INVESTIGATION OF THE IDENTITY AND BIOCORROSIVE ABILITY OF A NOVEL DEEP-SEA BACTERIUM, BELONGING TO THE GENUS *HALOMONAS*, FROM THE *TITANIC*

by

Bhavleen Kaur

Submitted

in partial fulfillment of the requirements

for the degree of

DOCTOR OF PHILOSOPHY

Biological Engineering

at

DALHOUSIE UNIVERSITY

Halifax, Nova Scotia April, 2004

Your file Votre référence
ISBN: 0-612-93284-2
Our file Notre référence
ISBN: 0-612-93284-2

DALHOUSIE UNIVERSITY

To comply with the Canadian Privacy Act the National Library of Canada has requested that the following pages be removed from this copy of the thesis:

Preliminary Pages
- Examiners Signature Page
- Dalhousie Library Copyright Agreement

Appendices
- Copyright Releases (if applicable)

TABLE OF CONTENTS

Page

LIST OF TABLES

LIST OF FIGURES

LIST OF SYMBOLS AND ABBREVIATIONS

16S rRNA	16S ribosomal ribonucleic acid
amp	Ampicillin
ATP	Adenosine Triphosphate
BHS	Bushnell Haas medium
BLAST	Basic Local Alignment Search Tool
C	Carbon
Ca	Calcium
Cl	Chlorine
CM	Cell membrane
DDSA	2-dodecenyl succinic anhydride
DMP	2,4,6 – tris [(dimethylamino)methyl]phenol
DNA	Deoxyribonucleic acid
dNTP	de-oxyribose nucleotide trisugar phosphate
e	electron
EB buffer	QIAGEN miniprep kit elution buffer
EDS	Energy Dispersive X-ray Spectrometry
EDTA	Ethylenediaminetetraaceticacid
EPS	Extracellular polymeric substances
ESEM	Environmental Scanning Electron Microscope
F	Furrowing
Fe	Iron
$Fe(OH)_2$	Iron hydroxide
GLC	Gas liquid chromatography
HCl	Hydrochloric Acid
HPLC	High pressure liquid chromatography
KAc	Potassium acetate
Kb	Kilobase
LB	Liquid broth
M	Metal
MIS	Microbial Identification System
N3 buffer	QIAGEN miniprep kit neutralisation buffer
Na	Sodium
NaCl	Sodium chloride
NaOH	Sodium hydroxide
NR	Nucleoid region
O	Oxygen
OD	Optical density
OH	Hydroxide
OM	Outer membrane
P1 buffer	QIAGEN miniprep kit precipitation buffer 1
P2 buffer	QIAGEN miniprep kit precipitation buffer 2
PB buffer	QIAGEN miniprep kit precipitation buffer 3

pBS	Plasmid Bluescript SK+
PCR	Polymerase chain reaction
PS	Periplasmic space
R	Ribosomes
RE	Restriction enzyme
RMS	Royal Mail Steamship
SDS	Sodium dodecyl sulphate
SEM	Scanning electron microscope
SSU	Small Subunit
TAAB	tetrabenzol[b,f,j,n][1,5,9,13]tetraazacyclohexadecine
TE	Tris-HCl EDTA buffer
TEM	Transmission Electron Microscopy

ACKNOWLEDGEMENTS

Often in life you realise the significance of lessons, long after you have received them. That, I believe, is how I am going to feel after I graduate. Dr. Henrietta Mann has made a deep impact on my life, both academically and personally. She has taught me about independent research: helping me plan and set-up the experimental design, reviewing my progress, helping me when I got stuck, keeping me on track, suggesting alternatives and finally, analysing and developing the layout for the thesis. Working under Dr. Mann has given me confidence in my decisions and my public speaking skills. Personally, she has been a friend, watching out for me, and helping me get adjusted to build a life in this country. Most importantly, she has reinforced my belief that if you put efforts, anything is possible.

I would like to extend my gratitude to Dr. Song Lee for helping me understand and conduct the molecular biology experiments, in his laboratory. His analysis of the results, of the identity of the isolate, gave me the confidence to reach the conclusions. I would like to thank the members of my supervisory committee for regularly reviewing my progress and ensuring that I kept going.

Special thanks to Frank Thomas at Bedford Institute of Oceanography for his assistance with using the ESEM and EDS. I also owe thanks to Mary Ann Trevors at the EM facility in Dalhousie University, for processing the samples for TEM and for helping me learn to use the TEM. Audrey Maw at the Department of Biology has been a constant source of media, glassware, microbial samples and light microscope. None of this study would be possible without the contribution of the rusticle samples by George Tulloch. I owe a sincere thanks to Muhannad Al Darbi for helping me set-up the corrosion experiments and to analyse the results obtained.

My family has been a constant source of support through my degree, and always. I thank my parents for believing in me and for supporting me in my decision to pursue a Ph. D. My brothers Kanwarpreet and Deepjot have been great moral supports through it all.

Finally, a very special mention of my friend Jaspreet, who has been here to keep me from giving up at the last moment and for proofreading my write-ups. His moral support has been unquestionable and heartening.

ABSTRACT

The morphology, ultrastructure, biochemical characteristics and 16S rRNA gene sequence of a bacterium, designated strain BH1, isolated from the rusticles that were removed from the wreck of the Royal Mail Steamship (RMS) *Titanic*, were determined. Strain BH1 was rod-shaped, Gram-negative and produced circular, off-white, opaque colonies on marine agar. Both long and short rod forms, ranging in size from 2 - 6 μm in length and 0.5 – 0.8 μm in width, were observed. Transmission electron microscopy revealed that strain BH1 had a typical Gram-negative cell wall structure and possessed 2 - 6 peritrichous flagella. 16S rRNA gene sequence comparison placed strain BH1 in the genus *Halomonas* of the family *Halomonadaceae* within class gammaproteobacteria of the phylum *Proteobacteria*. It showed 98 % sequence similarity with the species *Halomonas variabilis*. However, cells of *H. variabilis* are vibrio-shaped, monoflagellated and obligately aerobic. This implies that strain BH1 could be a novel species within the family.

In addition, the biocorrosive ability of the strain BH1 was studied by testing its effect on corrosion of mild steel coupons. Strain BH1 cells were able to adhere to the metal surface, and caused the formation of tubercles. Localised corrosion was observed under these tubercles, implicating the role of strain BH1 in microbially influenced corrosion. ESEM and EDX analysis inferred the presence of goethite and green rust crystals within the corrosion products. Both these formations are abundantly present in rusticles. Thus, this indicates that strain BH1 may have been part of a transient consortium that was involved in the formation of the rusticles, on the *Titanic*.

1. INTRODUCTION AND LITERATURE REVIEW

1.1 Understanding the deep-sea environment

The deep sea is often seen as an icy cold, dark inhospitable place, with bone crushing pressure, which is devoid of food and, thus, life: a marine desert, so to say. As a matter of fact, the British oceanographer, Edward Forbes, in the 1840's, was of the opinion that there was no life below the depth of ~ 600m. Nevertheless, after the end of the Second World War, Zobell and co-workers helped to progress the science of deep-sea biology and to dispel the myths of inhospitability (Austin, 1988).

The average temperature in the deep-sea is between 3 – 4 ^{o}C and salinity is 3.5 %. At a depth of about 10,000 m, the pressure in the water may be a 1000 times that on the surface ~ 1 tonne/cm^2. Deep beneath the surface, a current system driven by the differences in salt content and temperature (thermo-haline system) stirs up the ocean waters. This circulation mixes the water, keeps the chemistry uniform and carries oxygen from the atmosphere to the deeper layers, making it suitable for life (Rice, 2000). The amount of oxygen, in the deep sea, is often greater than 50 % of saturation levels of air, i.e. ~ 4 mg/l. These high levels of oxygen may be due to the extremely low rates of oxygen consumption by the deep sea organisms (Austin, 1988).

Food, either in the form of sporadic large chunks, such as, dead fish that settle at rates of 50 - 500 m/h or, as a more continuous settlement of organic particles - that settle at a much slower rate - reaches the bottom of even the deepest trenches. The organic particles may be remnants of surface-layer phytoplankton and zooplankton, their faecal matter and other recalcitrant molecules. These comprise the so-called "marine snow". They sink in the form of micro/macro aggregates (Silver *et al.,* 1978; Rice, 2000; Turner, 2002). Kiorboe (2001) described the process of formation of these aggregates. He demonstrated that fluid motion caused collisions between small primary particles (e.g. phytoplankton) and made them stick together to form aggregates. As they settle, bacteria from the water

column are able to colonise the aggregates (Simon *et al.,* 2002), and solubilise and remineralise them. This solubilisation causes the organic solutes to leak out of sinking aggregates, which can then guide small zooplankters to the aggregate.

The deep sea sustains the existence of a range of microorganisms, that can, not only, tolerate high hydrostatic pressures, extremes of pH and antibiotics, but can also flourish in environments that are at extremes of temperature, and salinity, or that have vanishingly low or exceedingly high levels of potential nutrients (Postgate, 1994). Takami *et al.* (1997) attempted to characterize the microbial flora found on the deepest sea floor, from a mud sample collected from the Mariana Trench. They found that the microbial flora was composed of actinomycetes, fungi, non-extremophilic bacteria, and various extremophilic bacteria such as alkaliphiles, thermophiles, and psychrophiles. A wide range of taxa were represented when the 16S rDNA sequences were studied.

These microorganisms play a major role in food web dynamics and biogeochemical cycles in the oceans (Kirchman and Williams, 2000). By investigating how they survive in nutrient-poor environments like the deep-oceans, microbial ecologists can understand their impact on other oceanographic and ecological processes.

1.2 RMS *Titanic* and its microbes

The wreck of the RMS *Titanic*, with its rich microbial diversity, provides an inimitable opportunity to forward our understanding of deep-sea microbial life forms.

The Royal Mail Steamship (RMS) *Titanic* was conceived as a luxury liner, which would rival all other ships of its time in size, speed and opulence. The 50,000-ton ship, when built, occupied a distance of two city blocks between the bow and the stern, and stood the height of a ten-storey building from the keel to the boat deck (MacInnis, 1992). Alas, that was not the distinction for which it would be remembered. The sinking of the *Titanic*, after striking an iceberg, only three days into its maiden voyage, with a loss of over 1500

lives, became a legend of the twentieth century that has spawned books, scientific research, documentaries, websites and, even movies.

Its remains were first uncovered during an expedition led by Dr. Ballard, in 1985, aboard a Woods Hole research vessel *Knorr*. This discovery set-off a new phase of research on the *Titanic*. In 1991, another expedition carried out from the Russian Academy of Science vessel *Akademik Keldysh* recovered artifacts, biological samples, sediment cores and scientific impressions from the wreck of the *Titanic* using the manned submersible MIR-2 (MacInnis, 1992; Stoffyn and Buckley, 1992). Scientists observed that the wreck was covered on all sides by rust and several icicle-like structures – coined "rusticles" by Dr. Ballard – hung off all other parts (Ballard, 1989; MacInnis, 1992). The microstructure of the rusticles indicated that they were biogenic in origin (MacInnis, 1992). Later expeditions have learnt that rusticles continue to grow larger and denser, thus hastening the deterioration of the wreck (Cullimore and Johnston, 2000).

The rusticles that were collected have since been the subject of vast research (Stoffyn-Egli and Buckley, 1993; Mann, 1997; Wells and Mann, 1997; Cullimore, 1999; Cullimore *et al.*, 2002). They are complex bioconcretious structures, composed of an iron oxy-hydroxide shell, with a smooth orange-red outer surface made of goethite, a rough orange inner surface made of lepidocrocite, and many internal structural formations like goethite-dominated mesh-like matrix, iron-plate like structures, porous spongelike regions, water channels, ducts and thread-like spans (Stoffyn-Egli and Buckley, 1993; Pellegrino and Cullimore, 1997; Pellegrino, 2000; Cullimore *et al.*, 2002). Figure 1.1 is an illustration of the typical components in a dissected rusticle.

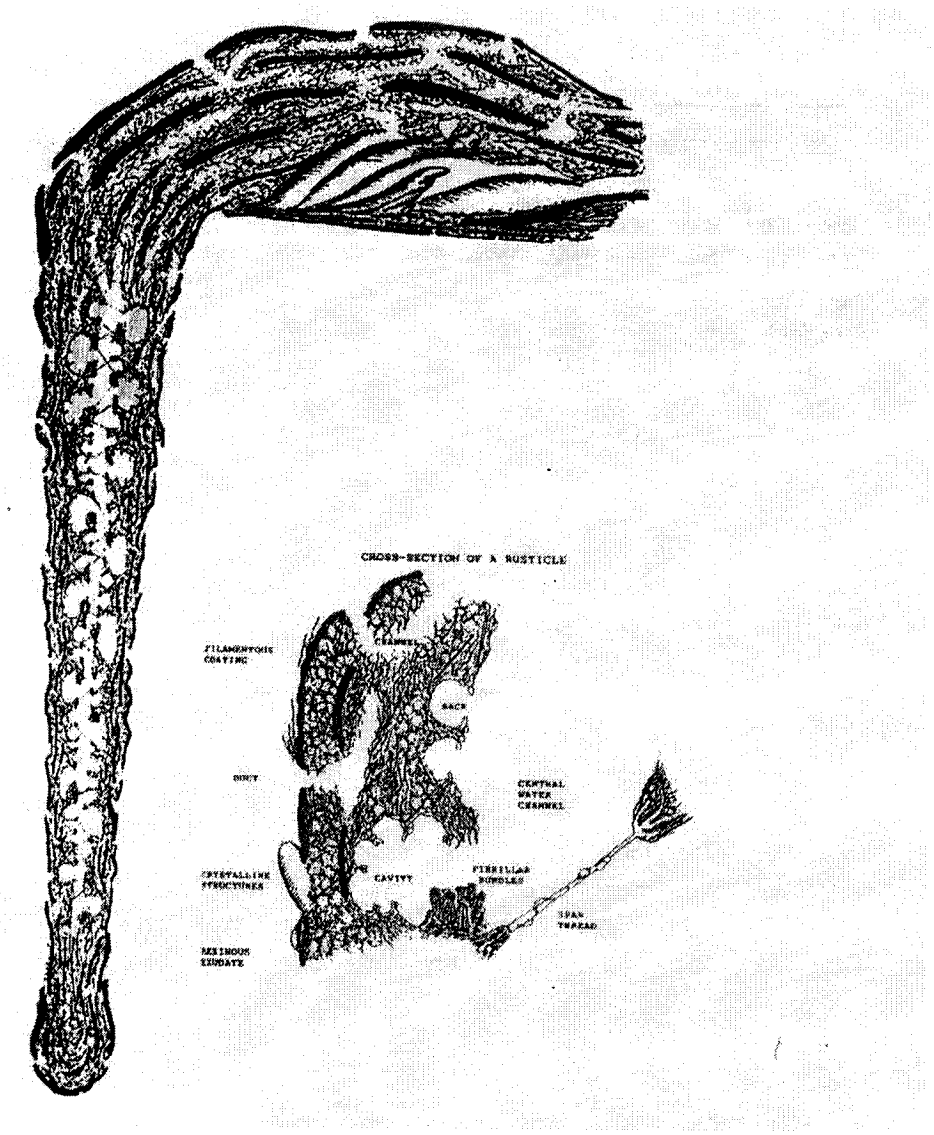

Figure 1.1 Illustration of the typical components in a dissected hanging rusticle. The left side of the diagram is a vertical cross section through a hanging rusticle showing a central water channel with sac-like extensions into the porous cortex of the rusticle. The outside of the rusticle is coated with iron-rich plates. To the lower right is an illustration of the structures found associated with the central water channel; these include the spans of threadlike materials forming a major structural support (upper left), the cavities and sac within which water may collect, the very porous concretious cortex, and the iron-rich plates toward the outside of the rusticle. Passageways (ducts) connect the central water column with the outside environment through these plates. Scales: left hand diagram, 1 mm is equivalent to 20 mm; lower right diagram, 1 mm is equivalent to 0.1 mm. (Pellegrino, 2000).

Rusticles are believed to be formed by the synergistic actions of a consortia of different microbes like sulfate-reducing bacteria, iron bacteria, heterotrophic aerobic bacteria, microaerophilic slime forming bacteria, various fungi, etc, that inhabit and establish themselves within its cortex (Stoffyn-Egli and Buckley, 1995; Wells and Mann, 1997; Cullimore *et al.,* 2002). These strains were identified using the Biological Activity Reaction Tests (BART™, Droycon Bioconcepts Inc., Canada), that detect different types of microbes, based on growth across redox and nutrient gradients.

A consortial theory of microbial associations within the rusticles was put forth by Cullimore *et al.* (2002). They suggested that these consortia may be vital or transient depending upon whether the strains involved in their formation could function independently, when removed from the consortium. The microbial species within the consortium survive by feeding not only on the materials being released from the ships structure, but also on the macro/microaggregates and small creatures that are constantly pouring down from surface water column.

Cullimore (1993) reported that the positively charged iron surface of the wreck probably attracts the negatively charged microbial cells, which then adhere to it by producing polymers, such as, glycocalyx (Allison and Sutherland, 1987). Then, some of these microbes mineralize and solubilize the metal, by various processes that lead to the formation of the basic physical structure of the rusticles. With time, the older microbes themselves, get mineralized, and become a part of the rusticular structure, and other bacteria then begin to grow on their remains. As the biomineralised remains of other bacteria, microorganisms, sand, clay, debris and " marine snow" accumulate, the rusticle becomes more complex, porous and semi-hard (Wells and Mann, 1997).

The complex network of water channels, cavities, and ductwork formed within the rusticles, allows for the constant circulation of water throughout the rusticles and thus, supports the consortia of microbes that live within its cortex (Cullimore *et al.,* 2002). In

the beginning stages, there is more circulation of water through the rusticle. But as biomineralisation proceeds, the water flow becomes more restricted. This creates different microenvironments within the rusticle, thus making it suitable for the arrival and establishment of newer species. Brown (1997) reported that rusticles may support a variety of halophilic and halotolerant microbes as the water inside may become more saline due to less circulation.

Rusticles are extreme examples of metal corrosion influenced by microbial growth. They provide an interesting and exciting opportunity to observe the microbial degradation of metal structures in the deep ocean. Cullimore *et al.* (2002) have investigated the corrosive potential of the consortia of rusticular bacteria. They found that rusticles were capable of extracting iron from steel at significant rates and, thus, could seriously compromise the physical structure of ships to which they were attached and cause heavy replacement costs to the maritime industry. The bacteria in the rusticles were also found to be capable of accumulating heavy metals, which when mobilised could become potential sources of pollution (Alford, 1999; Cullimore *et al.*, 2002).

1.3 Bacterial identification

The zoological definition of species as "groups of interbreeding or, potentially interbreeding natural populations that are reproductively isolated from other such groups" (Ravin, 1963) cannot be applied to bacteria. Other approaches, thus, have to be explored to define bacterial species, which is the most important taxonomic group in bacterial systematics (Brenner *et al.*, 2001). The polyphasic approach to bacterial taxonomy involves the collation and analysis of many levels of information, from molecular to ecological, to delineate consensus groups (Gillis *et al.*, 2001).

Chemotaxonomic studies of cellular fatty acids, quinones, polar lipids, polyamines, and molecular techniques like nucleic acid pairing studies, DNA and RNA sequence analysis, electrophoretic patterns of proteins, are some of the newer techniques, in addition to the

traditional methods of investigation like study of morphology, physiology, enzymology and serology that are currently used in the polyphasic approach to bacterial classification (Gerhardt *et al.,* 1994; Stackebrandt and Goebel, 1994; Vandamme *et al.,* 1996; Gillis *et al.,* 2001).

Different techniques have different levels of taxonomic resolution. Molecular biology techniques like DNA sequencing and DNA probes have very high discriminatory taxonomic power, revealing information from family to strain level. Other techniques like chemotaxonomic markers, FAME, BIOLOG, API, DNA-DNA hybridization, mol % G + C, etc have narrower levels of taxonomic resolution (Vandamme *et al.,* 1996). Choosing a number of complementary techniques is, thus, the first step in the consensus polyphasic approach.

The analysis of genes encoding for SSU rRNA (16S rRNA) is currently the most extensively used classification technique in prokaryotic classification. The potential, of sequence analysis of 16S rRNA genes, in inferring the evolution of taxa through billions of years has been extensively documented (Woese, 1987, Olsen and Woese, 1993, Olsen *et al.,* 1994, Ludwig and Schleifer, 1994, Ludwig *et al.,* 1998) and thus, it forms the backbone for structuring the second edition of Bergey's Manual of Systematic. The ribosomal RNA gene does not contain the code for a protein product, but transcribes ribonucleic acid molecules that fold to form a structural component of ribosomes. rRNAs and ribosomes together function as protein-synthesising machines of the cell. Therefore, the rRNA molecules are ancient and have highly conserved structures (Stackebrandt and Goebel, 1994; Giovannoni and Rappé, 2000). If we compare many copies of rRNAs side by side, we will find regions of base sequence that never change, other regions that are found in only members of a kingdom, or genus, and still other regions that vary from species to species (Giovannoni and Rappé, 2000). Thus, for every phylogenetic group of organisms, we can find a set of oligonucleotide "signature" sequences within the rRNA gene that occur with relatively high frequency only within that group (Woese *et al.*, 1980;

Stackebrandt and Goebel, 1994; Giovannoni and Rappé, 2000; Ludwig and Klenk, 2001). The composition at a given position and/or, the frequency and patterns of permissible variation in sequence at that position can be characteristic of a given phylogenetic group (Woese *et al.*, 1985; Ludwig and Klenk, 2001). By analyzing these in the 16S rRNA gene sequence, one can identify the phylogenetic group of an unknown. A comprehensive library of 16S rRNA gene sequences is available to make comparisons with other known bacteria (NCBI, 1988; www.mikro.biologie.tu-muenchen.de/pu/ARB).

Eventhough the 16S rRNA gene sequence is very useful in assigning an isolate to a genus, it falls short of species delineation, if the sequence similarity between two or more related species is greater than 97 %. In that case, DNA relatedness must be used to determine whether the strains belong to different species. Amann *et al.* (1992) showed that at high 16S rRNA gene homology values, DNA-DNA reassociation had a higher species resolving power than sequence analysis. Stackebrandt and Goebel (1994) showed that eventhough the correlation between 16S rRNA gene homology and DNA-DNA reassociation values was non-linear, yet, at sequence homologies below 97.5 %, it was unlikely that two organisms would have more than 60 to 70 % DNA similarity.

Double stranded DNA can be reversibly dissociated into its two complementary strands, at high temperature. Hybridisation is based upon the ability of dissociated DNA from one bacterium, to form heteroduplexes with any complementary sequences, present in the dissociated DNA of another bacterium. The percentage of unpaired bases in the heteroduplex gives an indication of the degree of divergence between the two. This can be approximated by comparing the thermal stability of the heteroduplex with the thermal stability of a homologous duplex (Brenner *et al.*, 2001). Various methods of DNA- DNA hybridization (Crosa *et al.*, 1973; Brenner *et al.*, 1982) are currently in use. Based on these comparisons, the definition of species as strains with approximately 70% or greater DNA-DNA relatedness and, with 5 ^{o}C or less ΔT_m (the temperature at which there is 50 % strand separation) is accepted (Wayne *et al.*, 1987).

Since DNA-DNA hybridization is a laborious technique, it is often restricted to a minimum number of strains, which have been defined based on other approaches like 16S rRNA gene sequencing (Gillis *et al.,* 2001).

1.4 Biofilms and microbially influenced corrosion

Biofilms are localized concentrations of microorganisms attached to a substratum and consist of a population of single species, or more often a multi-species community (White *et al.,* 1997). They are formed due to the adhesion of bacteria to metal surfaces in aqueous media or humid environments (Verran and Hissett, 1997; Medilanski *et al.,* 2002). The structure of the biofilm can be influenced by the extent of bacterial adhesion and the adhesion pattern, both of which depend on factors like a) bacterial characteristics - cell size, possession of flagella and pili, cell surface hydrophobicity and charge (van Loosdrecth *et al.,* 1990), b) chemical composition, surface roughness, crevices and inclusions on the metal surface and its coverage by oxide films or organic coatings (Videla *et al.,* 1987; Flint *et al.,* 2000), and c) the composition, ionic strength and flow regime of the aqueous medium (van Loosdrecth *et al.,* 1989; Scheuerman *et al.,* 1998).

Some researchers report that higher surface roughness increases the extent of bacterial accumulation (Vanhaecke *et al.,* 1990; Verran *et al.,* 1991; Verran *et al.,* 1994; Barnes *et al.,* 1999) and adhesion takes place preferentially at surface irregularities (Geesey *et al.,* 1996), whereas other studies (Taylor *et al.,* 1998) found reduced adhesion to rougher surfaces. The opposing observations regarding the influence of surface roughness on bacterial adhesion may be credited to the degree of surface roughness, the bacterial species tested, the physicochemical parameters of the surface, the bulk fluid phase under study and, the adhesion test method used to detect bacteria on the surface (Flint *et al.,* 2000).

Biofilms are held together by extracellular polymeric substances (EPS), which mediate cohesion as well as adhesion to surfaces. The EPS matrix consists mainly of

polysaccharides and proteins (Christensen, 1989; Neu and Marshall, 1990; Neu, 1991; Cooksey, 1992; Lazarova and Manem, 1995) with considerable amounts of nucleic and humic acids (Jahn and Nielsen, 1996). Substantial amounts of lipids can occur in waste water biofilms; abiotic particles such as clay, silt and gypsum can also be trapped by EPS and be integrated in the slime matrix (Flemming *et al.*, 1997). The composition of the EPS matrix can vary depending upon the organisms involved (Costerton *et al.*, 1987), the nutrient conditions (Uhlinger and White, 1983) and, the physicochemical conditions (Christensen and Characklis, 1990). As EPS contain many groups, which are capable of hydrogen bonds, electrostatic and, van der Waals interactions, they determine the physical and physico-chemical properties of biofilms (Flemming *et al.*, 1997).

Biofilms can be a significant problem in numerous disciplines, including biotechnology, medicine, oil industry, biocorrosion, biodeterioration and biofouling. There are many disadvantages of these biomasses: increase of the headloss, protection of pathogens, generation of anaerobic zones in aerobic environments, which favour the growth of sulphate-reducing bacteria that can induce biocorrosion, link in the food chain leading to the appearance of macroinvertebrates, etc. In some cases, the presence of biofilms is beneficial, e.g. on purifier supports or bioreactors in industries, waste-water treatment plants, etc (AGHTM Biofilm European Working Group, 1997; Sanders, 1997).

Corrosion and Biofouling

The surfaces of metals that are immersed in natural or industrial waters undergo two main processes: corrosion, and biofouling (Videla, 2001). Corrosion causes the deterioration of the properties of the metal due to charge –transfer reactions that take place at the interface between the metal and the aqueous environment (Bockris and Reddy, 1970). This corrosion reaction can be influenced by various physicochemical factors and microbial build-up (Borenstein, 1994; Sawant and Venugopal, 1996; During, 1997; Medilanski *et al.*, 2002).

The primary reaction is the dissolution of the metal, which releases electrons as ions, e.g.

$$Fe \longrightarrow Fe^{2+} + 2e^-$$

This reaction proceeds only if the electrons formed are removed by

a) hydrogen production which takes place in acidic solutions

$$2H^+ + 2e^- \longrightarrow H_2$$

b) oxygen reduction in neutral solutions

$$O_2 + 2H_2O + 4e^- \longrightarrow 4OH^-$$

The corrosion products that are thus formed can then adhere to the metal surface, which can alter the rate and type of corrosion: they may slow down the corrosion reactions due to a phenomenon called passivity (Videla 2001) and/or, make the surface amenable to attachment of microorganisms. The attached microorganisms, in turn, may influence the corrosion process by several different mechanisms that work simultaneously or consecutively (Videla, 1986), leading to a build-up of microbiological deposits on the metal surfaces. This is called biofouling.

The sequence of biological and inorganic changes that leads to biofouling can be summarized as follows: firstly, a very thin film (less than 100 nm thick) of inorganic and organic macromolecules (polysaccharides or glycoproteins) begins to form on the metal surface (Videla, 2001). This adhesion influences the distribution of electrostatic charges and the wettability of the metal surface (Dexter, 1976; Marshall, 1985). Due to these changes, the microbial cells start to adhere to the wetted metal surface. The adhesion, which, at first, is weak and reversible - caused mainly due to intermolecular forces and interfacial tension effects – gradually transforms into a more permanent irreversible adhesion caused due to the microbial production of EPS (Costerton *et al.,* 1985; Marshall, 1985). Thus, a biofilm consisting mainly of water, bacterial cells and their EPS is formed. This bacterial adhesion on stainless and mild steels can cause problems such as microbially induced corrosion (Costerton *et al.,* 1995) or represent a chronic source of microbial contamination, e.g. in the food industry (Barnes *et al.,* 1999).

Microbially influenced corrosion

The microbes in the biofilms may, in turn, influence corrosion by a number of different processes (During, 1997):

1) Depolarisation of cathode: The metabolic activities of the microbes may absorb the hydrogen that is formed at the cathode, thus activating the electrochemical cell.
2) Metabolic products: some products, like, sulphides, sulphuric acid, nitric acid, etc, produced during bacterial metabolism can attack the metal
3) Electrochemical cells: The differences in pH, salt concentration, aeration, that arise beneath the corrosion product deposits may create pockets of electrochemical activity, thus causing corrosion.

Other indirect ways, in which bacterial growth can influence corrosion, may be by degradation of the metal coatings or by decomposition of corrosion inhibitors (During, 1997).

Some of the most studied corrosive bacteria are the anaerobic sulphate-reducing bacteria (Tiller, 1982; Hamilton, 1985; Costerton *et al.,* 1995; Sanders, 1997) like *Desulfovibrio*, aerobic iron oxidizing bacteria like *Gallionella* and *Leptothrix* (Booth, 1971; Borenstein, 1994), and aerobic sulphur bacteria like *Thiobaccillus* (During, 1997). They have a chemolithotrophic type of nutrition (Moat and Foster, 1988). All of them are known to induce corrosion by one or more of the above MIC processes.

Identifying microbially influenced corrosion is not easy and is often overlooked for other physical causes of corrosion. To identify it correctly, it is essential to study the morphology of the attack, the composition of the deposits, the microbes present and the environmental conditions (During, 1997).

1.5 Benefits and malefits of marine microorganisms

Biodegradation of pollutants

Biodegradation is a natural process by which microbes alter and break down pollutants into other substances. Various marine microorganisms have been reported to degrade complex molecules, such as, naphthalene (Raymond, 1974, Voronin, *et al.,* 1977), pesticides (Gibson and Brown, 1975), wood pulp (Vance *et al.,* 1979) and petroleum hydrocarbons (Floodgate, 1984; Yakimov *et al.,* 1998). Of these, the petroleum degradation ability has been of great significance in accidents where the discharge of hydrocarbons from damaged ships, such as the *Amoco Cadiz*, *Exxon Valdez* and the *Torrey Canyon*, has occurred.

Prodigious amounts of crude oil are extracted from the earth and transported across the ocean each year. About 0.1 % of this total each year ends up in the marine systems (Albaiges, 1989). While accidental spills are the most spectacular, petroleum hydrocarbons also enter the coastal marine environment as exhaust particulates, fuel spills, tank washings, urban run-off, drilling and the by-products of biomass combustion (Johnston, 1980; Atlas, 1984).

Petroleum is a complex mixture of many thousands of compounds that include readily degradable *n*-alkanes, iso-alkanes, cyclo-alkanes, aromatics, naphthenoaromatics, heterocyclics (resins) and asphaltenes. Almost all samples of seawater contain bacteria capable of oxidizing some of the multitudinous components of petroleum (Atlas and Bartha, 1972; Jobson *et al.,* 1972; Cerniglia and Heitcamp, 1989; Delille and Siron, 1993, Siron *et al.,* 1995; Hedlund and Staley, 2001). Floodgate (1984) defines microbial degradation of oil in the marine environment as "the degradation of a complex and variable mixture of hundreds of substrates by unknown mixed population of microorganisms in an erratically changing medium". This ability is reported in a wide range of marine bacterial genera like *Pseudomonas, Acinetobacter, Vibrio, Bacillus, Arthrobacter, Micrococcus*, etc (Floodgate, 1984).

Microorganisms degrade these hydrocarbons to produce carbon dioxide, water, and partially oxidized biologically inert by-products (Floodgate, 1984; Minas and Gunkel, 1995). They use the organic contaminants that make up the oil, as carbon sources and transform them to less harmful compounds through aerobic and anaerobic respiration, fermentation, cometabolism and, reductive dehalogenation (Minas and Gunkel, 1995).

Biodeterioration/biofouling of objects in the sea

Besides being of consequence in their role as degraders of pollutants, marine microorganisms are also infamous for their role in biodeterioration of useful objects, such as wooden dockyard pilings, cotton fishing nets and ropes, bridges, piers and ships. Biofouling - which involves the undesirable accumulation of microbiological deposits - on the undersurface of ships, can destroy the structure of ships, cause accidents and, pollution, all of which have huge economic costs (Austin, 1988; Cullimore *et al.,* 2002).

Biotechnology

Marine microorganisms have the ability to produce and secrete polymers and enzymes, like DNases, lipases, alginases and proteases, that are commercially very valuable in the confectionery (lactases) and detergent (proteases) industries (Austin, 1988). They may be of interest in the production of biochemical compounds, single cell proteins (Phaff, 1986), biopolymers and pharmaceutical compounds (Sutherland, 1990 and 1998; Tombs and Harding, 1998) that could be of value in aquaculture or re-stocking programmes, health industry, production of degradable thermoplastics, cleansing agents for oil tankers, etc (Patel and Hou, 1983; Austin, 1988; Rodriguez-Valera, 1992). Finally, marine bacteria may harbour plasmids, which could be of value to molecular biologists.

Thus, the marine microbes have a huge potential as resources for new products, which have a lot uses for humans.

1.6 Objectives of this study

The objectives of this study were two-fold. The first was to identify a bacterial isolate, designated strain BH1, isolated from the rusticles, retrieved from the wreck of the RMS *Titanic*. The second objective was to study the ability of strain BH1 to cause microbially influenced corrosion and to assess its ability to degrade crude oil.

2. MATERIAL AND METHODS

2.1 Rusticle collection and storage

Rusticle samples for this study were collected by Dr. Steve Blasco (personal communication) during the *Akademik Keldysh* expedition, in 1991, to the RMS *Titanic* wreck site. These rusticle pieces were removed from the hull using the articulating arm of the Mir-2 submersible. They were transferred to plastic collection bags, along with sea water and then transported aseptically to the surface (Low, 1991). Until 1993, they were stored under dark, vacuum-sealed conditions at 4 °C at the Bedford Institute of Oceanography, Dartmouth, NS.

2.2 Isolation of strain BH1

These steps were performed by Dr. Henrietta Mann (personal communication) in 1997. The rusticle samples were aseptically removed from the collection bags and rinsed three times in sterile seawater. The rusticle was then dissected and a portion from the interior used to streak plate Bacto Marine Agar 2216 media (DIFCO Laboratories, Detroit; Appendix A). This helped to isolate, cultivate and enumerate heterotrophic, marine bacteria (Difco, 1984), that were found in conjunction with the rusticle. The plates were incubated at 4 °C ± 2 °C and the bacterial isolates obtained were then pure cultured and stored. Bacterial stock cultures were maintained in 50 % glycerol at -20 °C. The samples were periodically re-cultured to ascertain that there was no contamination of the samples. In 2000, one of the purified bacterial strains, designated strain BH1, was recultured on Bacto Marine agar and Bacto Marine broth (Appendix A), for this study.

2.3 Characterisation of strain BH1

Colony morphology

Colonial morphology of strain BH1 was described after growth for 24 - 48 h on Marine Agar petri plates at 4 °C. Growth of strain BH1 on Triple Sugar Iron Agar (DIFCO Laboratories, Detroit; Appendix A) was also recorded.

Gram staining technique

A smear using a pure culture of strain BH1 was made. It was then covered with crystal violet for 20 sec. Distilled water was used to wash off the stain. Next, the smear was covered with Gram's iodine solution for 1 min. The slide was flooded with 95 % ethyl alcohol (10 - 20 sec) and subsequently rinsed with water. Safranin was used to counter-stain the smear (20 sec). After rinsing the slide with distilled water, it was dried and observed under oil immersion lens of a light microscope.

Negative staining

Negative staining provides information on refractile inclusions such as poly-β-hydroxybutyrate granules and spores (Robinow, 1960). These preparations reveal unstained bacteria standing out brightly against a blue-black background. A loopful of strain BH1 cell suspension was dispersed in a drop of nigrosine, placed at the edge of a clean microscope slide. Using a spreader slide, the suspension was dragged across the bottom slide. After the slide was dry, it was observed under oil immersion lens of a light microscope.

2.4 Physicochemical and biochemical factors for growth

pH range

To establish the pH range of strain BH1, Marine broth solutions of pH 4.0, 5.0, 6.0, 7.0, 8.0 and 9.0 were prepared and growth was monitored at 27 °C. HCl and NaOH were used to adjust and control the pH of the medium. Growth was monitored by using the 4040 Novaspec II spectrophotometer to record the optical density (OD) readings at 660 nm.

Temperature range

For temperature range, Marine broth samples inoculated with strain BH1cell suspensions were kept at 4 °C, 15 °C, 27 °C, and 37 °C. A difference of 10 ± 2 °C between consequent temperature values was used to cover the temperature range from 4 °C to 37 °C. Growth

was monitored by using the 4040 Novaspec II spectrophotometer to record the OD readings at 660 nm.

Salt tolerance

Since strain BH1 was recovered from the deep-sea, it was logical to assess its range of salt tolerance to establish if it is halotolerant, moderately halophilic or, extremely halophilic. To test the salt tolerance limit of the strain, salt concentrations of 0.26 %, 2.2 %, 8.0 %, 14.5 %, 20.0 % and 32.0 % (wt/vol) were prepared with NaCl using glucose medium with 0.026 M $MgCl_2.6H_2O$, 0.01 M KCl, 0.031 M $(NH_4)_2SO_4$ and 0.0001 M $FeSO_4.7H_2O$ (Vreeland and Martin, 1980) and kept at 27 °C, since that was the optimum temperature of growth. Growth was monitored by using the 4040 Novaspec II spectrophotometer to record the OD readings at 660 nm.

Biochemical tests

The Api 20E and Api 50CH biochemical test strips were used to establish the biochemical profile of strain BH1, since no other miniaturised test strips specific for marine bacteria are commercially available. In addition to the strips, catalase, methyl red and nitrate reduction tests were also carried out. All these tests were carried out by Nelson Laboratories, Inc., Utah (Appendix B). The biochemical profile generated was used to make comparisons with related species.

Fatty Acid analysis using MIDI

The MIDI Microbial Identification System (MIS) was used to identify the organism. The MIS Similarity Index is a numerical value, which expresses how closely the fatty acid composition of an unknown compares with the mean fatty acid composition of the strains used to create the library entry listed as its match. This value is a software generated calculation of the distance, in multi-dimensional space between the profile of the unknown and the mean profile of the closest library entry. It is an expression of the relative distance from the population mean. An exact match of the fatty acid makeup of

the unknown and the mean of the library entry would result in a similarity index of 1.000 (Appendix B).

Strains with a similarity index of 0.500 or higher with a separation of 0.100 between the first and the second choice are considered good library comparisons. If the similarity index is between 0.300 and 0.500 and well separated from the second choice, it may be a good match but an atypical strain. A value lower than 0.300 suggests that the organism is not in the database, but indicates the most closely related species.

Strain BH1cells were plated on Trypticase Soy agar and incubated at 27 - 29 °C until growth was observed. Fatty acids were then extracted and analysed using gas chromatography. The results were compared the results with the MIS library. The MIS library search report lists the most likely matches with the unknown composition and provides a similarity index for each match.

These tests were carried out by Nelson Laboratories, Inc., Utah (Appendix B).

2.5 Ultrastructure of strain BH1

Transmission electron microscopy

Ultrathin sections of bacteria embedded in plastic can be used to assess their internal details, by first chemically fixing them and, then, staining them with salts of heavy metals to increase differential contrast. The transmission electron microscope (TEM) permits the formation of an ultrastructural image of the bacterium using the electrons transmitted through the ultrathin sections (Beveridge *et al.,* 1994). In this study, cell preparations of strain BH1 grown in Marine broth, Marine agar, Triple sugar iron broth and Triple sugar iron agar were used.

Fixation and observation

Bacterial cells were harvested from late stationary phase by centrifugation at 15000 g for 5 min. Primary fixation was done with 2.5 % glutaraldehyde in sodium cacodylate buffer (pH 7.3) for 2 h, at 4 °C. Even though strain BH1 was isolated from a marine environment, NaCl was not added to the buffer as it was found to be halotolerant. After washing in buffer, postfixation was done in 1 % osmium tetroxide for 2 h, followed by staining in 0.25 - 0.5 % uranyl acetate for 24 h. The cell preparation was then dehydrated with acetone at 4 °C:

50 % acetone once for 10 min

70 % acetone twice for 10 min

95 % acetone twice for 10 min

After bringing the dehydrated cell preparation to room temperature, it was infiltrated with Epon Araldite resin (Appendix A):

3:1 (acetone: epon araldite) for 3 h

1:3 (acetone to epon araldite) overnight

100 % epon araldite twice for 2 h

Following infiltration, the cell preparation was embedded in 100 % epon araldite and cured at 45 °C in a vacuum oven for 24 h. Then, allowed the resin to harden at 60 °C for 24 h.

Thin sections were cut with Reichert Jung Ultracut E ultramicrotome. Silver and gold sections (60 - 90 nm) were picked up on uncoated copper grids. Double staining was done with lead citrate for 10 min and uranyl acetate for 4 min. Sections were observed using Philips 300 transmission electron microscope at 60 kV. Micrographs were obtained with fine grain positive film and printed on resin coated Kodak paper.

Negative staining

Unfixed strain BH1 cells were placed on formvar coated copper grids and allowed to settle. The grids were then covered with uranyl acetate stain for 30 sec. Excess stain was removed. The grids were air-dried for 10-15 min and observed under TEM.

2.6 Genetic characterisation

For this study, the DNA of the strain BH1 was extracted, its 16S rRNA gene isolated and amplified, using primers, the amplified product restriction digested and ligated with plasmid pBluescript (pBS), the ligated product transformed into XL1- Blue *Escherichia coli* cells, and the gene sequenced. *Pst*I and *Hin*dIII sites were inserted into the primers because pBS contains cutting sites for these restrictions enzymes (RE). The gene fragment could thus be ligated to the plasmid. The components and preparation of all the reagents used in the following experiments are listed in Appendix A.

Isolation and PCR amplification of 16S rRNA gene

A well separated colony of strain BH1 was picked, with a toothpick, from a 24 h pure culture grown on Marine agar. The colony was dispensed into100 µl of TE buffer and boiled at 100 ^{0}C for 5 min. Two microliters of this sample was taken as DNA template for polymerase chain reaction (PCR). PCR mixture was prepared as listed in Table 1.

The PCR mixture was overlaid with 100 µl of mineral oil and 30 cycles of the PCR amplifion were run: 94 ^{0}C for 1 min, 50 ^{0}C for 1 min and 72 ^{0}C for 1 min. Figure 2.1 illustrates the amplification of the gene fragment through the cycles.

After amplification, mineral oil was removed from the top of the mixture and, 100 µl of chloroform was added and centrifuged for 3 min at 3000 rpm. Five microliters of the PCR product was run on an agarose gel in an electrophoresis chamber. The agarose gel was prepared and poured into a casting tray, with a comb, to allow it to set (30 min). Five

microliters of the PCR product was mixed with 2.5 µl of coomassie blue on a paraffin film. The PCR product turned purple. Once the gel was set, the comb was removed and the gel was placed into an electrophoresis chamber. Fifteen microliters of ethidium bromide was added to 1 % TAE buffer, which was used to fill the electrophoresis chamber. The lanes of the gel were loaded with 1 Kb ladder and 7.5 µl of PCR product. The gel was run for 25 - 35 min at 102 volts in the electrophoresis chamber. After that, the gel was removed and placed under UV light to observe the DNA bands.

Table 1: PCR mixture

Reagent	**Quantity**
10 X PCR buffer	10 µl
10 mM dNTP's	2 µl
50 mM $MgCl_2$	4 µl
Taq DNA polymerase (5 U/µl) [Invitrogen, Burlington]	1 µl
*Primer BK1 (10 pmoles/µl)	10 µl
*Primer BK2 (10 pmoles/µl)	10 µl
DNA template	2 µl
dH_2O	61 µl
Total	100 µl

*PCR primers

GG**AAGCTT**agagtttgatcctggctcag : BK1

***Hin*dIII cutting site**

AC**CTGCAG**aaggaggtgatccagccgca : BK2

***Pst*I cutting site**

After ascertaining that the PCR product was of the correct size, the next step was to ligate the strand to plasmid pBS (Appendix C).

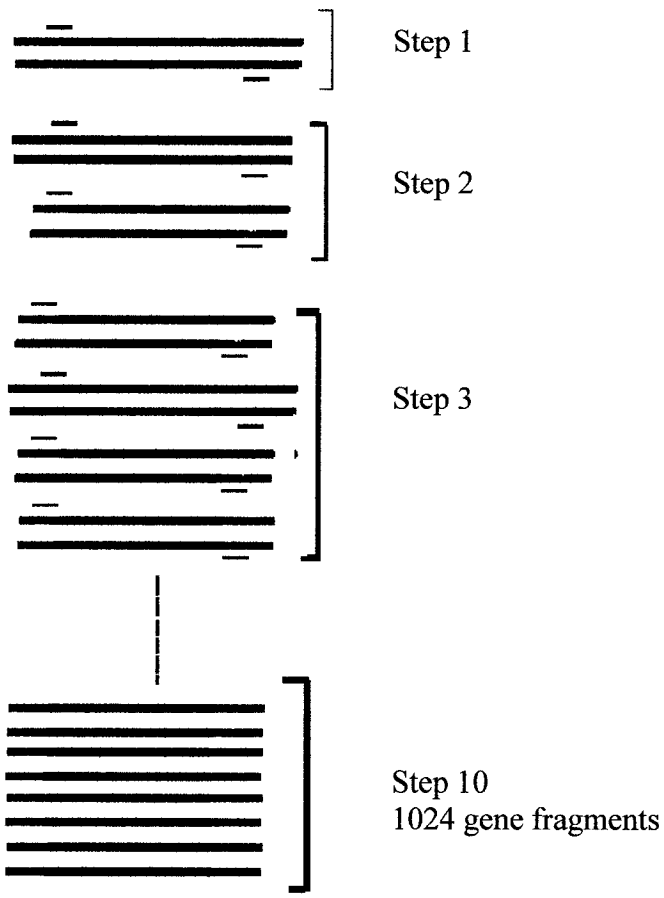

Figure 2.1 PCR amplification of the 16S rRNA gene. The green lines represent the bacterial DNA. The small red fragments represent the primers. The green lines with red ends represent copies of the PCR amplified 16S rRNA gene. By the 10th step, there will be 1024 copies of the 16S rRNA gene.

Isolation of pBluescript using the miniprep protocol

Plasmid pBS was isolated by performing a miniprep. pBS carrying *E. coli* cell culture (1.5 ml) was dispensed into an eppendorf tube. The tube was centrifuged for 2 min and, the supernatant quickly discarded. The tube was vortexed, after adding 100 µl of GTE, until the pellet was suspended in the GTE. In another eppendorf tube, 186 µl of dH_2O, 10 µl of 20 % SDS and 4 µl of NaOH were added, along with 2 µl of RNase. Then, this solution was mixed and added to the tube with the GTE and cell suspension. The tube was inverted 2 - 3 times and left at room temperature for 5 min. Then, 150 µl of KAc solution was mixed in by inversion. The tube was stored on ice for 10 min, then, centrifuged at high speed for 5 min. The supernatant was carefully extracted into a new tube. After adding 0.5 ml of chloroform and shaking very hard for 1 min, the tube was centrifuged for 3 min. Again, the supernatant was carefully extracted to a new tube. The tube was then stored at -70 ^{0}C for 30 min after adding 1 ml of 95 % ethanol. After centrifuging the tube for 10 min, the supernatant was discarded and 1 ml of 70 % ethanol was added. Again, after centrifuging for 6 min, the supernatant was discarded. The contents of the tube were vacuum dried. The plasmid DNA, thus obtained, was then suspended in 10-20 µl of TE.

Restriction digestion of pBS and PCR product

pBS and PCR product were both cleaved with 2 restriction enzymes *Hin*dIII and *Pst*I (Invitrogen, Burlington). The digests were setup according to the instructions of the manufacturer. The products were run on an agarose gel to see if they were successfully digested.

Purification of the restriction digested fragments

The portions of the gel, where the required fragments were present, were excised. Then, the excised gel portions were placed in a dialysis bag, and 500 µl of TE was added to the bag. The bag was, then, sealed with a clip and run in an electrophoresis chamber at 100 V for 1 h. After 1 h, the current was reversed for about 20 sec to remove the DNA

from the wall of the bag. The bag was observed under UV light to see if the DNA had come out of the gel.

Two petridishes, one with 7 ml of low salt solution and another, with 7ml of high salt solution were set up. The tip of a DNA elution column was cut off. Three milliliters of high salt solution was filled into a syringe and run through the column. The same process was repeated twice with low salt solution. The liquid contents of the dialysis bag were sucked out with a 1000 µl pipette. The contents of the pipette were poured into the syringe. The dialysis bag was washed with 200 µl of low salt solution. This solution was then sucked up into the syringe. The contents of the syringe were forced into the elution column. The column was washed again with 3 ml of low salt solution. Finally, the column was washed with 3 ml of high salt solution and the first 20 drops of the solution were collected into an eppendorf tube. One milliliter of 95 % ethanol was added and stored at -70 ^{0}C for 40 min. Then, the solution was centrifuged for 10 min. Ninety-five percent ethanol was poured off and 1 ml of 70 % ethanol was added and centrifuged for 5 min. Seventy percent ethanol was poured out and the tube was vacuum dried. The purified fragments were then ligated.

Ligation

The purified DNA fragments obtained from the procedure above were ligated, using T_4 DNA ligase (1U/µl), by setting up the mixture as indicated by manufacturer (Invitrogen, Burlington). The mixture was left at room temperature for 30 min to allow the pBS to ligate to the 16S rRNA gene fragment. Figure 2.2 is an illustration of the pBS plasmid with the 16S rRNA gene insert.

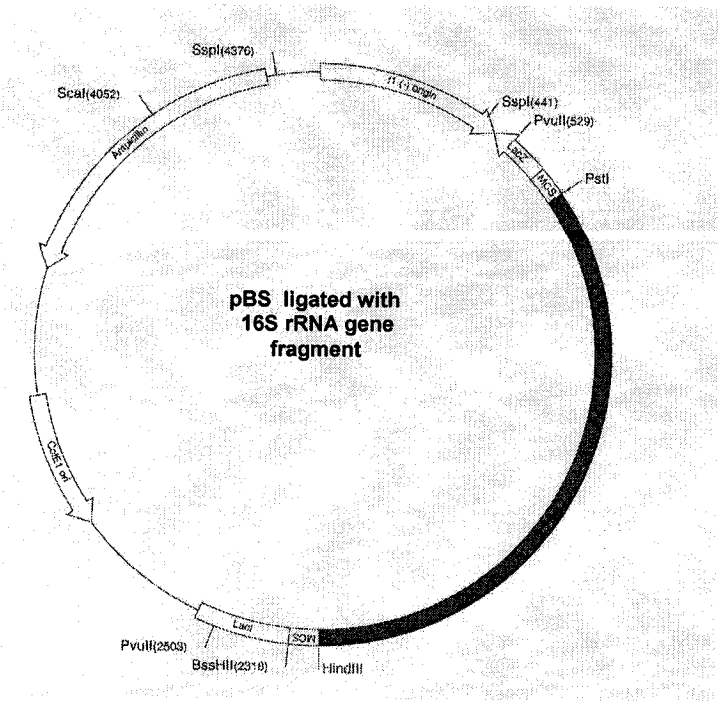

Figure 2.2 The restricted fragments of pBS and 16S rRNA gene come together because of the sticky ends and then ligate. The dark insert represents the16S rRNA gene fragment

Transformation of the ligated plasmid

200 µl of XL1-Blue competent *E. coli* cells and 100 µl of Tfm 3 were added to the ligation mixture and placed on ice for 45 min. Then the tube was put in a water bath (37 ^{0}C) for 2 min and finally, left at room temperature for 10 min. After that, 500 µl of LB was added to the tube and placed in a water bath (37 ^{0}C) for 1 h. LB agar plates were prepared with 160 µl of ampicillin (50 mg/ml) and 240 µl of tetracycline (10 mg/ml). The antibiotics were added to prevent the growth of XL1-Blue *E. coli* cells which did not pick up the plasmid. Only cells with the plasmid have resistance to the antibiotics. The plates were streaked with 200 µl of sample, 4 µl of IPTG and 50 µl of X-gal, and left overnight at 37 ^{0}C. This will allow the XL1-Blue *E. coli* cells to pick up the ligated plasmid and then multiply, making more copies of the ligated plasmid. Figure 2.3 is an illustration of the transformation of the ligated plasmid into the XL1-Blue cells.

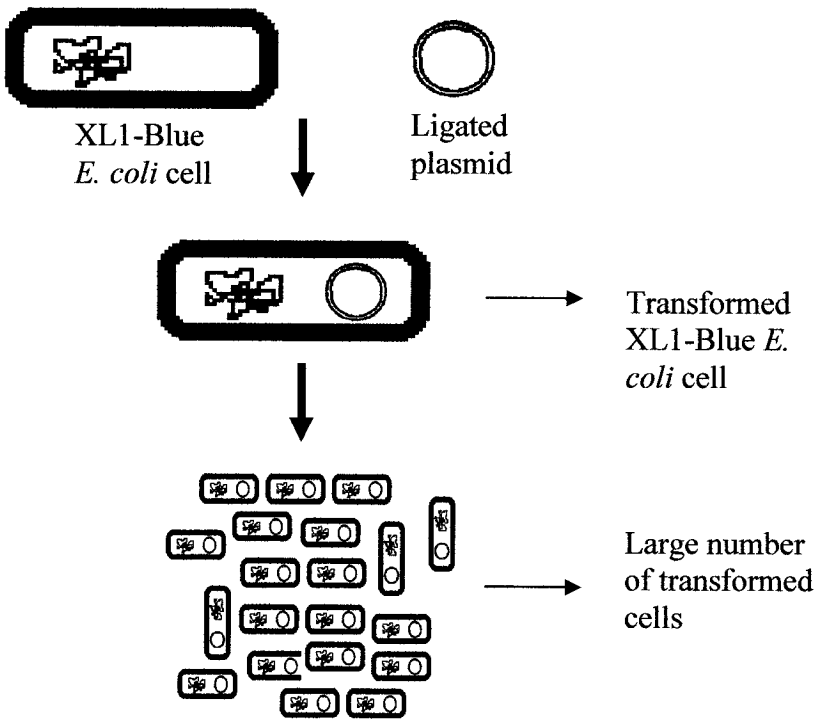

Figure 2.3 Transformation of the ligated plasmid into the XL1-Blue competent *E. coli* cells.

X-gal is a histochemical substrate for β-galactosidase enzyme that yields a blue precipitate upon hydrolysis. β-galactosidase is the gene product of the Lac Z gene. pBS carries the Lac Z gene. However, the 16S rRNA gene fragment gets inserted within the Lac Z gene sequence. So the transformed XL1-Blue *E. coli* cells, which carry the recombinant plasmid, do not synthesize β-galactosidase. This was used for the detection of the transformants with the correct insert.

Thus, only the white colonies were picked out from the transformants on the plates. These were then cultured, overnight at 37 ^{0}C, in test tubes containing 2 ml of LB and 4 µl of ampicillin. The plasmids were isolated from the transformants by doing a miniprep. The transformants were stored at -20 ^{0}C after adding 500 µl of 50 % glycerol to the tubes.

The extracted plasmids were restriction digested with *Hin*dIII and *Pst*I as specified by manufacturer (Invitrogen, Burlington). After 1 h, the digests were run on an agarose gel to observe the size of the fragments to determine, which transformants had the right plasmid.

Subcloning of gene

Subcloning of the transformant with the correct plasmid was done to get shorter fragments of the 16S rRNA gene because sequencing very large fragments is not reliable. The plasmid was restriction digested with several different restriction enzymes *Sma*I, *Kpn*I, *Bam*HI, *Cla*I, *Not*I, *Xba*I and *Hin*cII to see if there were any restriction sites in the 16S rRNA gene. All the digests were setup as specified by the manufacturer (Invitrogen, Burlington). Restriction sites were obtained for *Sma*I and *Hin*cII. Figure 2.4 illustrates the cutting sites for the enzymes in recombinant pBS.

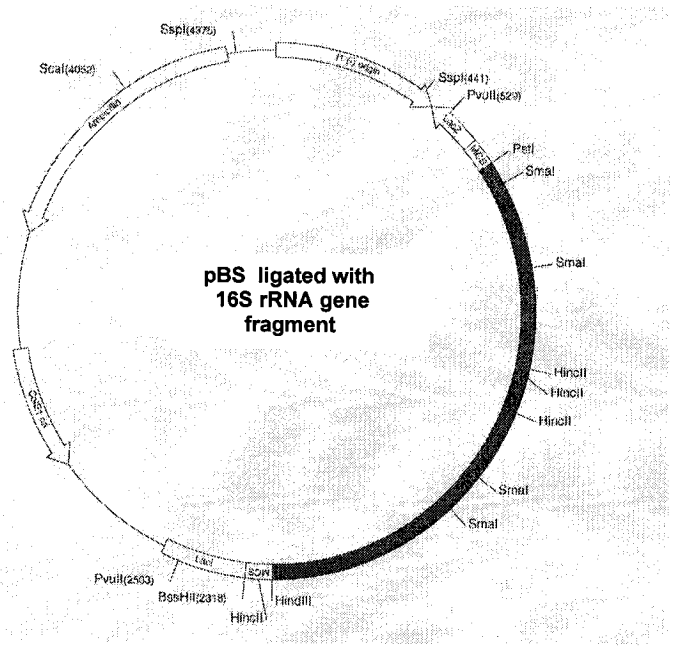

Figure 2.4 The recombinant pBS with the dark 16S rRNA gene fragment insert showing cutting sites for *Sma*I and *Hin*cII in the insert.

The *Sma*I and *Hin*cII digested plasmids were run on an agarose gel. The desired fragments were excised from the gel and extracted electrophoretically. The fragments were allowed to ligate and then, transformed into XL1-Blue competent *E. coli* cells. The transformants were grown on LB agar plates prepared with160 µl of ampicillin (50 mg/ml) and 240 µl of tetracycline (10 mg/ml). The plasmids were extracted from the transformants by doing a miniprep and then run on an agarose gel to determine which were the correct transformants. Figure 2.5 illustrates the 16S rRNA gene fragments in plasmids, obtained after subcloning.

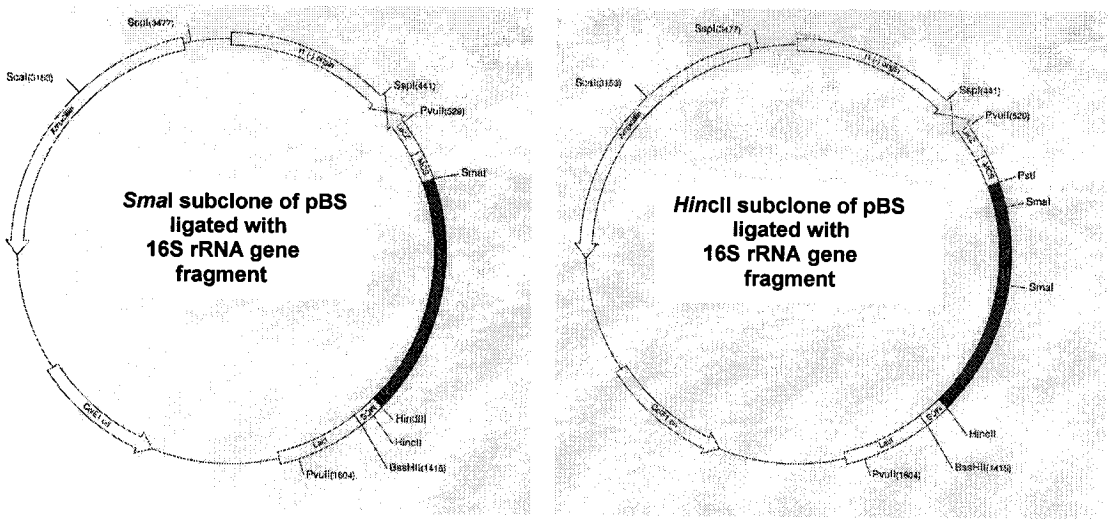

Figure 2.5 Plasmids restriction digested with *Sma*I and *Hin*cII and, then, ligated to get subclones that contain shorter dark fragments of the 16S rRNA gene.

QIAGEN spin prepMini prep protocol

QIAGEN spin prepMini prep kit (QIAGEN Inc., Mississauga) was used to extract plasmids from the three transformants with the right 16S rRNA gene fragments: full 16S rRNA gene, *Sma*I subclone gene fragment and *Hin*cII subclone gene fragment.

The transformants were pelleted in eppendorf tubes by centrifuging at 3000 rpm for 2 min. Two hundred fifty microliters of P1 buffer was added to the bacterial pellet and vortexed. Next, 250 µl of P2 buffer was added and inverted slowly 4-5 times. Finally, 350 µl of N3 buffer was added and inverted slowly 4-5 times. The tubes were centrifuged for 10 min. The supernatant was added to a spin column placed in collection tube and spun for 1 min. The flow through was discarded. Then, 750 µl of PB buffer was added into the column and centrifuged for 1 min. Again, the flow through was discarded. The column was placed into a new microcentrifuge tube and 50 µl of elution buffer EB was added. The tube was allowed to stand for 1 min and centrifuged for 1 min. The collected elute was stored at -20 ^{0}C. Two microliters of the purified plasmids were run on an agarose gel along with a double-stranded DNA standard (0.2 µg/µl) to determine the concentration of the plasmids.

Sequencing of gene

The purified plasmids were sent for sequencing to Laval University, Quebec. T_3 and T_7 primers were used to sequence the full gene. T_3 primer was used for the *Sma*I subclone and T_7 primer for the *Hin*cII subclone.

Sequencing primers

5' taaccctcactaaaggg 3' : T_3 primer

5' gccctatagtgagtcgtattac 3': T_7 primer

16S rRNA gene sequence comparisons

The 16S rRNA gene sequence of the strain BH1 was compared with that of other bacteria using BLASTn provided by the National Centre for Biotechnology (NCBI, 1988). DNA Strider was used to obtain the restriction map of the sequence.

2.7 Hydrocarbon degradation

The ability of the strain BH1 to degrade hydrocarbons found in crude oil was tested using Bushnell Haas (BHS) medium (DIFCO Laboratories, Detroit; Appendix A), since it contains all the nutrients required for bacterial growth except the carbon source.

Media for crude oil experiments

Santa Barbara crude oil (Caleb Brett, Dartmouth) (density 813.5 Kg/m^3) was used for testing the hydrocarbon degradation capacity of strain BH1. The oil was sterilized by autoclaving at 121 °C for 15 min. Two concentrations - 0.1 % and 0.4 % (w/v) - of the oil were prepared in BHS broth. Oil at a concentration of 0.25 % (w/v) was added to sterilized sea water as the third test concentration.

Degradation experiments

0.4 ml each, of 24 h cultures grown in Marine broth, were inoculated into two 250 ml erlenmeyer flasks containing 50 ml of BHS each and, 0.06 ml and 0.2 ml of Santa Barbara crude oil, respectively. Strain BH1 cell suspension (0.4 ml) was also inoculated into an erlenmeyer flask containing 50 ml of sterilized seawater and 0.1 ml of crude oil. Table 2 shows the concentrations of different components in the samples. All the flasks were incubated at 27 °C and placed on a shaker agitated at 150 rpm. Sterile flasks incubated under identical conditions were used as controls to monitor changes in oil due to physical and chemical processes. Two more controls with strain BH1 cell suspensions, one in BHS media and one in sterilized seawater, were set up to monitor the growth of the strain BH1 in the absence of oil. The experiments were run in triplicate.

Bacterial growth measurements

Bacterial growth was monitored by measuring OD at 660 nm using the 4040, Novaspec II spectrophotometer. BHS medium appears slightly brownish and absorbs near the blue end of the visible spectrum. Growth was measured on day 1, 4, 7, 10 and 12. Growth of

strain BH1 under test conditions was used as an indicator of its capacity to degrade oil as no other source of carbon was added to the medium.

Different dilutions (1:16, 1:8, 1:4, 1:2, 1:1) of a 48 h culture of strain BH1, grown in Marine broth at 27 °C, were made and their OD was measured at 660 nm. Plate counting was done for the dilutions to obtain the number of cells/ml.

Table 2: Concentration of the different components in the experimental samples

Contents / Concentration	BHS (ml)	Seawater (ml)	Strain BH1 sample (ml)	Crude oil (ml)
Control 1 (Blank)	50	-	-	-
Control 1	50	-	0.4	-
Test 1 (Blank)	50	-	-	0.06
Test 1	50	-	0.4	0.06
Test 2 (Blank)	50	-	-	0.2
Test 2	50	-	0.4	0.2
Control 2 (Blank)	-	50	-	-
Control 2	-	50	0.4	-
Test 3 (Blank)	-	50	-	0.1
Test 3	-	50	0.4	0.1

2.8 Corrosion of metal coupons

The ability of strain BH1 to influence the corrosion of mild steel was tested to determine if it was involved in microbially influenced corrosion.

Metal coupon preparation

Mild steel (1018/1020) coupons of 2 cm^2 surface area and 0.2 cm thickness were cut from a plate. The average weight of the coupons was 3.3 - 3.5 g. A small hole was made in the top centre of each coupon to help suspend them in the flasks. The coupons were polished using 240 grit, 400 grit and 600 grit sandpaper, and degreased using acetone. All the

coupons were dried and weighted. The coupons were rewashed with acetone and sterilized with 95 % ethanol before being suspended into flasks using a copper wire.

Experimental setup

To analyse the influence of physicochemical factors on corrosion of the coupons, the samples were setup as in Table 3. Erlenmeyer flasks (250 ml) filled with 125 ml of Marine broth were autoclaved. The coupons were suspended into the flasks using insulated copper wire, ensuring that the coupons were completely immersed in the Marine broth. Ten microliters of 24 - 48 h cultures of the strain BH1 were inoculated into the appropriate flasks. Based on preliminary experiments a bigger inoculum volume resulted in a very rapid growth. The flasks were incubated at appropriate temperatures (27 ^{0}C and 5 ^{0}C), in high (5 mg/l) and low (2 mg/l) dissolved oxygen environments, and under static or agitated conditions. For low dissolved oxygen conditions, flasks were placed in candelabra jars and a candle was lit to use up the oxygen in the jars. For testing the effect of agitation on corrosion, the flasks were placed on a low speed (100 rpm) shaker. Multiple samples were setup for each point per replicate.

Table 3: Experimental runs at different temperatures, high and low dissolved oxygen, static and agitated conditions

Sample	Coupon	Marine broth	Strain BH1	Temperature (^{o}C)	Motion	Dissolved Oxygen
Control 1	-	125 ml	-	27	100 rpm	5 mg/l
Control 2	-	125 ml	10 µl	27	100 rpm	5 mg/l
Test 1	600	125 ml	-	27	100 rpm	5 mg/l
Test 2	600	125 ml	10 µl	27	100 rpm	5 mg/l
Control 3	-	125 ml	10 µl	27	Static	5 mg/l
Test 3	600	125 ml	-	27	Static	5 mg/l
Test 4	600	125 ml	10 µl	27	Static	5 mg/l
Control 4	-	125 ml	10 µl	27	Static	2 mg/l
Test 5	600	125 ml	-	27	Static	2 mg/l
Test 6	600	125 ml	10 µl	27	Static	2 mg/l
Control 5	-	125 ml	10 µl	5	Static	5 mg/l
Test 7	600	125 ml	-	5	Static	5 mg/l
Test 8	600	125 ml	10 µl	5	Static	5 mg/l

To analyse the effect of surface roughness on the rate and type of corrosion, the samples were setup as in Table 4. Three types of coupons were used

a) polished, consecutively with 240, 400 and 600 grit sandpaper
b) polished with 240 grit sandpaper
c) unpolished

The flasks were incubated at 27 ^{0}C in an aerobic environment on a low speed (100 rpm) shaker.

Table 4: Experimental setup for testing the effect of surface roughness

Sample	Coupon	Marine broth	Strain BH1
Test 1a	600[a]	125 ml	-
Test 1b	600[a]	125 ml	10 µl
Test 2a	240[b]	125 ml	-
Test 2b	240[b]	125 ml	10 µl
Test 3a	unpolished[c]	125 ml	-
Test 3b	unpolished[c]	125 ml	10 µl
Control 1	-	125 ml	-
Control 2	-	125 ml	10 µl

[a] polished consecutively with 240, 400 and 600 grit sandpaper
[b] polished with 240 grit sandpaper
[c] unpolished original surface

Observations

The coupons were removed after 3, 7, 11 and 22 days of testing. Growth of strain BH1 was monitored by reading OD at 660 nm using the 4040, Novaspec II spectrophotometer. The metal coupons were observed visually to note the extent and colour of the corrosion products. Photographs were taken to maintain a record of the changes. The coupons were washed with abundant water, air dried and weighted to calculate the corrosion rate weight loss. E3 ElectroScan ESEM (ElectroScan, Massachusetts), operating at a pressure of 1 – 2 Torr, was used to observe the surface features of the metal coupons and crystal structures of the corrosion products. Energy dispersive X-ray spectrometer (EDS), attached to the ESEM, was used to determine the elemental composition of the corrosion

products, formed on the metal coupons. Gram staining was done to ensure that there was no contamination. The tests were carried out in triplicate, i.e., the weight loss is listed as an average of three specimens studied under identical experimental conditions.

3. RESULTS

3.1 Characterisation of strain BH1

Colony characteristics

On Marine agar, circular, smooth surfaced, raised, off-white, opaque and glistening colonies were produced. In Marine broth, cells grew both on the surface of the media and at the bottom of the tube. Strain BH1 showed slower growth, under low dissolved oxygen conditions, created in the candelabra jars. On Triple Sugar Iron agar, strain BH1 produced smooth surfaced, raised, reddish-brown, translucent and glistening colonies.

Staining reactions

Negative staining illustrated clear rod shaped cells, against a purple background. Both long and short rod forms were seen. The cells turned pink in color after Gram staining indicating a Gram-negative response. They ranged in size from 2 - 6 μm in length to 0.5 – 0.8 μm in width.

3.2 Physicochemical and biochemical growth factors

pH range

Strain BH1 showed growth in the pH range from 6.0 – 9.0. There was no growth at pH 4.0 and 5.0. The maximum growth rates at the pH tested were observed at pH 8.0 and 9.0 (Figure 3.1).

Temperature range

Strain BH1 showed growth in the temperature range from 4 °C to 37 °C. The maximum growth rates at the temperatures tested was seen at 27 °C (Figure 3.2).

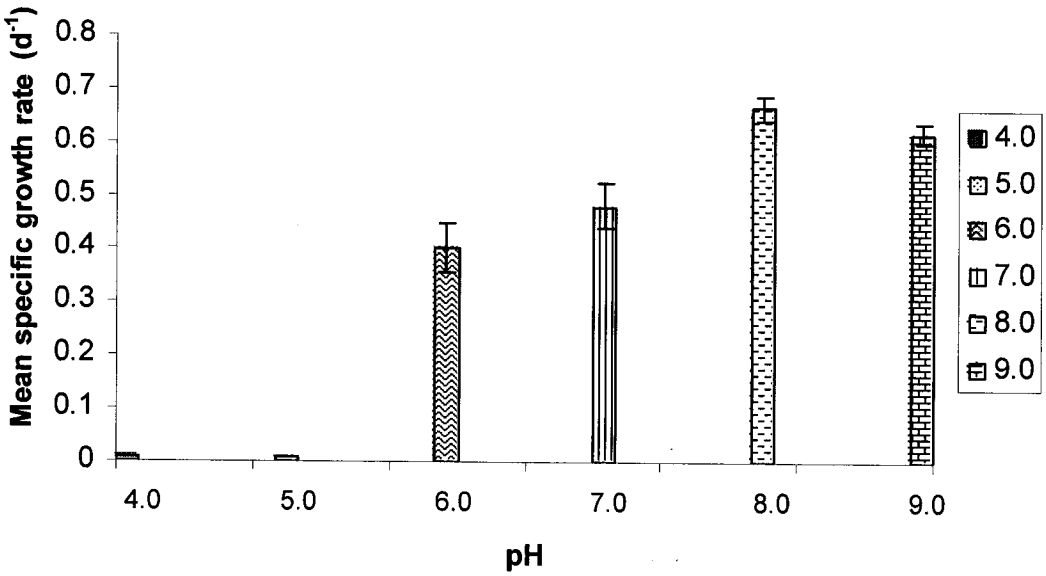

Figure 3.1 Relationship between pH and growth rate of strain BH1.

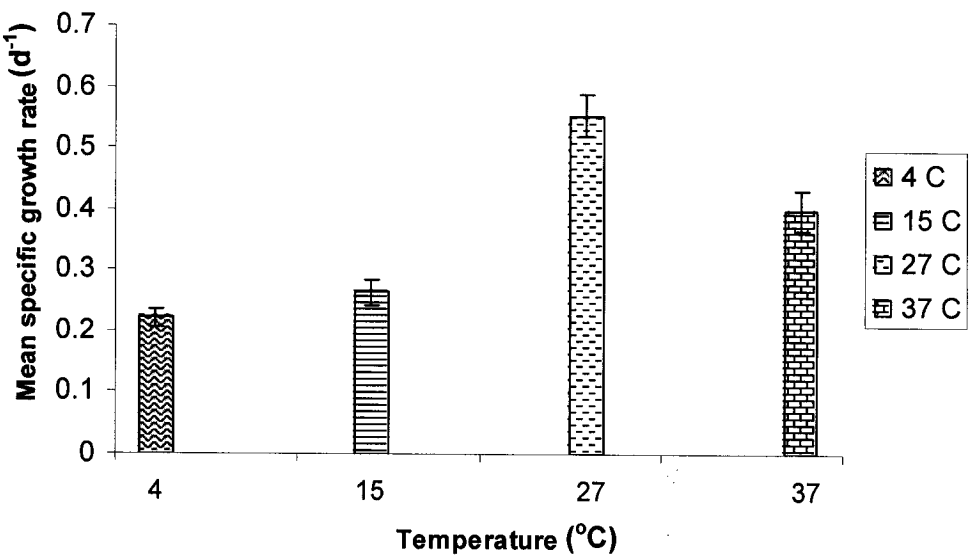

Figure 3.2 Relationship between temperature and growth rate of strain BH1.

Salt tolerance range

Strain BH1 showed growth at NaCl concentrations of 0.26 %, 2.2 %, 8.0 %, 14.5 % and 20.0 % (wt/vol). There was no growth at 32.0 % NaCl. Even at 20.0 % NaCl, the specific growth rate was very low (Figure 3.3). The maximum growth rate at the NaCl concentrations tested was seen at NaCl concentration of 8.0 % (wt/vol).

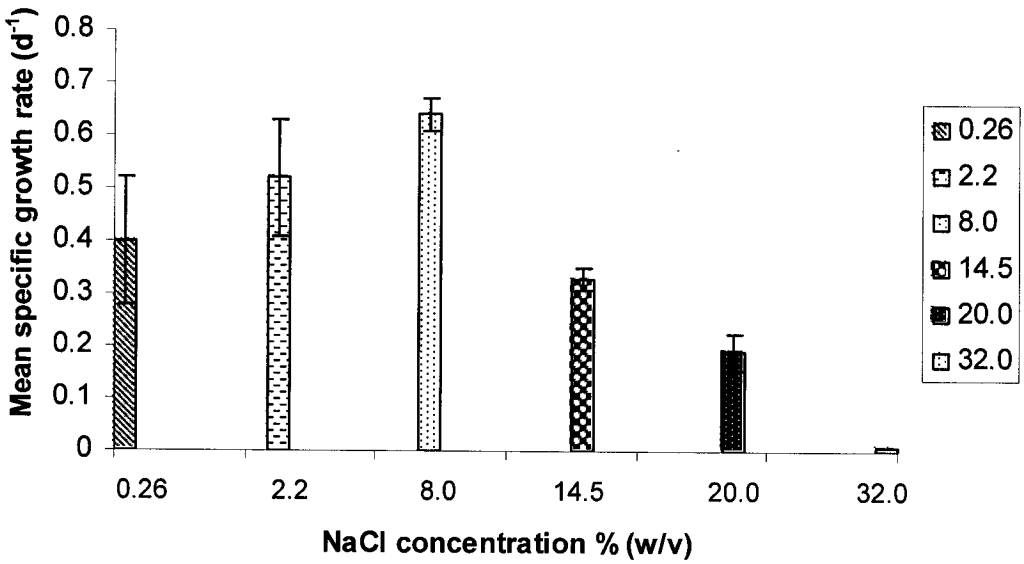

Figure 3.3 Relationship between salt concentration and growth rate of strain BH1.

Biochemical tests

The biochemical profile of strain BH1 is listed in Tables 5, 6 and 7. It was found to be catalase and oxidase positive; methyl red and urease negative. It was unable to grow on starch, sucrose, mannitol, inositol, sorbitol, rhamnose, amygdalin, arabinose, erythritol, adonitol, B-methyl-xyloside, dulcitol, a-methyl-D-mannoside, a-methyl-D-glucoside, esculin, salicin, lactose, maltose, trehalose, inulin, glycogen, and 2-keto-gluconate. It was able to utilize glucose, arginine, citrate, melibiose, ribose, L-arabinose, D-xylose, galactose, D-fructose, D-mannose, and D-fucose.

Table 8 shows the fatty acid profile of strain BH1 in TSA. The major fatty acids were $C_{16:0}$, $C_{18:1}\omega7c$ and $C_{15:0}$ Iso 2OH and/or $C_{16:1}$ $\omega7c$. The results of MIDI fatty acid analysis were used for comparison of strain BH1 against the strains in the MIDI Microbial Identification System library. It showed a 0.841 similarity index with *Pseudomonas putida* biotype A (Table 9). The high value of the similarity index indicated that it was a good library comparison. But the library did not contain any strains of the genus *Halomonas*.

Table 5: Results of the Api 20E test kit

Test	24 hr Result	48 hr Result
ONPG	-	-
Arginine	+	+
Lysine	-	-
Ornithine	-	-
Citrate	+	+
Urease	-	-
TDA	-	-
Indole	-	-
Voges-Prokauser	-	-
Gelatinase	-	-
Glucose	-	+
Mannitol	-	-
Inositol	-	-
Sorbitol	-	-
Rhamnose	-	-
Sucrose	-	-
Melibiose	-	+
Amygdalin	-	-
Arabinose	-	-
Oxidase	+	+

Table 6: Results of the Api 50CH test kit

Test	Result
Glycerol	+
Erythritol	-
D-Arabinose	borderline
L-Arabinose	+
Ribose	+
D-Xylose	+
L-Xylose	borderline
Adonitol	-
B-Methyl-xyloside	-
Galactose	+
Glucose	+
D-Fructose	+
D-Mannose	+
L-Sorbose	-
Rhamnose	borderline
Dulcitol	-
Inositol	-
Mannitol	-
Sorbitol	-
a-Methyl-D-mannoside	-
a-Methyl-D-glucoside	-
N-Acetyl-glucosamine	-
Amygdalin	-
Arbutine	-
Esculin	-
Salicin	-
Cellobiose	borderline
Maltose	-
Lactose	-
Melibiose	+
Sucrose	-
Trehalose	-
Inulin	-
Melezitose	-
D-Raffinose	-
Starch	-
Glycogen	-
Xylitol	-
B-Genitiobiose	borderline
D-Turanose	-
D-Lyxose	borderline

Table 6: Results of the Api 50CH test kit (continued)

Test	Result
D-Tagatose	-
D-Fucose	+
L-Fucose	-
D-Arabitol	-
L-Arabitol	-
Gluconate	-
2-Keto-Gluconate	-
5-Keto-Gluconate	-

Table 7: Results of additional biochemical tests

Test	Result
Catalase	+
Methyl Red	-
Nitrate	-

Table 8: Cellular fatty acid profile of strain BH1 in TSA

Fatty Acid	Percentage composition
$C_{10:0}$ 3OH	2.84
$C_{12:0}$	1.64
$C_{12:0}$ 2OH	5.13
$C_{12:1}$ 3OH	0.17
$C_{12:0}$ 3OH	3.78
$C_{14:0}$	0.28
$C_{15:0}$	0.22
$C_{16:0}$	27.65
$C_{17:0}$ Iso	0.13
$C_{17:1}$ ω8c	0.20
$C_{17:0}$ Cyclo	5.60
$C_{17:0}$	0.28
$C_{18:1}$ ω7c	23.72
$C_{18:0}$	0.51
$C_{19:0}$ Cyclo ω8c	0.35
*Summed feature 3	27.50

*Summed feature represents $C_{15:0}$ Iso 2OH and/or $C_{16:1}$ ω7c that could not be separated by GLC with the MIDI system.

Table 9: MIDI Similarity Index table

MIDI similarity index table	Organism
Pseudomonas putida biotype A	0.841

3.3 Ultrastructure of strain BH1

At low magnification transverse, oblique and longitudinal cross sections of the cells in Marine and Triple Sugar Iron broth (Figure 3.4) could be seen. Rod-shaped cells varying in size from 2 - 5 μm in length and 0.5 – 0.7 μm in width were visible. The cells were more elongated in Triple Sugar Iron broth than in Marine broth, some reaching lengths > 6 μm.

Three distinct layers were visible in the cell envelope (Figure 3.5). The outermost layer, outer membrane (OM) was electron dense and double layered, varying between 8 - 10 nm in thickness. On the inner side of the outer membrane was a thick (16 - 20 nm) lightly stained layer, the periplasmic space (PS). The innermost layer, cell membrane (CM) was again electron dense. It varied in size from 13 - 15 nm. These three layers are typical of Gram-negative cell wall structure.

The nucleoid region (NR) appeared as a lightly stained region (Figure 3.6). It was not restricted to the center of the cell but was scattered in the cytoplasm. Dense and thin fibrils were seen in this region and may represent the DNA. Ribosomes (R) were observed as dark almost circular spots spread throughout the cytoplasm. The size of these ribosomes ranged from 14 - 18 nm.

Figure 3.7 shows two cells, which were in the process of cell division. The cell undergoing division was elongated along the longitudinal axis and showed two distinct nucleoid regions. Large number of ribosomes were visible in the cytoplasm. Cell division seemed to occur via transverse fission; invagination of the cell envelope appeared to start near the center of the cell and proceeded inwards.

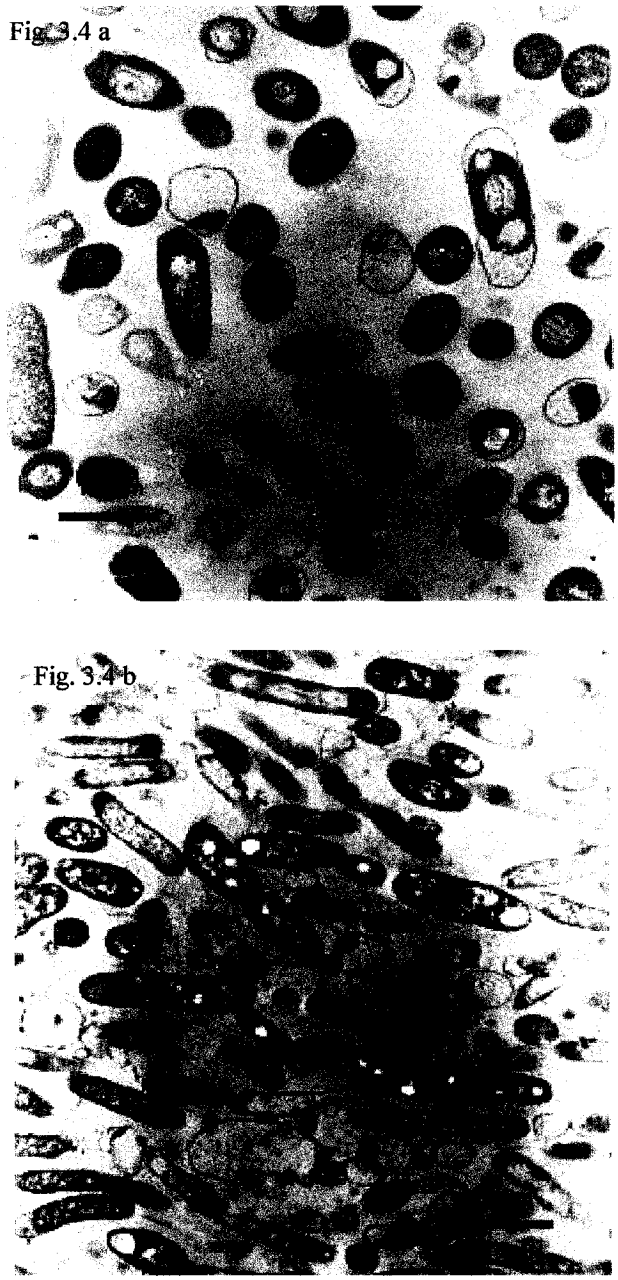

Figure 3.4 Low magnification micrographs of thin sections showing transverse, oblique and longitudinal views of strain BH1 cells in: (a) Marine broth, and (b) Triple Sugar Iron broth.

Fig. 3.5

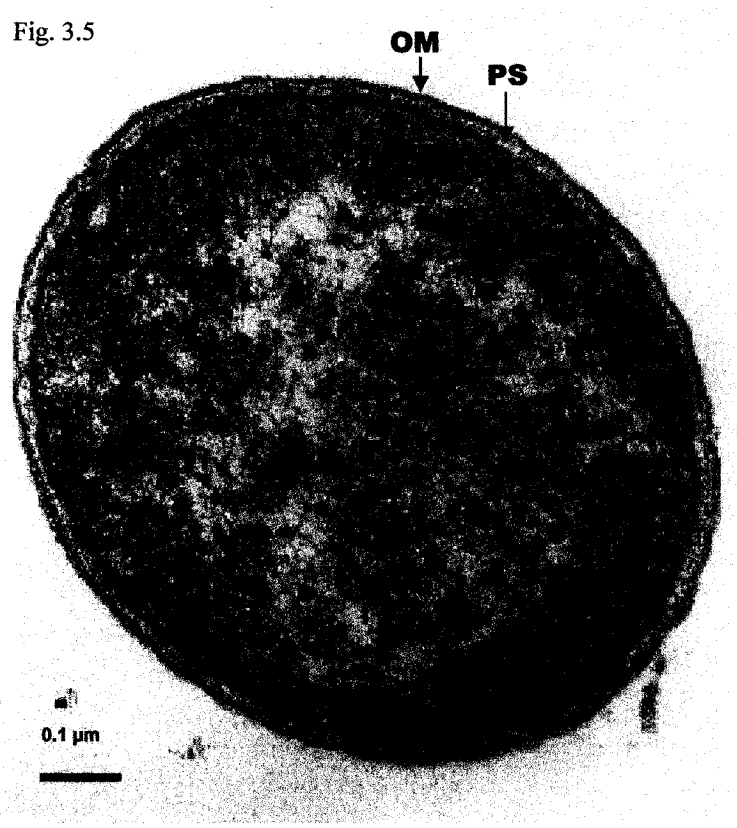

Figure 3.5 Thin section of strain BH1 cell showing three distinct layers of the cell envelope: dense outer membrane [OM], middle light zone periplasmic space [PS] and inner dense cell membrane [CM].

Fig. 3.6

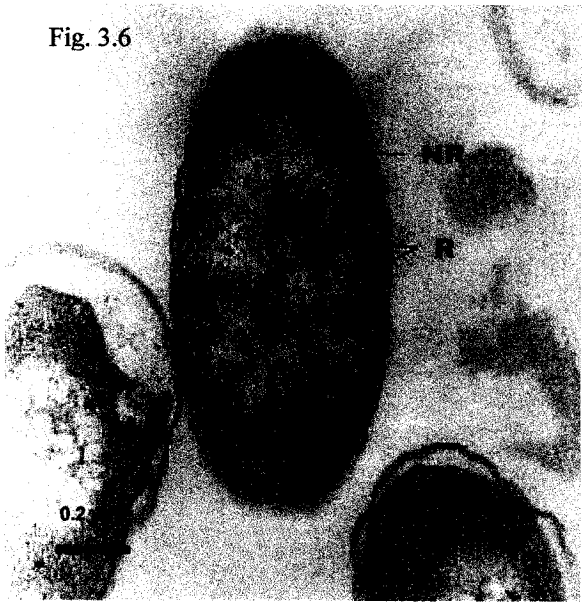

Fig. 3.7 a

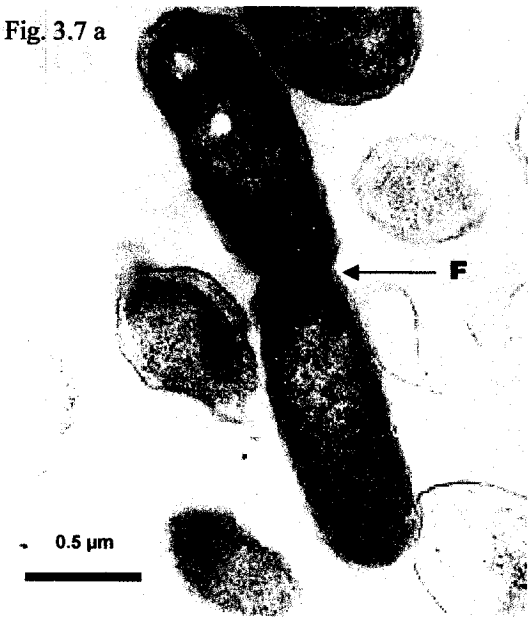

Fig. 3.7 b

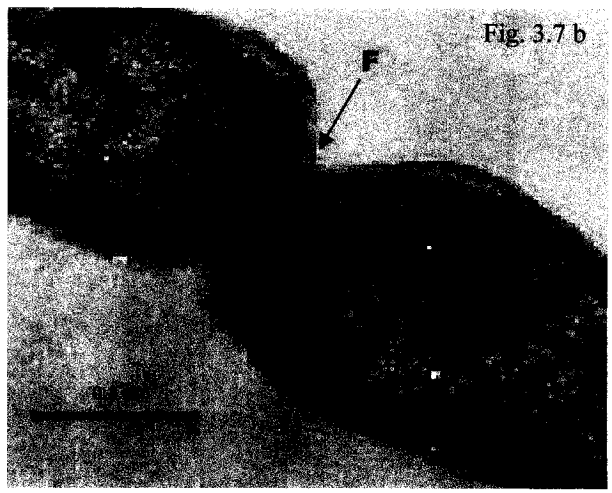

Figure 3.6 Cross section revealing the lightly stained nucleoid region [NR]; the nucleoplasm contains dense thin DNA fibrils and cytoplasm contains numerous ribosomes [R].

Figure 3.7 Thin-sections showing cells undergoing division; note the furrowing [F] of cell envelope.

Large number of membrane-bound, translucent (low electron density), circular, vacuole-like inclusions were seen in cells grown in Triple Sugar Iron Agar (Figures 3.8 a). No such inclusions were visible in Marine-media grown cells. However, some cells in Marine media had a single darkly stained inclusion of circular or ellipsoid contour that was polarly located within the cell (Figures 3.8 b and c). These may be some kind of volutin granules composed of polyphosphate or poly-β-hydroxy butyrate.

Negative staining

Negative staining illustrated the presence of flagella in strain BH1 (Figure 3.9). Varying numbers of flagella (2 - 6) were found on the cells. The flagella were 9 - 12 μm in length and 15 - 18 nm in diameter (Figure 3.10). These flagella were unsheathed. Some of the flagella had detached, lying freely in the stain. Very few of the cells grown in Triple Sugar Iron Agar showed flagella.

At higher magnification, the points of origin of the flagella were observed (Figure 3.11) and it was found that these were not restricted to any particular region of the cell. They appeared to arise from lateral and polar ends of the cell, i.e. they were peritrichous.

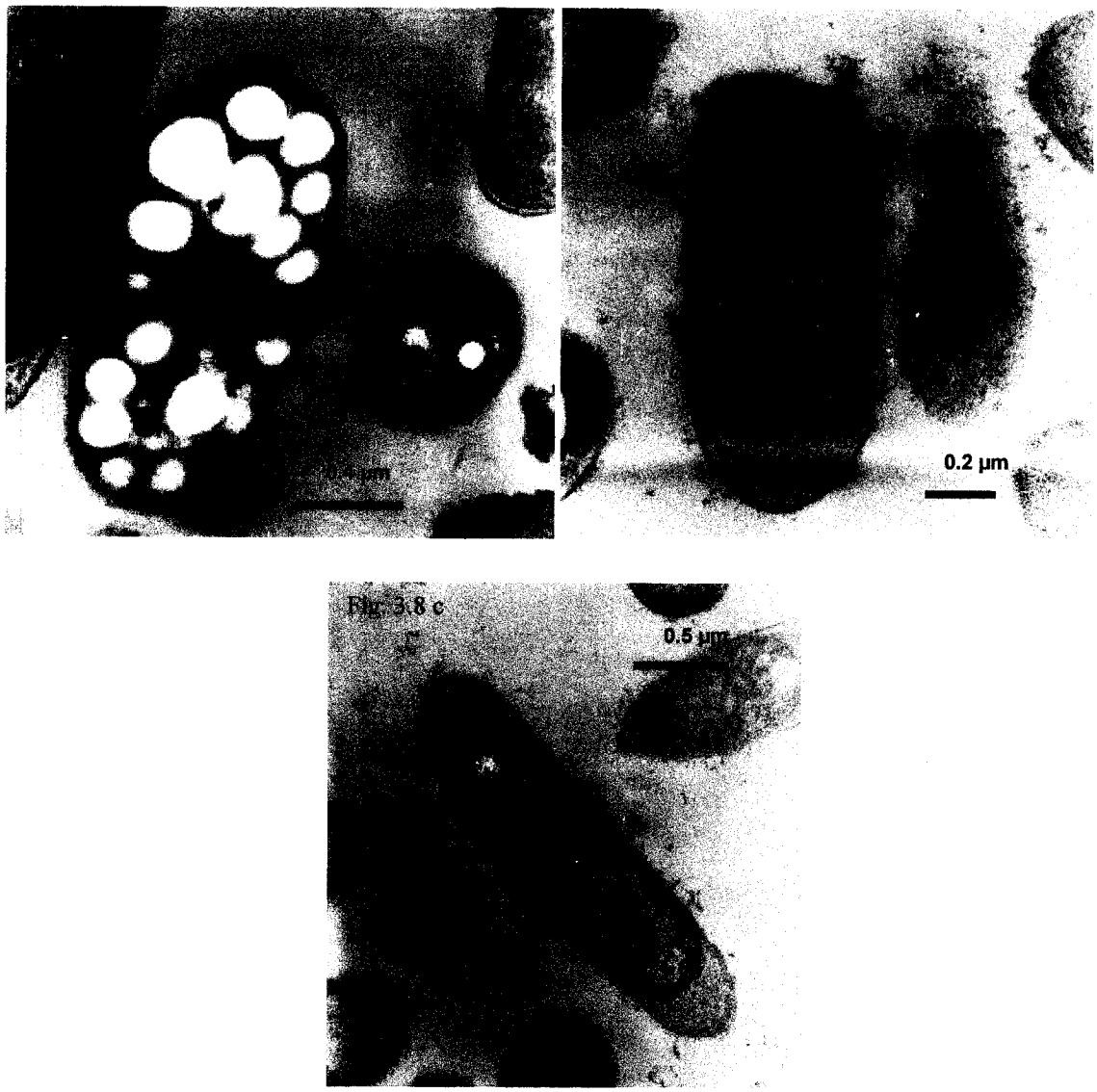

Figure 3.8 (a) Low electron-density, membrane-bound, vacuole-like inclusions visible in the cytoplasm of the cells grown in Triple Sugar Iron agar, (b) and (c) Marine media grown cells did not show such inclusions. However, a single inclusion with an electron dense membrane was found polarly located in these cells.

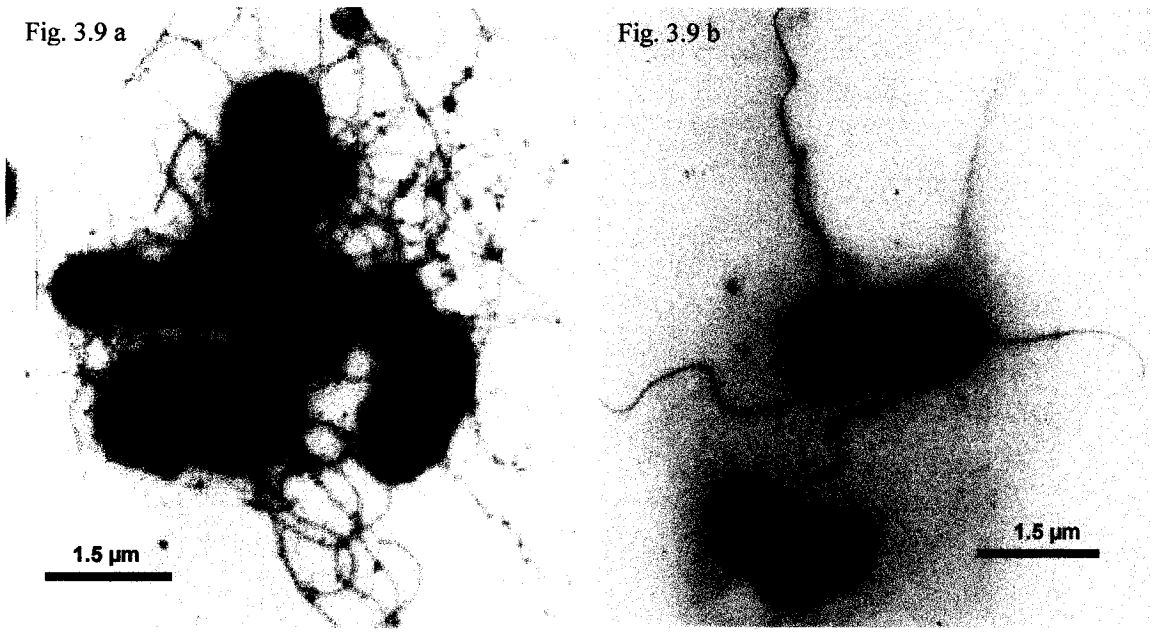

Figure 3.9 Negatively stained (uranyl acetate) cells showing flagellar arrangements. (a) Marine broth grown cells, and (b) Triple Sugar Iron broth grown cells.

Fig. 3.10 a

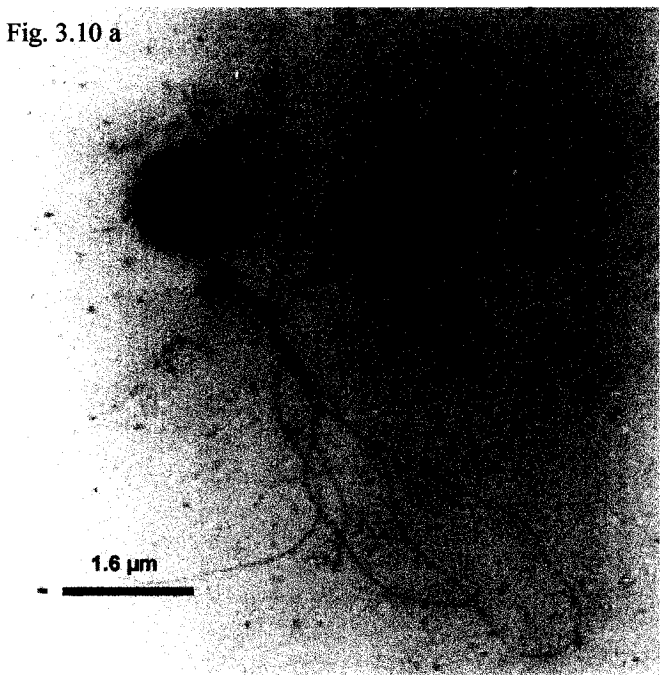

Fig. 3.10 b

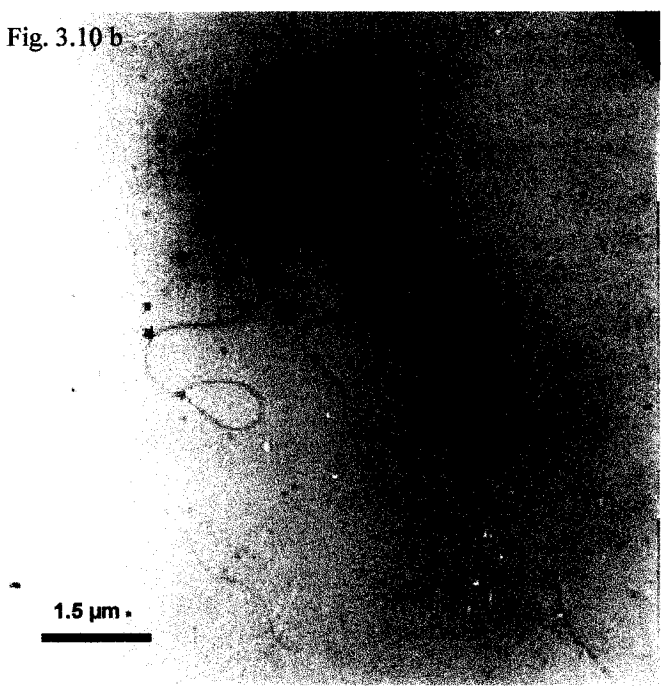

Figure 3.10 Negatively stained cells show varying numbers of unsheathed flagella, between 2 - 6. Length of flagella range from 9-12 µm and diameter from 15 - 18 nm.

Fig. 3.11a

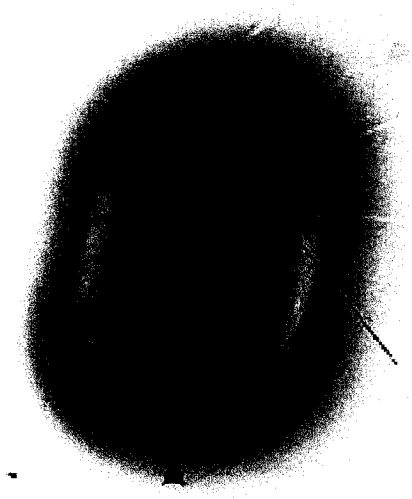

Fig. 3.11 b

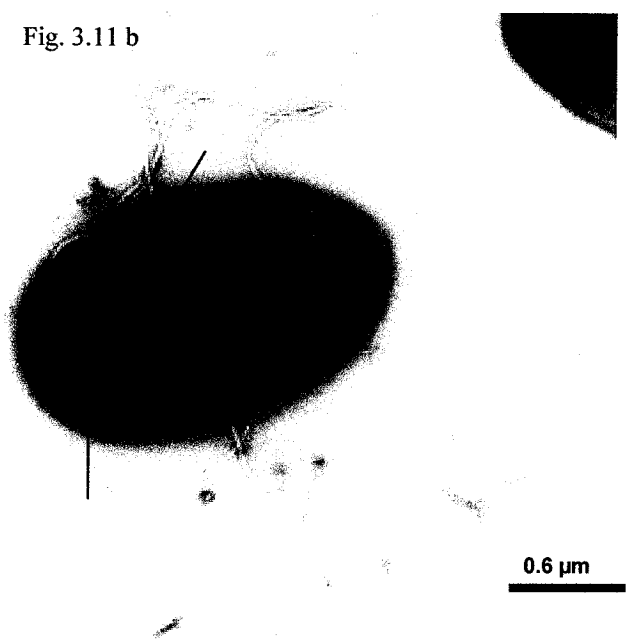

Figure 3.11 High magnification micrographs of negatively stained cells showing points of origin of the flagella (←). Both polar and lateral origin points indicate peritrichous flagella.

3.4 Genetic analysis

PCR product

A 1.6 Kb PCR product (Figure 3.12) was obtained after isolating and amplifying the 16S rRNA gene, using appropriate primers, as defined by Edwards *et al.* (1989). This is the approximate size of the 16S rRNA gene (Edwards *et al.*, 1989). After ligating the PCR product with the plasmid pBS - which runs as a 3 Kb fragment on an agarose gel - and transforming it, 14 transformants were obtained (Figure 3.13). The total size of the ligated plasmid should be approximately 4.6 Kb. But nicked linear fragments run as higher Kb fragments. So, the plasmids from all the transformants, which showed fragments bigger than 4.0 Kb: 1, 2, 8, 10, 13, were restriction digested and run on an agarose gel (Figure 3.14). Transformant 8 showed the correct size fragments after restriction: a 3.0 Kb plasmid fragment and a 1.6 Kb 16S rRNA gene fragment.

Sub clones

The pBS plasmid was then restriction digested with different RE's to test if there were RE cutting sites on it. *Sma*I and *Hin*cII showed cutting sites on the pBS plasmid. The plasmid from transformant 8, which contains the 16S rRNA gene fragment, was then digested with the two RE's *Sma*I and *Hin*cII, separately. Figure 3.15 illustrates the cutting sites for *Sma*I and *Hin*cII in the plasmid from the original transformant 8 that contains the full 16S rRNA gene.

Figure 3.16 shows the fragments obtained after the plasmid from the original transformant 8 was digested with *Sma*I and *Hin*cII. The larger fragments: 3.7 Kb for the *Hin*cII digest and 3.6 Kb fragment for *Sma*I digest, were then ligated and transformed. Twenty transformants for *Sma*I subclone and fifteen transformants for the *Hin*cII subclone were obtained. Of these, the plasmids from six transformants gave fragment sizes greater than 3.5 Kb when digested with *Sma*I for the *Sma*I subclone and six plasmids gave fragment sizes greater than 3.5 Kb when digested with *Hin*cII for the

Fig. 3.12

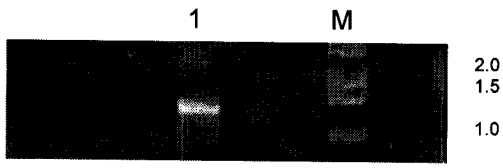

Fig. 3.13

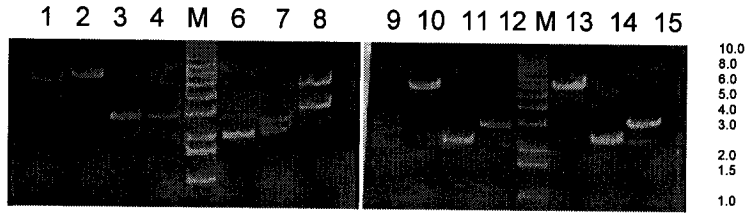

Fig. 3.14

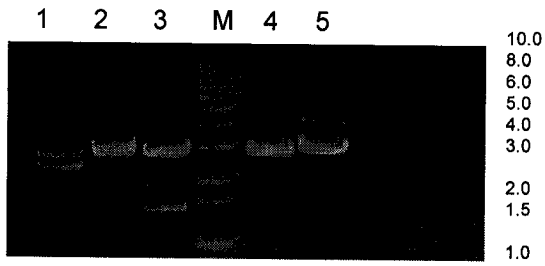

Figure 3.12 PCR mediated synthesis of the 16S rRNA gene of the strain BH1 using primers. Lane 1 shows a 1.6 Kb DNA fragment. Lane M shows the molecular weight marker, which is the 1 Kb ladder.

Figure 3.13 Plasmids from transformants that were obtained after ligating the 1.6 Kb DNA gene fragment to the pBS plasmid (3.0 Kb). Transformants in lanes 1, 2, 8, 10 and 13 show fragment sizes greater than 4.5 Kb. Lanes M indicate molecular weight markers, which are the 1 Kb ladders.

Figure 3.14 DNA fragments obtained after restriction digesting transformants 1, 2, 8, 10 and 13, in lanes 1, 2, 3, 4 and 5 respectively, with *Pst*I and *Hin*dIII. Plasmid from transformant 8 in lane 3 shows the appropriate 3.0 Kb and 1.6 Kb fragment sizes. Lane M shows the molecular weight marker, which is the 1 Kb ladder.

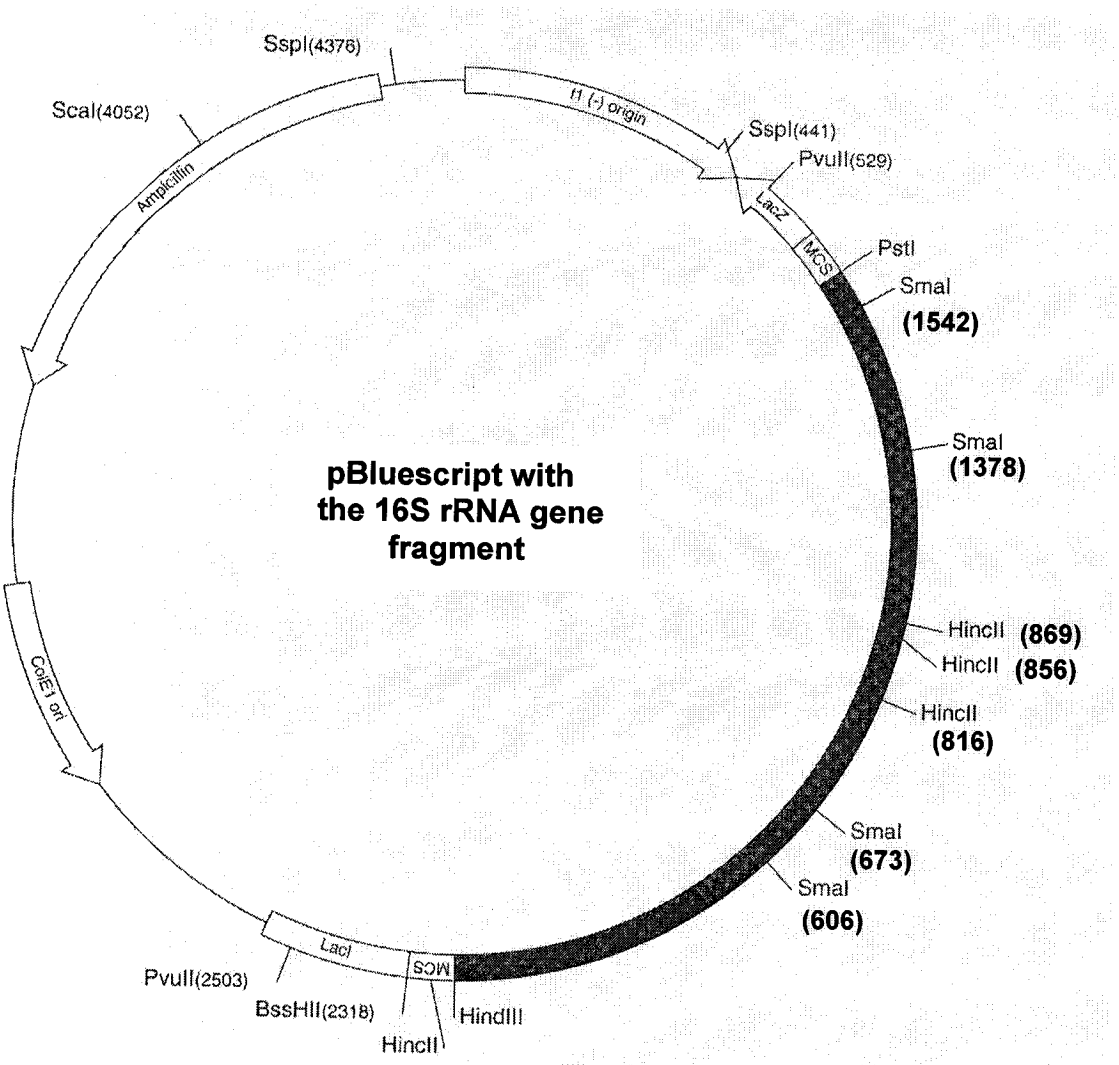

Figure 3.15 Illustration showing the cutting sites for *Sma*I and *Hinc*II in the recombinant plasmid from the transformant 8 that contains the dark insert representing the almost complete 16S rRNA gene fragment. The numbers are the cutting sites on the plasmid based on *E. coli* numbering.

Fig. 3.16

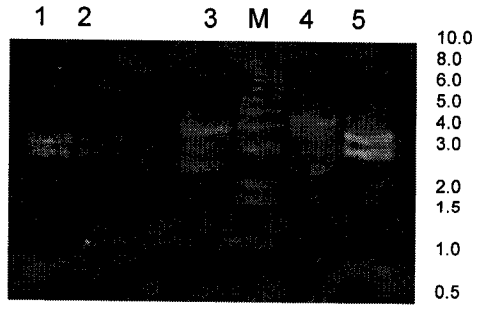

Fig. 3.17

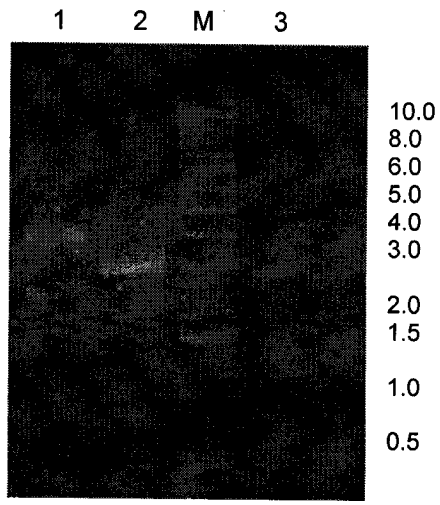

Figure 3.16 DNA fragments obtained after digesting the plasmid, obtained from transformant 8, with *Sma*I (lanes 1and 2) and *Hin*cII (lanes 4 and 5). One of the *Hin*cII cuts did not work (lane 4). Lane 3 contains the uncut plasmid. The larger fragments: 3.7 Kb for the *Hin*cII digest and 3.6 Kb fragment for *Sma*I digest, were then ligated and transformed. Lane M shows the molecular weight marker, which is the 1 Kb ladder.

Figure 3.17 DNA fragments obtained when the plasmid from transformant 8 was digested with *Sma*I and *Hin*dIII (lane 2), and *Hin*cII and *Pst*I (lane 3). Lane 1 contains the uncut plasmid. Lane M shows the molecular weight marker, which is the 1 Kb ladder.

*Hin*cII subclone. Figure 3.17 shows the fragments obtained when the plasmid from the original transformant 8 that contains the full 16S rRNA gene was digested with *Sma*I and *Hin*dIII, and *Hin*cII and *Pst*I respectively.

Transformants 13 and 14 had the right fragment sizes for the *Sma*I subclone: 3.0 Kb pBS fragment and 0.6 Kb 16S rRNA gene fragment. Of the *Hin*cII subclones, transformant 10 had the plasmid with the right insert: 3.0 Kb pBS fragment and 0.7 Kb 16S rRNA gene fragment.

The plasmids from the three transformants: plasmid from transformant 8 with the full 16S rRNA gene, plasmids from transformants 14 and 10 with a portion of the16S rRNA gene (subclones), were purified using the QIAGEN spin prep Mini prep kit and their concentrations estimated with a double-stranded DNA standard (0.2 μg/μl):
Plasmid from transformant 8: 800 ng/μl
Plasmid from transformant 14: 1600 ng/μl
Plasmid from transformant 10: 1280 ng/μl

At Laval University, they were sequenced:
Plasmid from transformant 8: sequenced using T_3 and T_7 primers
Plasmid from transformant 14: sequenced using T_3 primer
Plasmid from transformant 10: sequenced using T_7 primer

The gene sequence obtained is shown in Figure 3.18. It was compared with the 16S rRNA gene sequences of other bacteria using nucleotide-nucleotide BLAST (blastn) available on the National Centre of Biotechnology Information website (NCBI, 1988). The comparison yielded closest matches with *Halomonas* species. The highest similarity was with *Halomonas variabilis* (98 %). This indicates that strain BH1 is a member of the family *Halomonadaceae*, belonging to genus *Halomonas*.

*Hin*dIII
taagcttagagtttgatcctggctcagattgaacgctggcggcaggcctaacacatgcaagtcgagcggtaacag base pairs
attcgaatctcaaactaggaccgagtctaacttgcgaccgccgtccggattgtgtacgttcagctcgccattgtc 1 to 75

gggtagcttgctacccgctgacgagcggcggacgggtgagtaatgcataggaatctgcccgatagtgggggataa base pairs
cccatcgaacgatgggcgactgctcgccgcctgcccactcattacgtatccttagacgggctatcacccctatt 76 to 150

cctggggaaacccaggctaataccgcatacgtcctacgggagaaaggggcttcggctcccgctattggatgagc base pairs
ggacccctttgggtccgattatggcgtatgcaggatgccctctttcccccgaagccgagggcgataacctactcg 151 to 225

ctatgtcggattagctagttggtgaggtaatggctcaccaaggcaacgatccgtagctggtctgagaggatgatc base pairs
gatacagcctaatcgatcaaccactccattaccgagtggttccgttgctaggcatcgaccagactctcctactag 226 to 300

agccacatcgggactgagacacggcccgaactcctacgggaggcagcagtggggaatattggacaatgggggcaa base pairs
tcggtgtagccctgactctgtgccgggcttgaggatgccctccgtcgtcacccctataacctgttacccccgtt 301 to 375

ccctgatccagccatgccgcgtgtgtgaagaaggccctcgggttgtaaagcactttcagcgaggaagaacgccta base pairs
gggactaggtcggtacggcgcacacacttcttccgggagcccaacatttcgtgaaagtcgctccttcttgcggat 376 to 450

tcggttaatacccggtaggaaagacatcactcgcagaagaagcaccggctaactccgtgccagcagccgcggtaa base pairs
agccaattatgggccatcctttctgtagtgagcgtcttcttcgtggccgattgaggcacggtcgtcggcgccatt 451 to 525

tacggagggtgcaagcgttaatcggaattactgggcgtaaagcgcgcgtaggtggcttgataagccggttgtgaa base pairs
atgcctcccacgttcgcaattagccttaatgacccgcatttcgcgcgcatccaccgaactattcggccaacactt 526 to 600

agccccgggctcaacctgggaacggcatccggaactgtcaggctagagtgcaggagaggaaggtagaattcccgg base pairs
tcggggcccgagttggacccttgccgtaggccttgacagtccgatctcacgtcctctccttccatcttaagggcc 601 to 675

ntgtagcggtgaaatgcgtagagatcgggaggaataccagtggcgaaggcggccttctggactgacactgacact base pairs
nacatcgccactttacgcatctctagccctccttatggtcaccgcttccgccggaagacctgactgtgactgtga 676 to 750

gaggtgcgaaagcgtgggtagcaaacaggattagataccctggtagtccaccccgtaaacgatgtcgaccagccg base pairs
ctccacgctttcgcacccatcgtttgtcctaatctatgggaccatcaggtggggcatttgctacagctggtcggc 751 to 825

ttgggtgcctagagcactttgtggcgaagttaacgcgataagtcgaccgcctggggagtacggccgcaaggttaa base pairs
aacccacggatctcgtgaaacaccgcttcaattgcgctattcagctggcggacccctcatgccggcgttccaatt 826 to 900

aactcaaatgaattgacgggggcccgcacaagcggtggagcatgtggtttaattcgatgcaacgcgaagaacctt base pairs
ttgagtttacttaactgcccccgggcgtgttcgccacctcgtacaccaaattaagctacgttgcgcttcttggaa 901 to 975

acctacccttgacatctacagaagccggaagagattctggtgtgccttcgggaactgtaagacaggtgctgcatg base pairs
tggatgggaactgtagatgtcttcggccttctctaagaccacacggaagcccttgacattctgtccacgacgtac 976 to 1050

Figure 3.18 Nucleotide sequence of the 16S rRNA gene of strain BH1. Both strands are shown. The sequence comprises 1591 nucleotide bases. The red regions represent the primer sequences and the blue regions represent the cutting sites for *Hin*dIII and *Pst*I inserted into the primers.

```
gctgtcgtcagctcgtgttgtgaaatgttgggttaagtcccgtaacgagcgcaacccttgtccttatttgccagc base pairs
cgacagcagtcgagcacaacactttacaacccaattcagggcattgctcgcgttgggaacaggaataaacggtcg 1051 to 1125


gagtaatgtcgggaactctaaggagactgccggtgacaaaccggaggaaggtggggacgacgtcaagtcatcatg base pairs
ctcattacagcccttgagattcctctgacggccactgtttggcctccttccacccctgctgcagttcagtagtac 1126 to 1200


gcccttacgggtagggctacacacgtgctacaatggccggtacaaagggctgcgagctcgcgagagtcagcgaat base pairs
cgggaatgcccatcccgatgtgtgcacgatgttaccggccatgtttcccgacgctcgagcgctctcagtcgctta 1201 to 1275


cccttaaagccggtctcagtccggatcggagtctgcaactcgactccgtgaagtcggaatcgctagtaatcgtga base pairs
gggaatttcggccagagtcaggcctagcctcagacgttgagctgaggcacttcagccttagcgatcattagcact 1276 to 1350


atcagaatgtcacggtgaatacgttcccgggccttgtacacaccgcccgtcacaccatgggagtggactgcacca base pairs
tagtcttacagtgccacttatgcaagggcccggaacatgtgtggcgggcagtgtggtaccctcacctgacgtggt 1351 to 1425


gaagtggttagcctaacgcaagagggcgatcaccacggtgtggttcatgactggggtgaagtcgtaacaaggtag base pairs
cttcaccaatcggattgcgttctcccgctagtggtgccacaccaagtactgaccccacttcagcattgttccatc 1426 to 1500

                                  PstI
ccgtaggggaacctgcggctggatcacctccttctgcagcccgggggatccactagttctagagcggccgccacc base pairs
ggcatccccttggacgccgacctagtggaggaagacgtcgggccccctaggtgatcaagatctcgccggcggtgg 1501 to 1575


gcggtggagctccagc  base pairs
cgccacctcgaggtcg  1576 to 1591
```

Figure 3.18 Nucleotide sequence of the 16S rRNA gene of strain BH1. Both strands are shown. The sequence comprises 1591 nucleotide bases. The red regions represent the primer sequences and the blue regions represent the cutting sites for *Hin*dIII and *Pst*I inserted into the primers.

3.5 Hydrocarbon degradation

Crude oil degradation

Test 1: Strain BH1 cells in BHS medium with 0.1 % crude oil

Test 2: Strain BH1 cells in BHS medium with 0.4 % crude oil

Test 3: Strain BH1 cells in sterilized seawater with 0.2 % crude oil

Control 1 (blank): BHS medium

Control 2 (blank): Sterilized seawater

Control 1 (blank) was used to set reference for Test 1 and Test 2 and control 2 (blank) was used to set reference for Test 3. The OD of blank samples [Test 1(blank), Test 2 (blank) and Test 3 (blank)] was subtracted from OD of samples with strain BH1 [Test 1, Test 2 and Test 3] to account for the absorbance due to oil and also to account for loss of oil due to volatilization. Table 10 shows the mean OD for the test samples on different days.

Table 10: Mean OD of the test samples at 660 nm

Day / Samples	Day 1	Day 4	Day 7	Day 10	Day 12
Test 1	0.021	0.014	0.002	0.007	0.007
Test 2	0.017	0.017	0.046	0.041	0.006
Test 3	0.014	0.003	0.022	0.007	0.018

The increase in OD was used as an indicator of growth, which would have implied that the oil was being utilized by strain BH1 cells. But there was no significant increase in OD even after 12 days. Strain BH1 cells were still viable when transferred to Marine broth. To ascertain that the test media was not lacking in other essential nutrients, samples supplemented with varying concentrations of K_2HPO_4 and $(NH_4)_2SO_4$ were also run. Similar results were obtained, indicating that strain BH1 was unable to utilize the hydrocarbons in Santa Barbara crude oil for growth.

3.6 Corrosion of metal coupons

Quantitative analysis of the corrosion of metal coupons

Test 1: Coupon in aerobic agitated conditions at 27 ^{0}C without strain BH1 (sterile control)
Test 2: Coupon in aerobic agitated conditions at 27 ^{0}C with strain BH1

Figures 3.20 - 3.23 show mild steel coupons from Test 1 and Test 2. The electrolytes in the Marine broth caused the coupons to corrode right from the start. The corrosion products that were formed in the two tests, over time, were of different types. Some were very loose and fell off easily, while others were more adherent and did not come off even after vigorous washing. With time, there was a loss in the weight of the coupons, which was recorded (Figure 3.19).

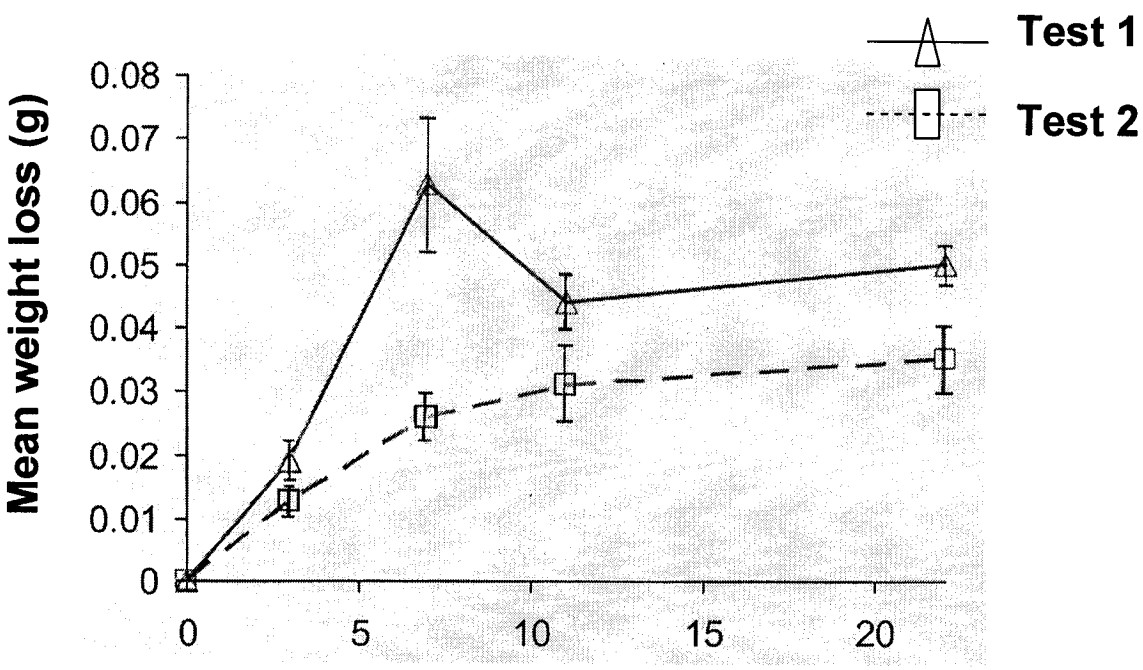

Figure 3.19 Mean weight loss in metal coupons in Test 1 and Test 2 from Day 1 to Day 22.

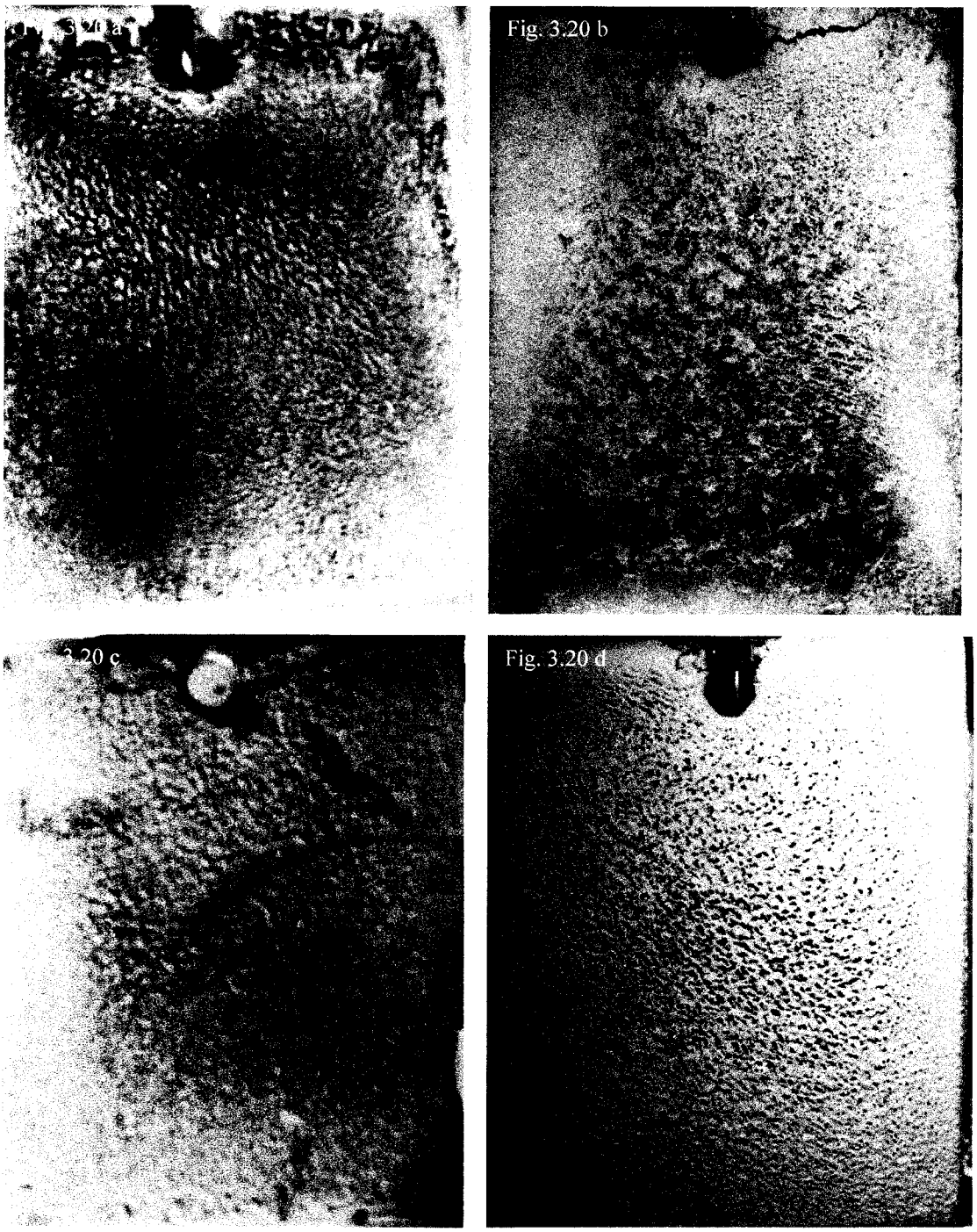

Figure 3.20 Low magnification (7 X) photographs showing the corrosion layer on entire metal coupons in Test 1 on a) Day 3, b) Day 7, c) Day 11 and d) Day 22.

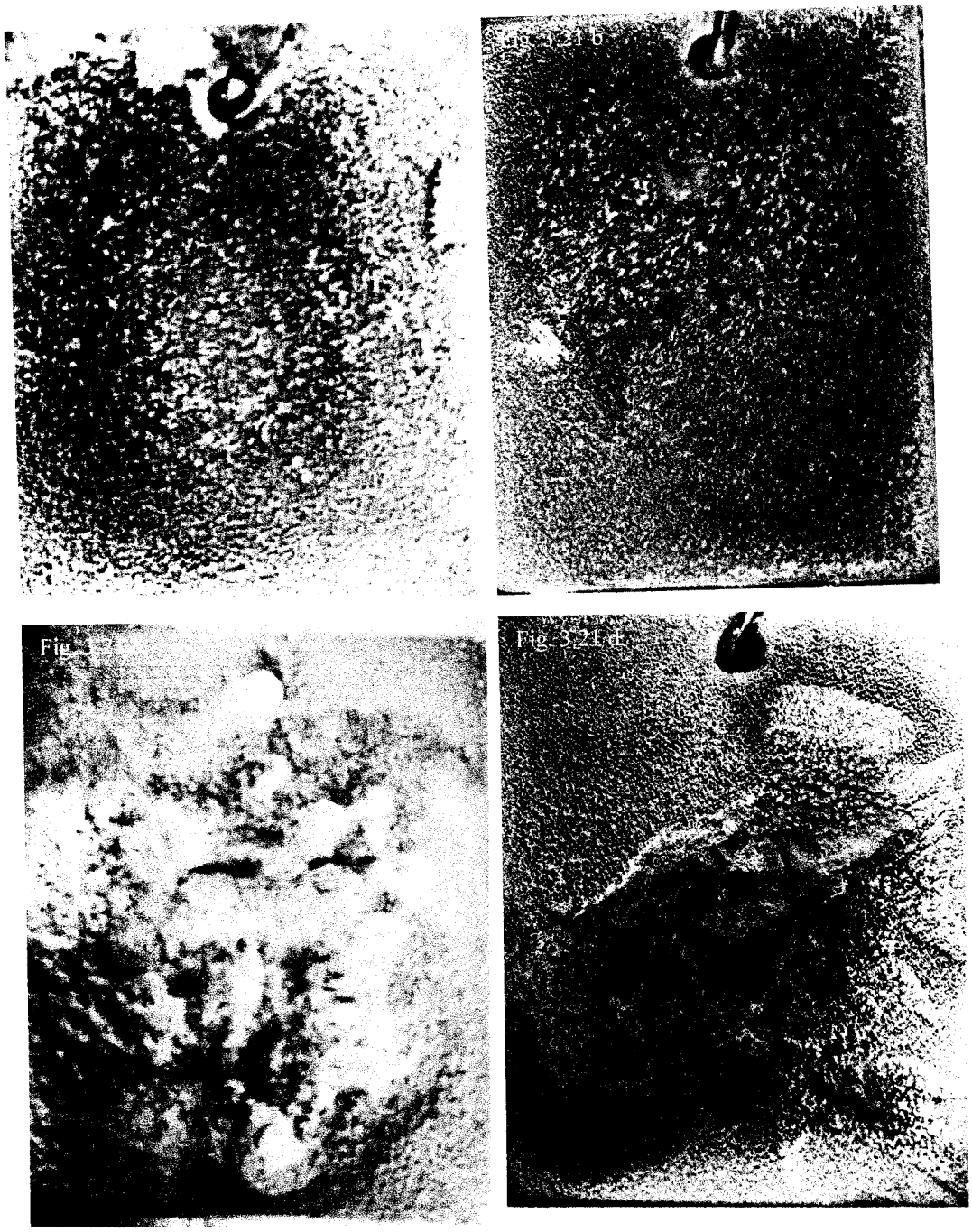

Figure 3.21 Low magnification (7 X) photographs showing the corrosion layer on entire metal coupons in Test 2 on a) Day 3, b) Day 7, c) Day 11 and d) Day 22.

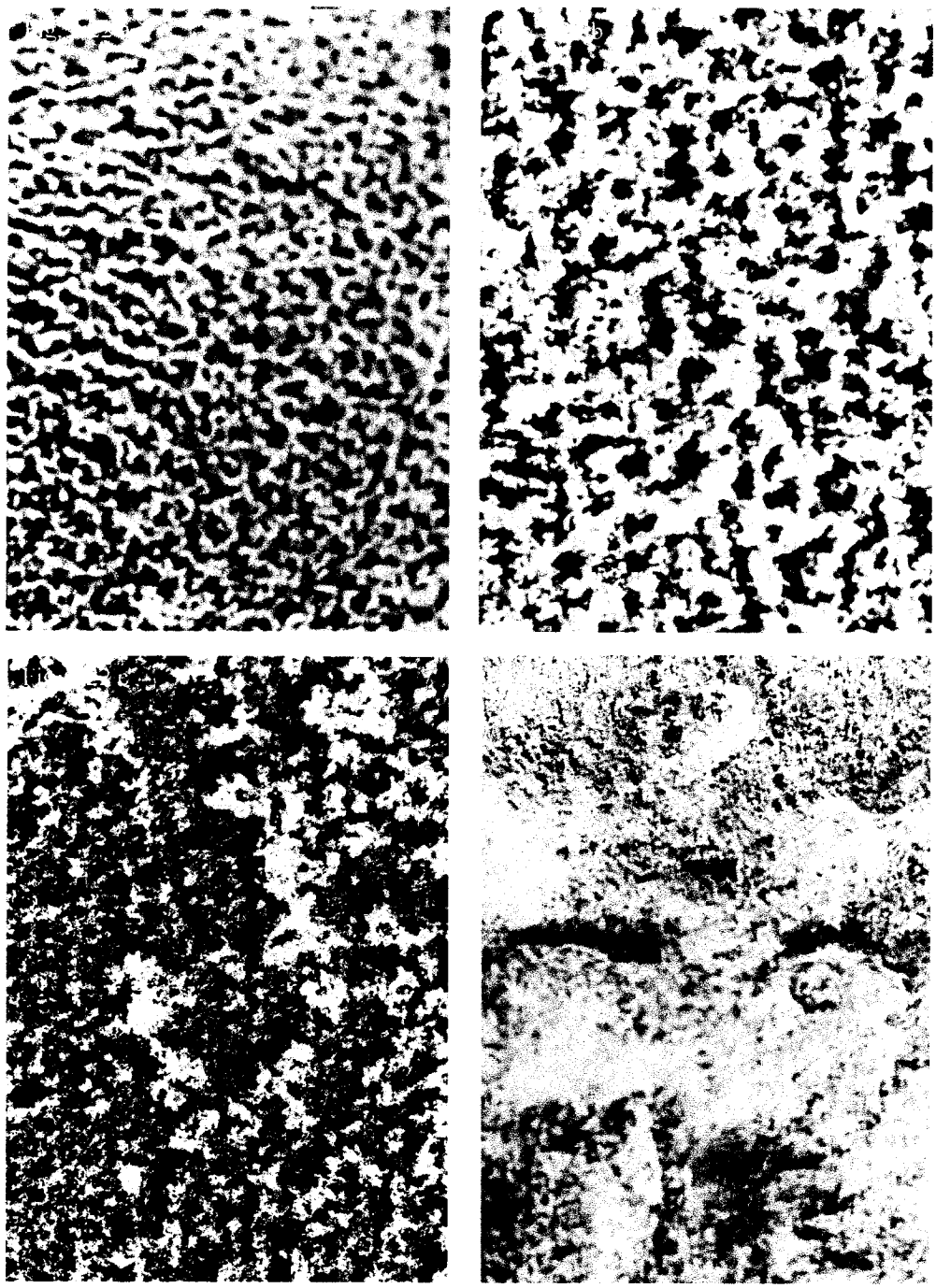

Figure 3.22 Higher magnification (10 X) photographs showing Test 1 metal coupons on a) Day 3 and b) Day 11. Notice the uniformly porous corrosion layer on both days. High magnification photographs (10 X) showing Test 2 metal coupons on c) Day 3 and d) Day 11. The corrosion layer appeared very irregular on Day 3 and very compact on Day 11.

Figure 3.23 Low magnification (7X) photograph showing the side view of the corrosion layer in Test 2 metal coupon on Day 22. The tubercles were 1 - 2 mm high, above the metal surface.

From Figure 3.19, it was revealed that the net weight loss in Test 1 was higher than in Test 2. There was an increase in the mean weight loss of coupons in Test 1 from Day 1 to Day 7, but after that, there was a decrease in the mean weight loss (Day 7 to Day 11). This was because the kinds of corrosion products produced, by Day 11, were more adherent to the metal surface and could not be washed off, even after vigorous brushing (Figure 3.24). In addition, the rate of weight loss after Day 11 was very small. This could be because the initial corrosion product layer that was formed started behaving as a passive layer, preventing further corrosion of the metal surface or slowing it down. Table 11 describes the changes that took place in the coupon in Test 1.

In Test 2, the mean weight loss increased exponentially from Day 1 to Day 11 and then reached an almost steady phase (Figure 3.19). But, in general, the net weight loss was lower than the net weight loss in Test 1. The other difference was that the area covered by adherent corrosion products, on the metal surface, was higher in Test 2 (Figures 3.25 and 3.26). Strain BH1 cells grew rapidly in the Marine broth, adhering to the metal surface and the corrosion products. The colour, compactness and texture of the corrosion products indicate that they were different from those formed in Test 1 (Figure 3.21). By Day 11, irregular bumps of corrosion products or tubercles were seen on the metal surface (Figure 3.21). Underneath these tubercles, pitting or localised corrosion was seen (Figure 3.25). There was an almost shiny metal surface visible after washing. But in the areas where there were no tubercles, there seemed to be a very thick and very adherent corrosion product layer. Table 12 describes the changes that took place in the coupon in Test 2.

The difference in the rate of corrosion and the type of corrosion products formed, in Test 2, compared to Test 1, suggests that the presence of strain BH1 cells in Test 2, alters the regular corrosion process, which takes place in Test 1. The lower net weight loss in Test 2, suggests that strain BH1 cells adherent to the metal surface act as a barrier, preventing the contact of the electrolyte with the metal surface and, thus preventing

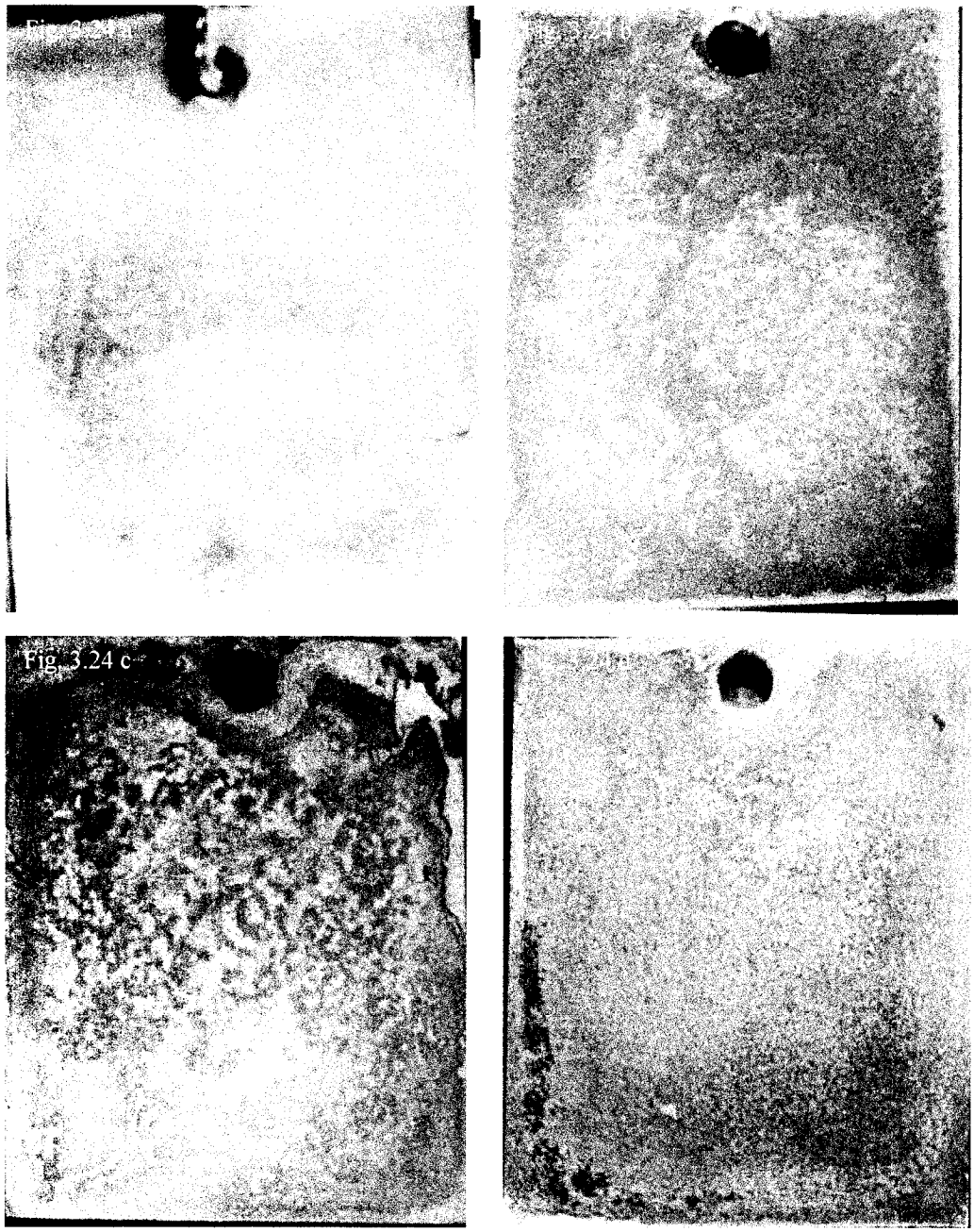

Figure 3.24 Low magnification (7X) photographs showing the surface of the entire metal coupons in Test 1 after the corrosion layer was washed off on a) Day 3, b) Day 7, c) Day 11 and d) Day 22.

Table 11: Corrosive changes in mild steel coupon in Test 1

Test coupon	Color of medium	Color of corrosion layer	Surface topography	General comments
Test 1 (Day 3)	Clear dark yellow solution with fine reddish brown precipitates on the bottom of flask.	Orange brown colour (dry rust).	Surface was regular with a uniform corrosion layer. Very loose and comes off easily.	After washing, the surface appeared clean and like the original color of the coupon. It was gritty.
Test 1 (Day 7)	Dark yellow brown solution. Reddish brown precipitates with fine fibrous particles on the bottom of flask.	Orange brown colour (dry rust).	Surface was regular with a uniform corrosion layer. Very loose and comes off easily.	After washing, the surface was clear with dark yellow/brown coloured spots almost uniformly covering the surface.
Test 1 (Day 11)	Clear dark yellow brown solution. Reddish brown precipitates with very fine particles on the bottom of flask.	Orange brown colour (dry rust).	Surface was regular with a uniform corrosion layer. Very loose and comes off easily.	After washing, the surface was clear with dark yellow/brown coloured spots almost uniformly covering the surface.
Test 1 (Day 22)	Clear light yellow solution. Reddish brown precipitates with very fine particles on the bottom of flask.	Orange brown colour (dry rust).	Surface was regular with a uniform corrosion layer. Very loose and comes off easily.	After washing, the surface was clear with dark yellow/brown coloured spots almost uniformly covering the surface. The edges had more adherent corrosion products.

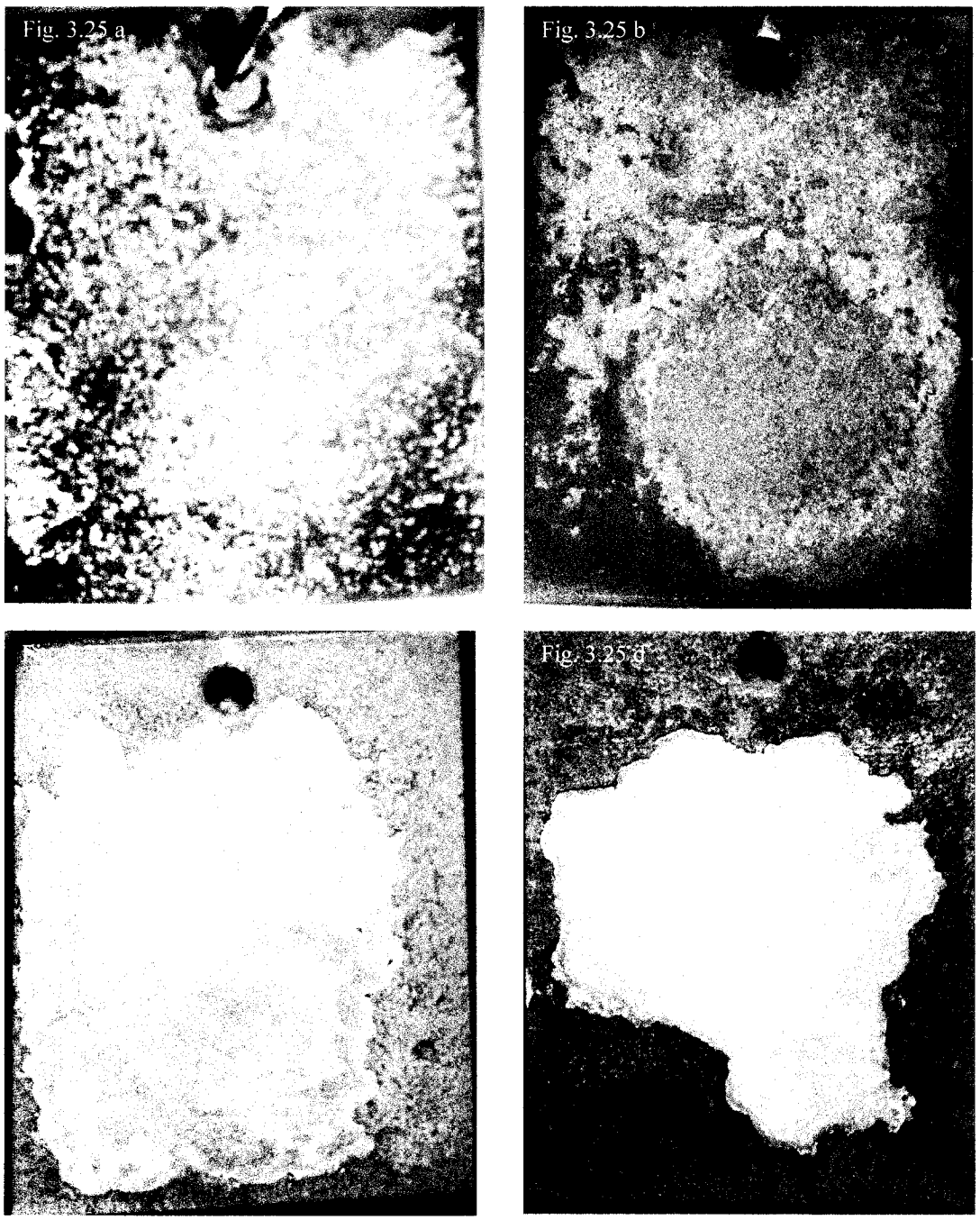

Figure 3.25 Low magnification (7X) photographs showing the surface of the entire metal coupons in Test 2 after the corrosion layer was washed off on a) Day 3, b) Day 7, c) Day 11 and d) Day 22.

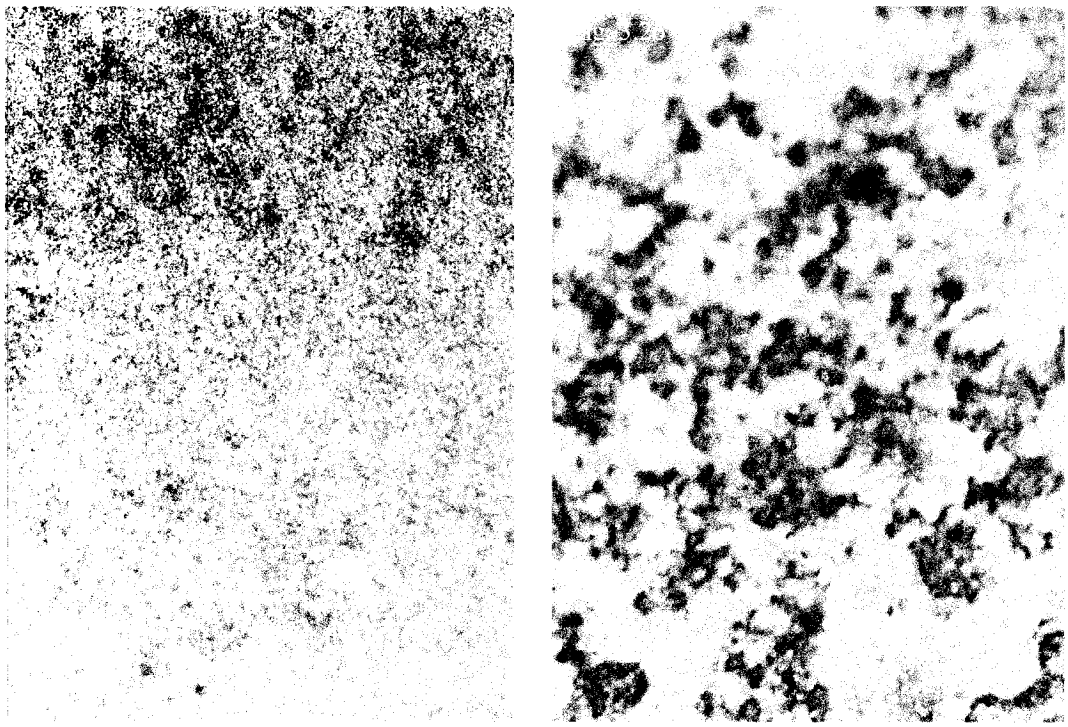

Figure 3.26 Higher magnification (10X) photographs showing surface of the metal coupons in a) Test 1 and b) Test 2 after the corrosion layer was washed off on Day 3. Notice the smoother surface of the metal coupon from Test 1, as compared to the metal coupon from Test 2, which had a rougher surface due to the increased adherence of corrosion products.

Table 12: Corrosive changes in mild steel coupon in Test 2

Test coupon	Color of medium	Color of corrosion layer	Surface topography	General comments
Test 2 (Day 3)	Opaque dark yellow solution with fine reddish brown precipitates on the bottom of flask. Strain BH1 growth apparent.	Orange brown colour (dry rust).	Surface was regular with a scattered corrosion layer. No bumps were seen.	The corrosion layer was harder to remove than that of Test 1. Localised corrosion spots were seen after the corrosion layer was removed with a plastic brush. The coupon had a peculiar smell.
Test 2 (Day 7)	Opaque dark yellow solution with fine reddish brown precipitates on the bottom of flask. Strain BH1 growth apparent.	Dark orange brown and black colour.	Surface was regular with a uniform corrosion layer. No bumps were seen. Loose and came off easily.	Localised corrosion spots were seen after the corrosion layer was removed with a plastic brush. The edges of the metal coupon were very dark black or brown.
Test 2 (Day 11)	Opaque dark yellow solution with fine reddish brown precipitates on the bottom of flask. Strain BH1 growth apparent.	Dark brown corrosion layer.	Severe corrosion attack with an irregular surface that had lots of bumps. The bumps were about 0.5 mm higher than the rest of the surface. These may be areas of localised corrosion.	The corrosion product layer sloughed off easily from the region covered by bumps and it was clean underneath but the edges had a very adherent corrosion product layer that did not come off even after vigorous brushing.

Table 12: Corrosive changes in mild steel coupon in Test 2 (continued)

Test coupon	Color of medium	Color of corrosion layer	Surface topography	General comments
Test 2 (Day 22)	Opaque dark yellow solution with fibrous reddish brown precipitates on the bottom of flask. Strain BH1 growth apparent.	Dark brown corrosion layer with black spots and bumps.	Severe corrosion attack with an irregular surface that had lots of bumps. The bumps were about 1-2 mm higher than the rest of the surface. These may be areas of localised corrosion.	The corrosion product layer sloughed off easily from the region covered by bumps and it was shiny underneath but the edges had a very adherent corrosion product layer that did not come off even after vigorous brushing.

electrochemical corrosion. However, the difference in the kinds of corrosion products formed and the initiation of localised corrosion, implicates a more active role of strain BH1 in the corrosion process.

Corrosion of metal coupons under static conditions

Test 3: Coupon in aerobic static conditions at 27 ^{0}C without strain BH1 (sterile control)
Test 4: Coupon in aerobic static conditions at 27 ^{0}C with stain BH1

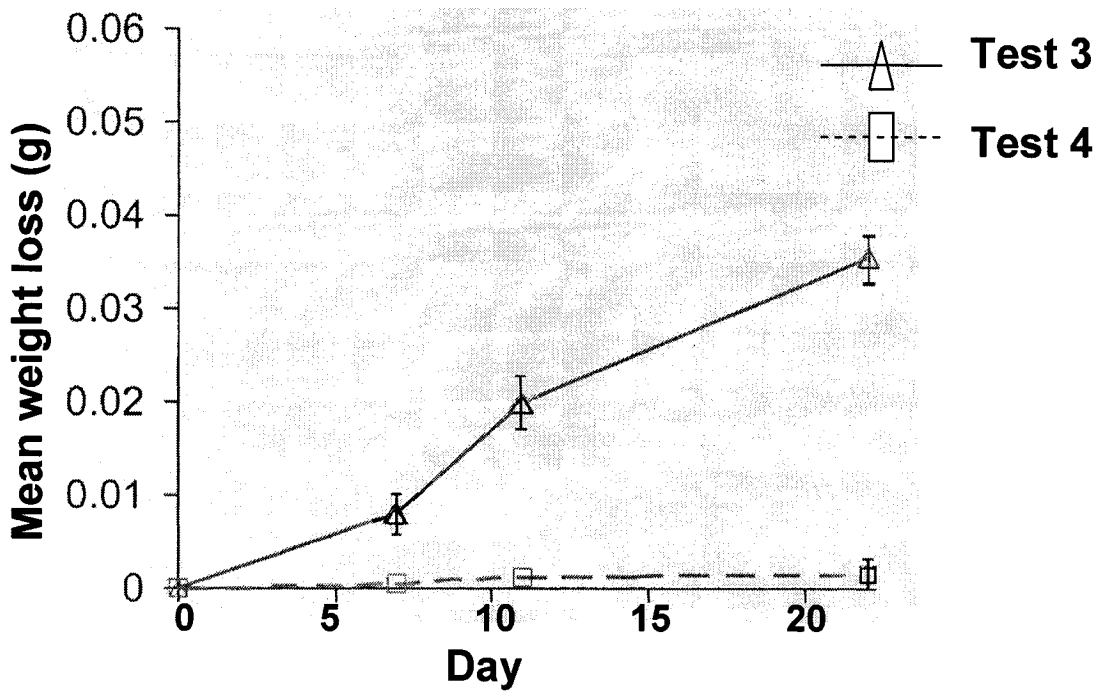

Figure 3.27 Mean weight loss in metal coupons in Test 3 and Test 4 from Day 1 to Day 22.

From Figure 3.27, it can be seen that the net weight loss in Test 3 was much higher than in Test 4. In Test 3, the mean weight loss increased almost exponentially from Day 1 to Day 22. On Day 7 a very thin uniform corrosion product layer that was easily washed off, was visible on metal coupons in Test 3 (Figure 3.28 a). On Day 22, the surface was more irregular but still easily washed off (Figure 3.28 b and 3.29). There were very little

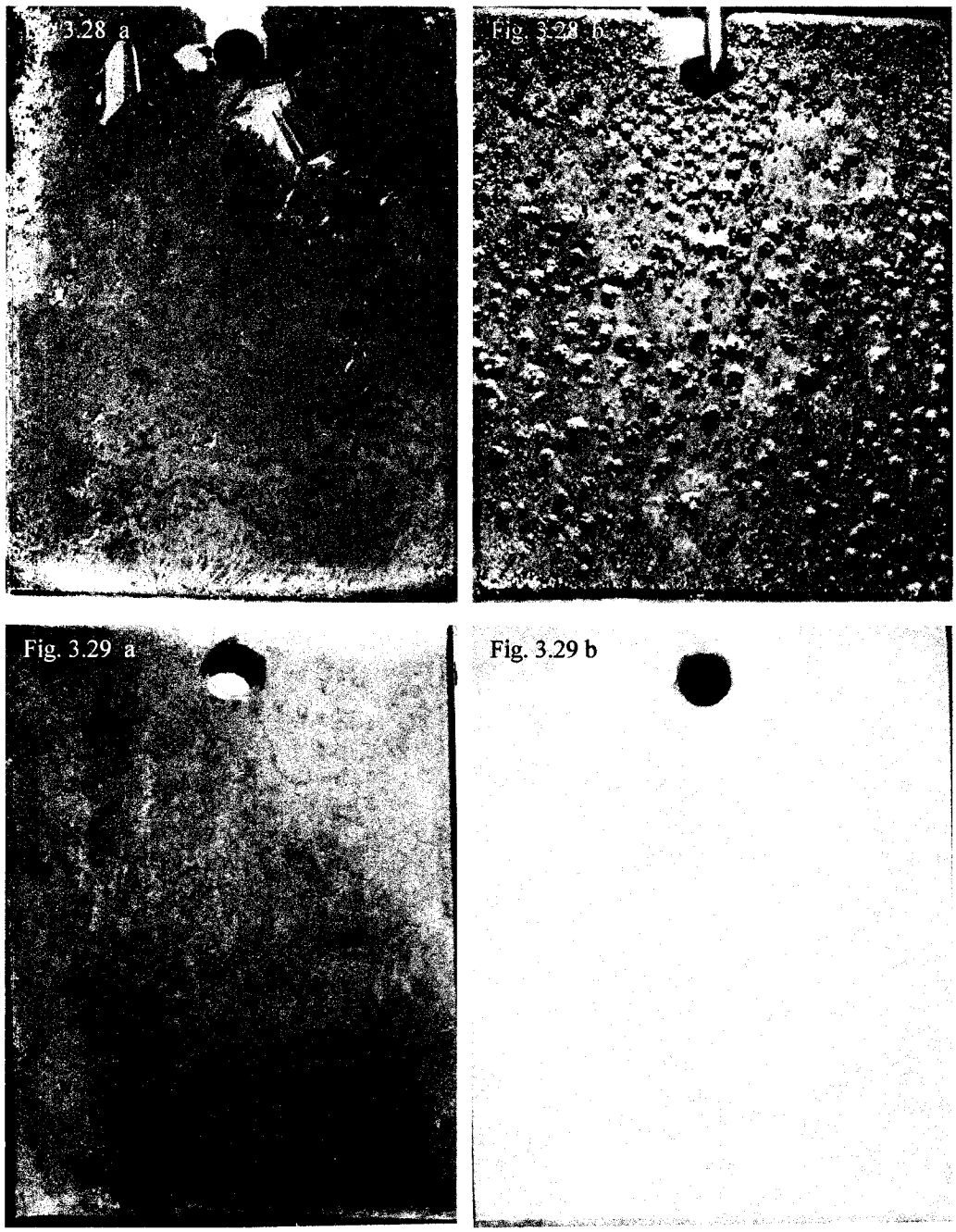

Figure 3.28 Low magnification (7X) photographs showing the corrosion layer on metal coupons in Test 3 on a) Day 7 and b) Day 22.

Figure 3.29 Low magnification (7X) photographs showing the surface of the metal coupons in Test 3 after the corrosion layer was washed off on a) Day 7 and b) Day 22.

adherent corrosion products. Table 13 describes the changes that took place in the coupon in Test 3.

In Test 4, the net weight loss was negligible. A thin transparent layer, consisting of adherent strain BH1 cells, was visible on the coupon surface (Figure 3.30), which appears to have slowed down or almost stopped the corrosion process. The metal surface had a yellow colour after the layer was washed off (Figure 3.31), but there were no apparent adherent corrosion products. Table 14 describes the changes that took place in the coupon in Test 4.

The net weight loss in Test 3 was almost half that in Test 1 (Figures 3.19 and 3.27), suggesting that agitation of the sample had a direct relation to the rate of corrosion. The negligible weight loss in Test 4, compared to Test 3, further supports the theory that the adherent strain BH1 cells act as barriers between the electrolyte and the metal surface, thus preventing the electrochemical corrosion process. The higher net weight loss in Test 2 compared to Test 4 (Figure 3.19 and 3.27) implies that strain BH1 cells were more successful in adhering to the metal surface in static conditions (Test 4) as compared to the agitated conditions (Test 2).

Table 13: Corrosive changes in mild steel coupon in Test 3

Test coupon	Color of medium	Color of corrosion layer	Surface topography	General comments
Test 3 (Day 7)	Murky dark yellow brown solution with very little, fine reddish brown precipitates on the bottom of the flask.	Dark reddish brown colour.	Surface was regular with a uniform very thin corrosion layer. No bumps were seen.	The corrosion product layer came off easily on washing with water. The surface underneath was clear with dark yellow/brown coloured spots almost uniformly covering the surface.
Test 3 (Day 22)	Clear light brown coloured solution with fine and coarse reddish brown and yellow brown precipitates on the bottom of flask.	Black-brown corrosion product layer with orange-yellow corrosion products stuck irregularly across the surface.	Surface was irregular with granular appearance due to yellow-orange corrosion products spread across the surface. No bumps were seen. The corrosion layer was loose and came off easily.	After washing, the surface appeared smooth, not shiny. It had some yellowish coloured spots and streaks across the surface.

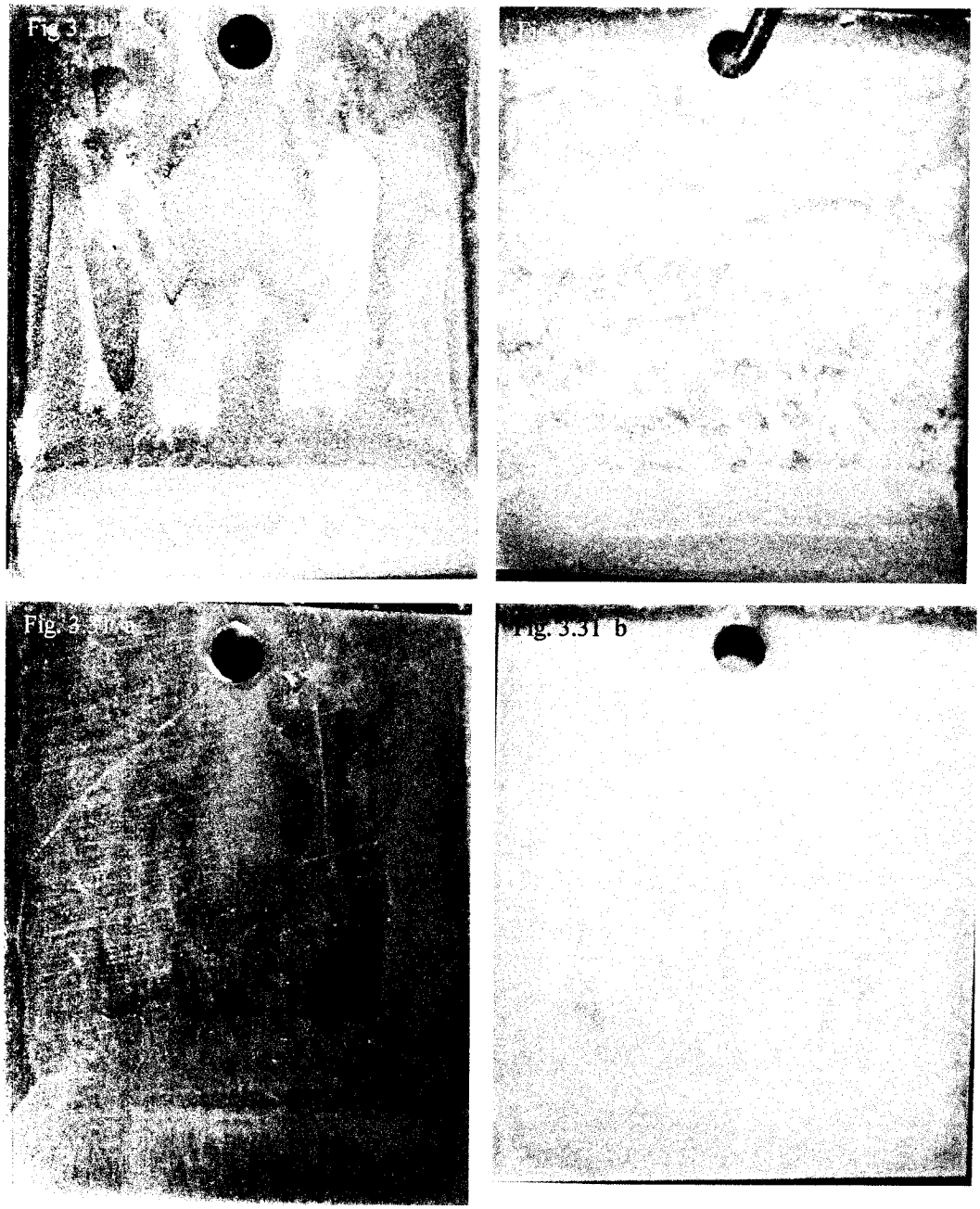

Figure 3.30 Low magnification (7X) photographs showing the corrosion layer on metal coupons in Test 4 on a) Day 7 and b) Day 22.

Figure 3.31 Low magnification (7X) photographs showing the surface of the metal coupons in Test 4 after the corrosion layer was washed off on a) Day 7 and b) Day 22.

Table 14: Corrosive changes in mild steel coupon in Test 4

Test coupon	Color of medium	Color of corrosion layer	Surface topography	General comments
Test 4 (Day 7)	Light yellow solution, almost like control. It had very little, very fine, reddish brown precipitates on the bottom of flask. Strain BH1 growth apparent.	There was very little corrosion. A very thin yellow coloured layer was visible.	Surface had a very thin layer that had an irregular pattern. No bumps were seen.	The yellow layer came off easily on washing with water. The surface underneath was clear with yellow coloured pattern corresponding to the areas, which had the layer.
Test 4 (Day 22)	Opaque yellow coloured solution with very few brown precipitates on the bottom of flask. Strain BH1 growth apparent.	There was very little corrosion. A very thin yellow coloured layer was visible.	Surface had a very thin layer that had an irregular pattern. No bumps were seen.	The yellow layer came off easily on washing with water. The surface underneath was clear with yellow coloured pattern corresponding to the areas, which had the layer.

Corrosion of metal coupons under low dissolved oxygen conditions

Test 5: Coupon under low dissolved oxygen static conditions at 27 ^{0}C without strain BH1 (sterile control)

Test 6: Coupon under low dissolved oxygen static conditions at 27 ^{0}C with strain BH1

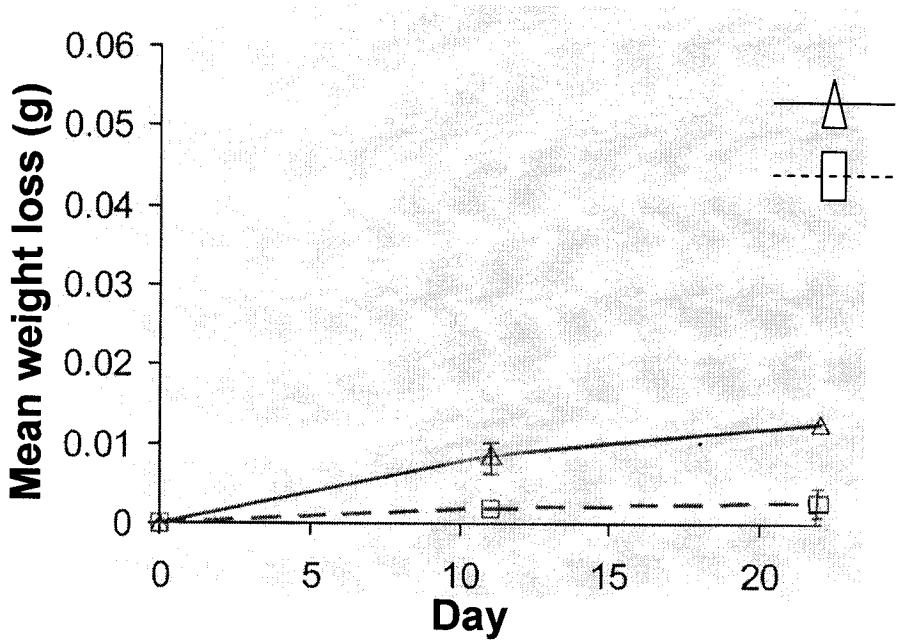

Figure 3.32 Mean weight loss in metal coupons in Test 5 and Test 6 from Day 1 to Day 22.

From Figure 3.32, it can be seen that the net weight loss in Test 5 was much higher than in Test 6. In Test 5, the mean weight loss increased from Day 1 to Day 22. A very thin uniform corrosion layer was visible on Day 22 and it was washed off easily (Figure 3.33). There were very little adherent corrosion products. Table 15 describes the coupon in Test 5.

In Test 6, the net weight loss was negligible. A thin transparent layer, consisting of adherent strain BH1 cells, was visible on the coupon surface in a random pattern (Figure 3.34 a). The metal surface had a yellow colour along the pattern after the layer was washed off (Figure 3.34 b), but there were no apparent adherent corrosion products. Table 15 describes the coupon in Test 6.

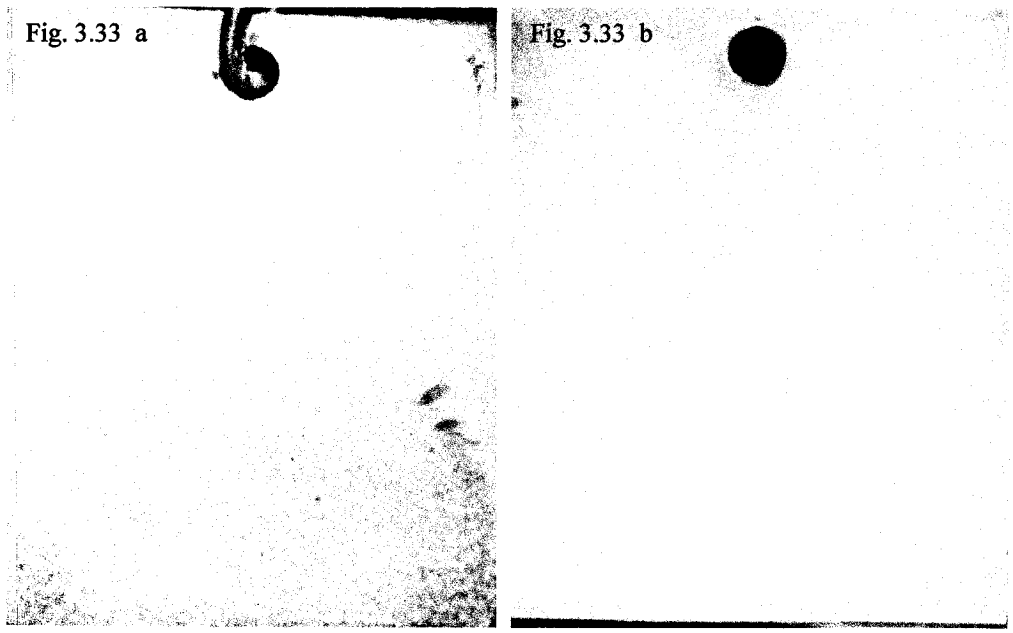

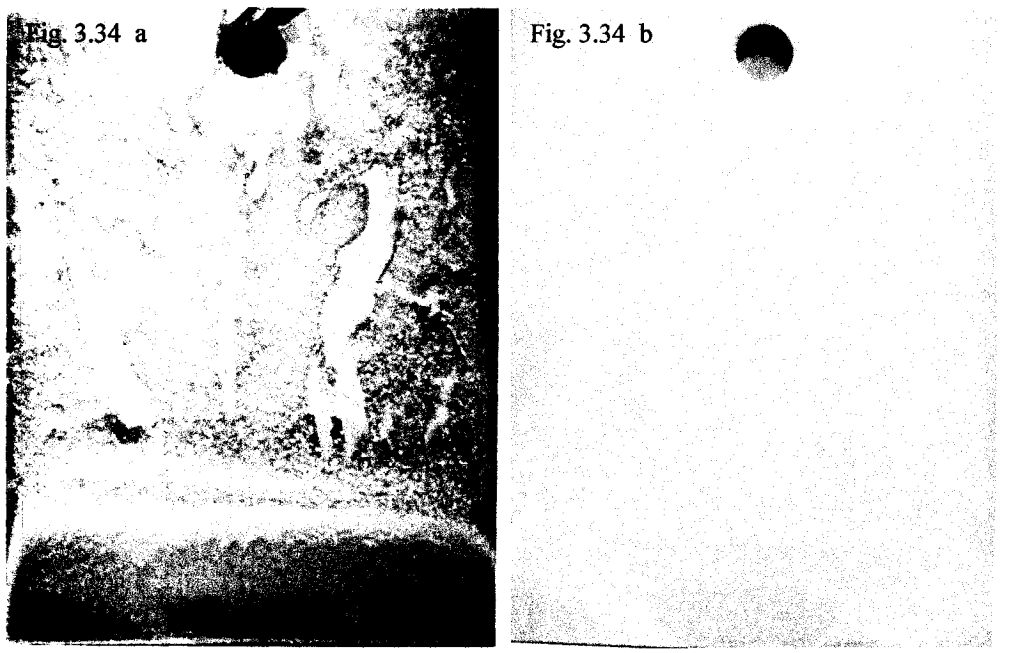

Figure 3.33 Low magnification (7X) photographs showing a) the corrosion layer and b) surface of the metal coupon after the corrosion layer was washed off, in Test 5, on Day 22.

Figure 3.34 Low magnification (7X) photographs showing a) the corrosion layer and b) surface of the metal coupon after the corrosion layer was washed off, in Test 6, on Day 22.

Table 15: Corrosive changes in mild steel coupons in Test 5 and Test 6

Test coupon	Color of medium	Color of corrosion layer	Surface topography	General comments
Test 5 (Day 22)	Clear reddish brown solution. No visible corrosion product precipitates.	There was very little corrosion. A very thin yellow coloured corrosion layer was visible.	Surface had a very thin corrosion layer that had a regular pattern. No bumps were seen.	The corrosion product layer came off easily on washing with water. The surface underneath was clear with yellow coloured spots all over the coupon.
Test 6 (Day 22)	Clear yellow solution. No visible corrosion product precipitates. Strain BH1 growth apparent.	There was very little corrosion. A very thin yellow coloured layer was visible.	Surface had a very thin corrosion layer that had an irregular pattern. No bumps were seen.	The yellow layer came off easily on washing with water. The surface underneath was clear with yellow coloured spots all over the coupon.

The net weight loss in Test 5 was almost half that in Test 3 suggesting that the amount of of dissolved oxygen in the media had a direct relation to the rate of corrosion. The negligible weight loss in Test 6 indicates that strain BH1 cells that were adherent to the metal surface in low dissolved oxygen conditions, were acting as a barrier in preventing even the minimal corrosion that would have taken place, had there been no strain BH1.

Corrosion of metal coupons under low temperature conditions

Test 7: Coupon in aerobic static conditions at 5 ^{0}C without strain BH1 (sterile control)
Test 8: Coupon in aerobic static conditions at 5 ^{0}C with strain BH1

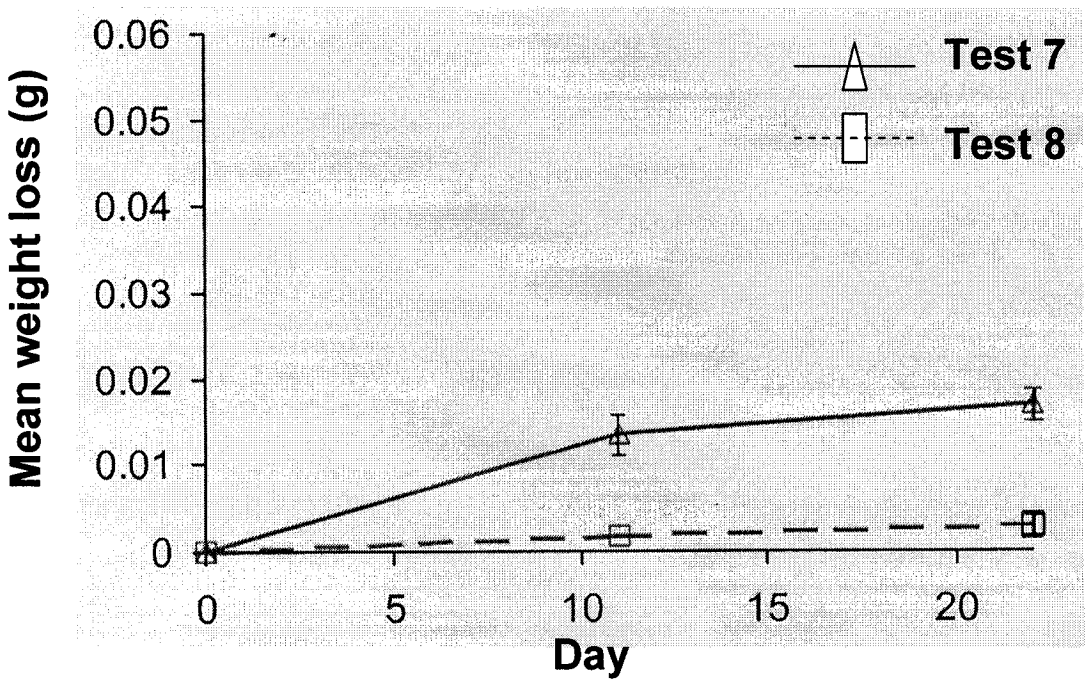

Figure 3.35 Mean weight loss in metal coupons in Test 7 and Test 8 from Day 1 to Day 22.

From Figure 3.35, it can be seen that the net weight loss in Test 7 was much higher than in Test 8. In Test 7, the mean weight loss increased from Day 1 to Day 22. A very thin fragile uniform corrosion layer was visible on Day 22 and it was washed off easily (Figure 3.36). The corrosion product layer was yellow-orange near the edges but the

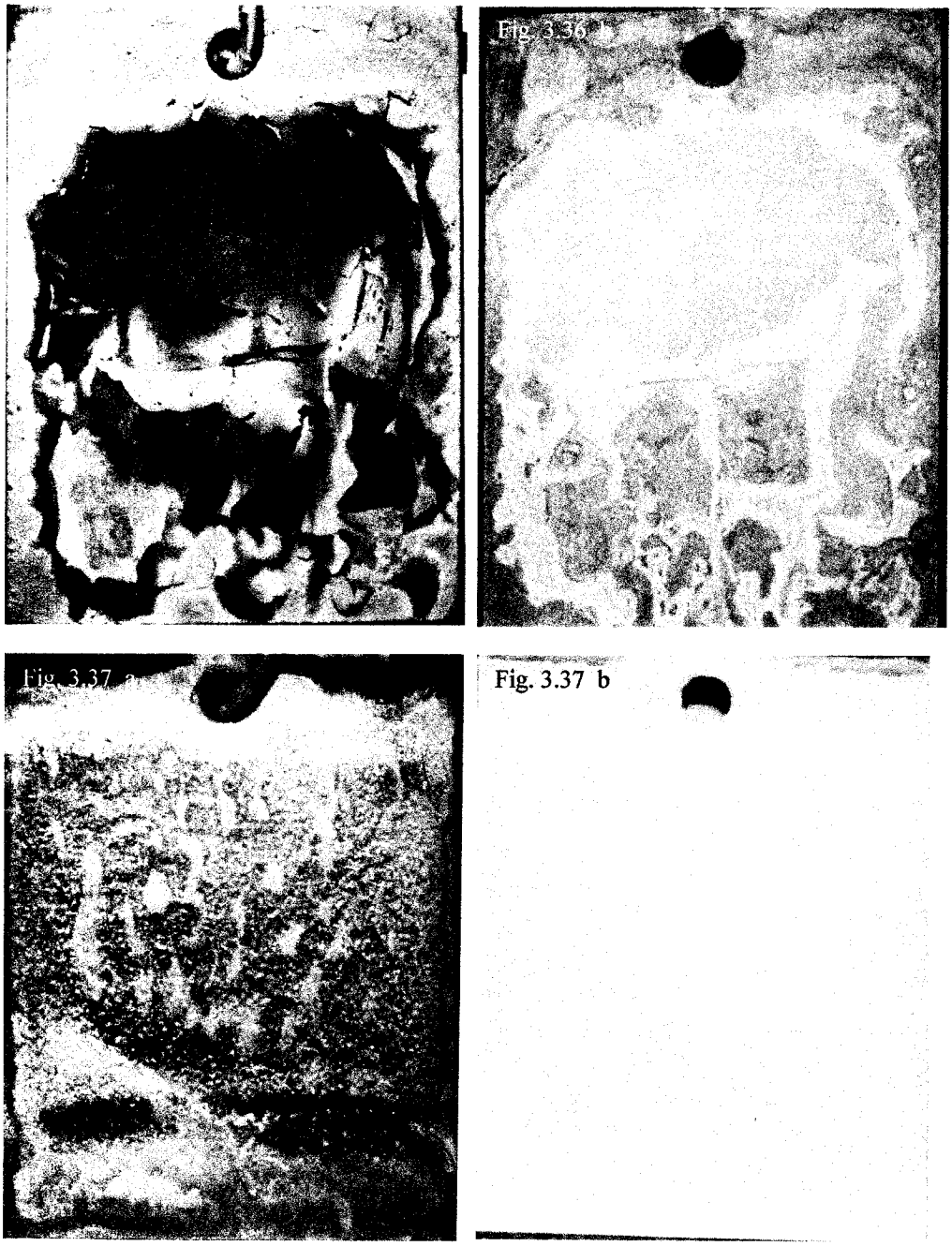

Figure 3.36 Low magnification photographs showing a) the corrosion layer and b) surface of the metal coupon after the corrosion layer was washed off, in Test 7, on Day 22.

Figure 3.37 Low magnification photographs showing a) the corrosion layer and b) surface of the metal coupon after the corrosion layer was washed off, in Test 8, on Day 22.

central regions were more reddish-brown. It was not uniform like the ones in Test 3 and Test 5. There were very little adherent corrosion products. Table 16 describes the coupon in Test 7.

In Test 8, the net weight loss was negligible. A thin transparent layer, consisting of adherent strain BH1 cells, was visible on the coupon surface in a random pattern (Figure 3.37 a). The metal surface had a yellow colour along the pattern after the layer was washed off (Figure 3.37 b), but there were no apparent adherent corrosion products. Table 16 describes the coupon in Test 8.

The net weight loss in Test 7 was almost half that in Test 3 (Figures 3.35 and 3.27), suggesting that temperature of the medium had a direct relation to the rate of corrosion. The net weight loss at low temperature was comparable to the net weight loss in low dissolved oxygen conditions (Figures 3.35 and 3.32). The low temperature also made the corrosion layer very fragile.

The negligible weight loss in Test 8 indicates that strain BH1 cells adherent to the metal surface in low temperature conditions, were acting as a barrier in preventing even the minimal corrosion that would have taken place had there been no strain BH1 cells.

Table 16: Corrosive changes in mild steel coupons in Test 7 and Test 8

Test coupon	Color of medium	Color of corrosion layer	Surface topography	General comments
Test 7 (Day 22)	Clear brownish orange solution. There were very little fine yellow corrosion precipitates at the bottom of the flask.	A very thin yellow brown coloured corrosion layer with a reddish brown central region.	Surface had a very thin corrosion layer that was uniform. Very loose and came off easily. No bumps were seen.	The corrosion product layer came off easily on washing with water. The surface underneath was brown and yellow with a patchy appearance like an abstract painting.
Test 8 (Day 22)	Opaque yellow coloured solution with very light yellow coloured precipitates on the bottom of the flask. Strain BH1 growth apparent.	There was very little corrosion. A very thin grayish yellow coloured layer was visible.	Surface had a very thin layer that had an irregular pattern. No bumps were seen.	The thin layer came off easily on washing with water. The surface underneath was clear with yellow coloured spots all over the coupon.

Qualitative analysis of the effect of roughness on corrosion

Sterile controls

Test 1a- 600 grit-polished coupon in aerobic agitated conditions at 27 ^{0}C without strain BH1

Test 2a- 240 grit-polished coupon in aerobic agitated conditions at 27 ^{0}C without strain BH1

Test 3a- Unpolished coupon in aerobic agitated conditions at 27 ^{0}C without strain BH1

In the sterile samples, it was observed that a uniform, orange-yellow coloured, loose corrosion product layer was formed (Figure 3.38). The corrosion product layer came off easily on washing. After washing, the surface of the coupon with the smoothest surface, Test 1a, was very smooth and clear, whereas in the more rougher samples, the surface was almost like an abstract painting, with variously coloured very adherent corrosion products (Figure 3.39). So as the roughness increased, the adherence of corrosion products increased. Table 17 describes the coupons in the three sterile controls.

Test samples

Test 1b- 600 grit-polished coupon in aerobic moving conditions at 27 ^{0}C with strain BH1

Test 2b- 240 grit-polished coupon in aerobic moving conditions at 27 ^{0}C with strain BH1

Test 3b- Unpolished coupon in aerobic moving conditions at 27 ^{0}C with strain BH1

In the samples with strain BH1 cells, a dark yellow coloured corrosion product layer, with dark elevated areas, tubercles, was observed (Figure 3.40). The tubercles were more evident in the smoother coupon in Test 1b. In the roughest coupon, Test 3b, the corrosion product layer was very loose and was unable to stay adherent to the coupon and sloughed off even before the coupon was removed. After washing the coupons, it was observed that the coupon in Test 3b had the least area of adherent corrosion products (Figure 3.41). The original coupon surface could be made out. Whereas in Test 1b (smoothest surface), the edges had more adherent corrosion products and the areas under the tubercles were

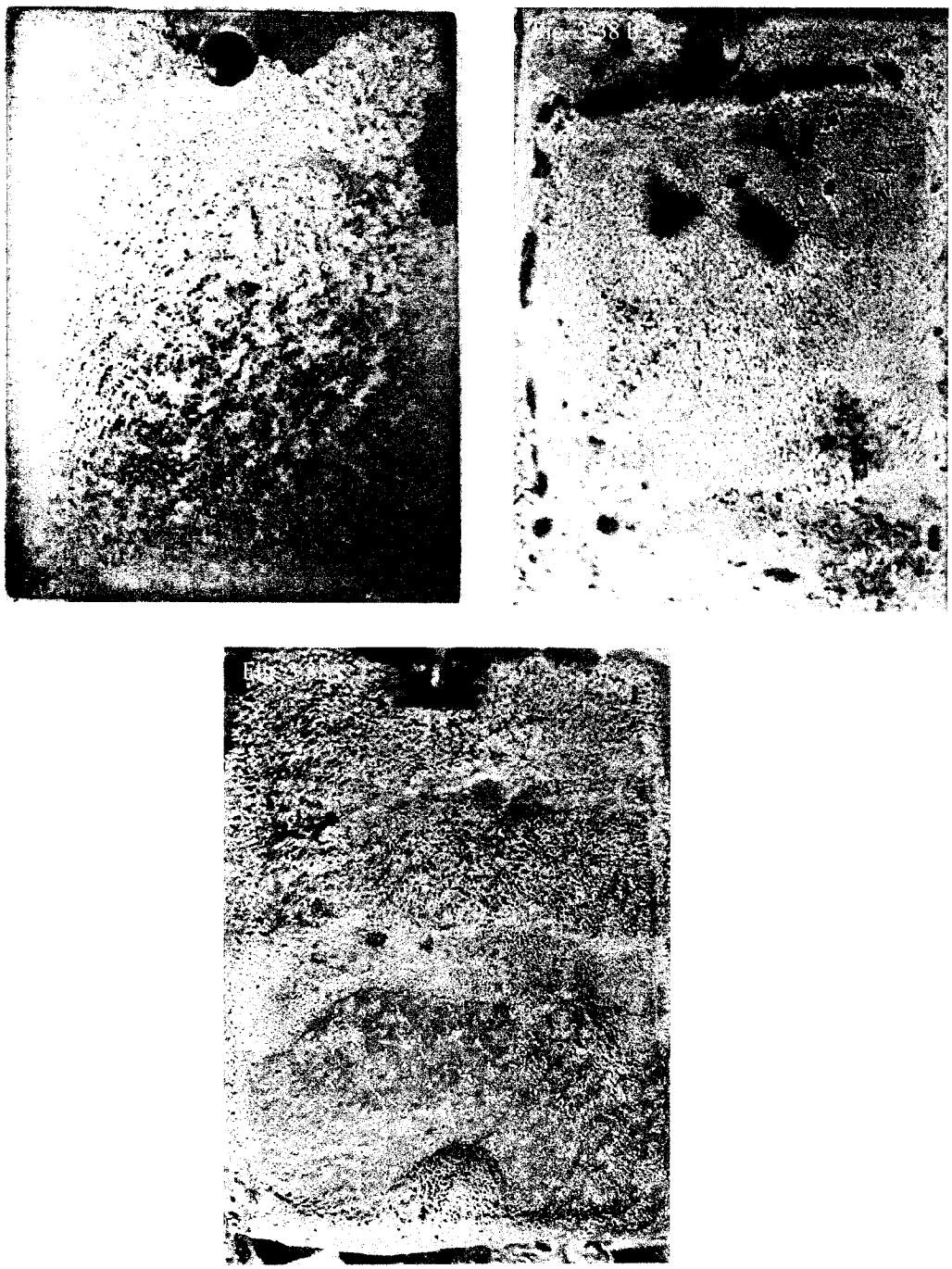

Figure 3.38 Low magnification (7X) photographs showing the uniform orange-yellow coloured porous corrosion layer in a) Test 1a, b) Test 2a, and c) Test 3a on Day 18.

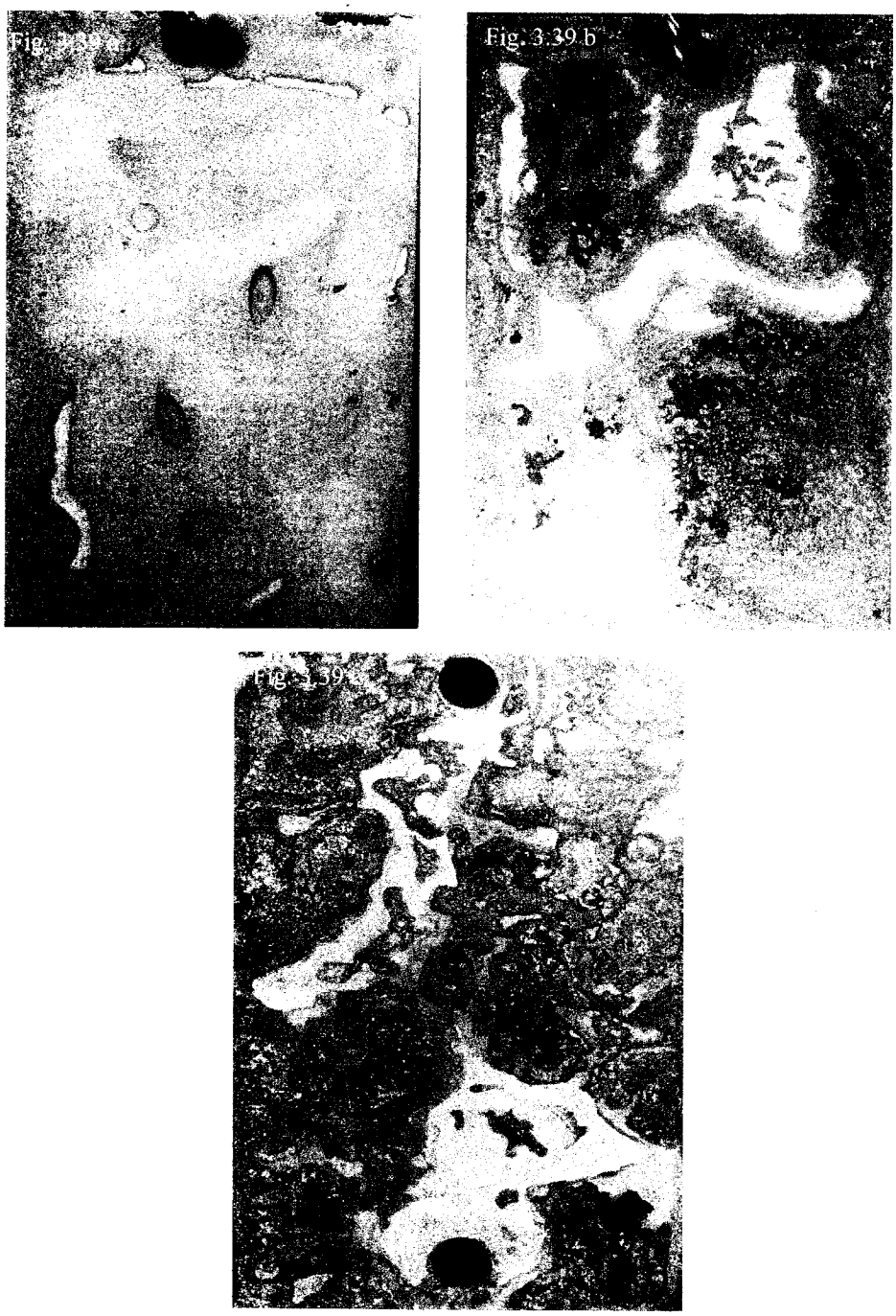

Figure 3.39 Low magnification (7X) photographs showing the surface of the metal coupons after the corrosion layer was washed off on Day 18 in a) Test 1a, the surface appeared smooth and clean b) Test 2a, surface appeared very irregularly coloured, like an abstract painting and c) Test 3a, surface appeared very irregularly coloured, like an abstract painting.

Table 17: Corrosive changes in mild steel coupons in Test 1a, Test 2a and Test 3a

Test coupon	Color of medium	Color of corrosion layer	Surface topography	General comments
Test 1a	Light yellow with fine reddish brown precipitates on the bottom of the flask.	Orange brown colour (dry rust).	Uniform corrosion layer. Very loose and came off easily.	The corrosion product layer came off easily on washing with water. The surface underneath was clean and smooth.
Test 2a	Light yellow with very fine reddish brown precipitates at the bottom of the flask.	Orange brown colour (dry rust).	Uniform corrosion layer. Very loose and came off easily.	The corrosion product layer came off easily on washing with water. The surface underneath was dark brown with a patchy appearance like an abstract painting.
Test 3a	Light yellow with very fine reddish brown precipitates at the bottom of the flask.	Orange brown colour (dry rust).	Uniform corrosion layer. Appeared slightly thicker than the other samples. Very loose and came off easily.	The corrosion product layer came off easily on washing with water. The surface underneath was dark brown with a patchy appearance like an abstract painting.

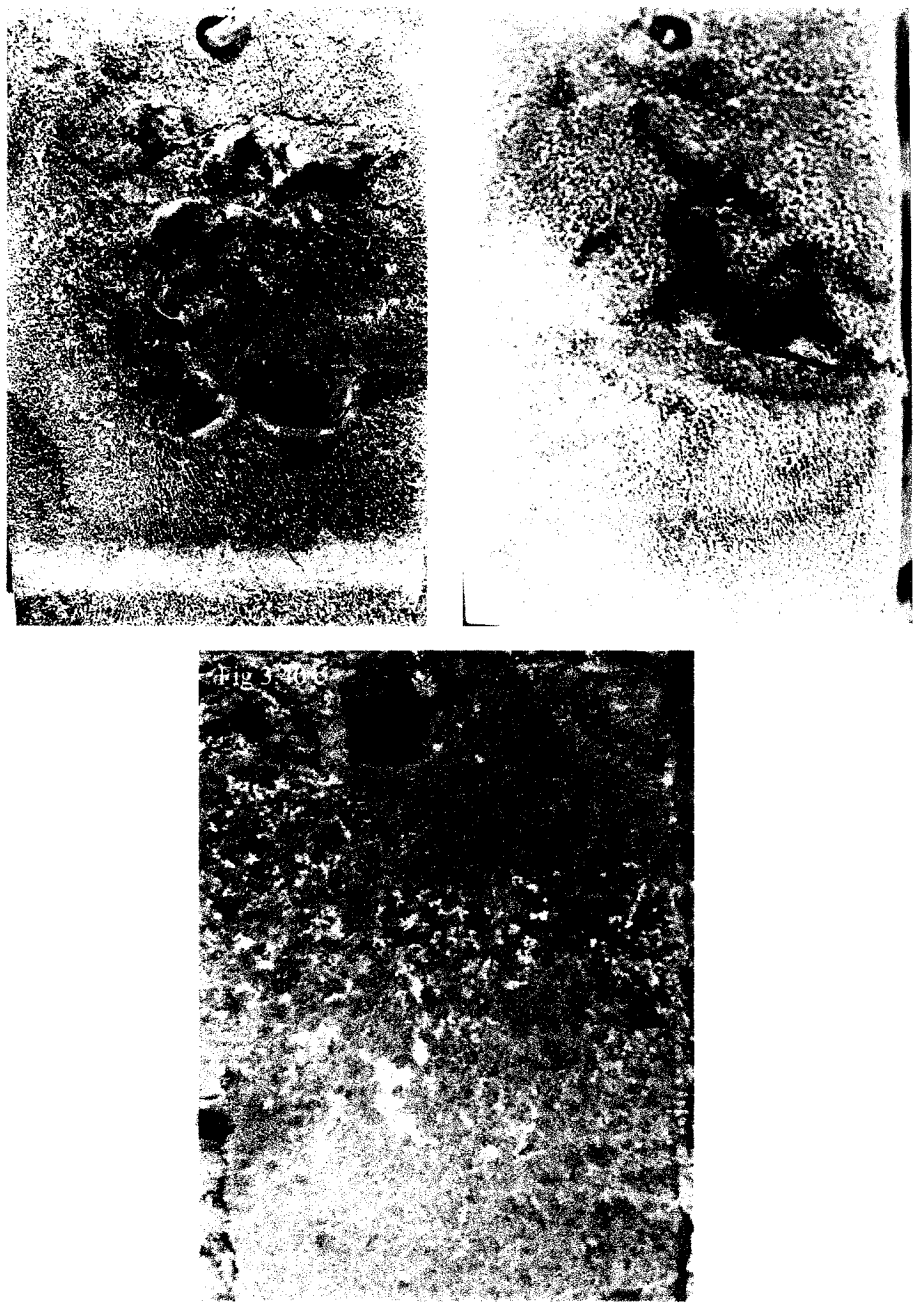

Figure 3.40 Low magnification (7X) photographs showing the corrosion layer on Day 18 in a) Test 1b, corrosion layer was very irregular, bumpy and compact, b) Test 2b, corrosion layer was very irregular, less bumpy and porous and c) Test 3b, corrosion layer was very fragile and had fallen off.

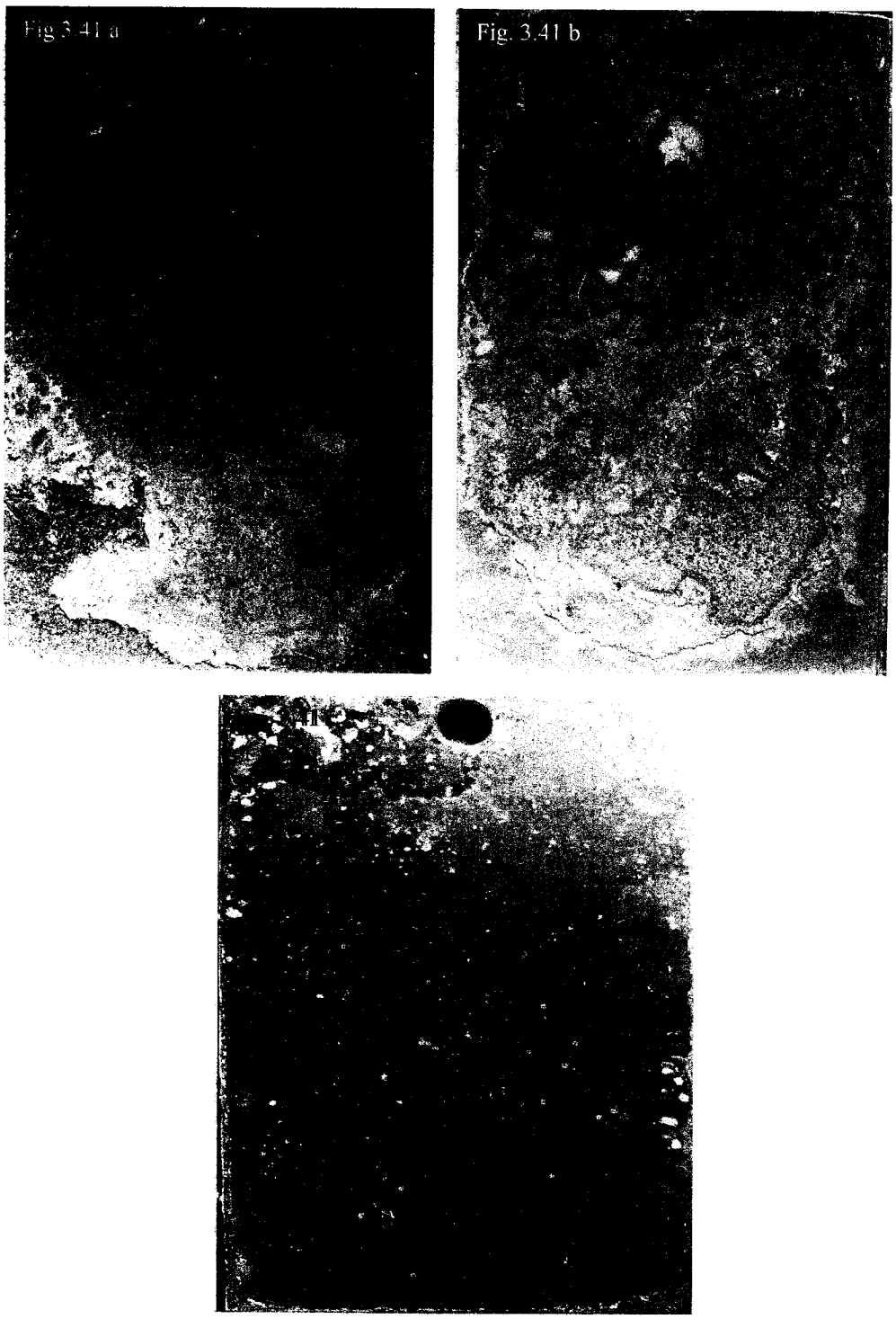

Figure 3.41 Low magnification (7X) photographs showing the surface of the metal coupons after the corrosion layer was washed off in a) Test 1b, b) Test 2b, and c) Test 3b on Day 18.

smoother. Test 2b was in between the other two tests, in that it had adherent corrosion products on the edges but also had more scattered variously coloured corrosion products in the central region, similar to the corrosion products in the rougher sterile samples. Compared to the sterile samples, the presence of strain BH1 cells increased the adherence of the corrosion products in all the cases. Table 18 describes the coupons in the three test samples.

ESEM and EDX analysis

The surface features of the coupons were observed using the Environmental Scanning Electron Microscope (ESEM) and, the Energy dispersive X-ray analysis (EDX) was done to find out the elemental composition of the surface structures on the coupons.

Under the ESEM, the corrosion product layer of the coupons from sterile sample (Test 1), appeared rough and irregular (Figures 3.42 a and b). At higher magnification, the irregular matrix of the corrosion product layer seemed to have many holes (Figures 3.42 c and d). No distinguishable crystal formations were visible. The underside of the corrosion layer, which had peeled off the coupon, showed flat needle like crystals (Figures 3.43 a and b). O and Fe were the prominent elements present in this layer, indicating the formation of ferric or ferrous oxides (Figure 3.44). On removing the corrosion product layer, the surface of the metal appeared smooth, with some white flaky deposits (Figures 3.45). EDX analysis of the bare metal surface showed a high Fe peak, as was expected (Figure 3.46).

The surface of the coupons from sterile samples (Test 3) that showed a thinner corrosion product layer, had a smooth texture with irregularly distributed bits of the rougher corrosion products (Figure 3.47). In the areas where the corrosion product layer was cracked, the smooth metal surface was visible (Figure 3.48). The thinner corrosion layer not only had high O and Fe peaks, but also showed chlorine (Cl) and sodium (Na) peaks. The Cl and Na peaks were probably due to the NaCl from the media that had precipitated

Table 18: Corrosive changes in mild steel coupons in Test 1b, Test 2b and Test 3b

Test coupon	Color of medium	Color of corrosion layer	Surface topography	General comments
Test 1b	Opaque dark yellow solution. Strain BH1 growth apparent. Reddish brown precipitates with large fibrous particles.	Rust coloured corrosion product layer with raised dark black areas.	Severe corrosion attack seen with many black spots and black bumps, which were 1-2 mm above the surface of the coupon. These may be areas of localised corrosion.	The outermost corrosion product layer came off easily. The area under the bumps was smooth but there was a very adherent corrosion layer on the outer edges, which did not come off even with vigorous brushing.
Test 2b	Opaque dark yellow solution. Strain BH1 growth apparent. Reddish brown precipitates with large fibrous particles.	Rust coloured corrosion product layer with raised dark black areas.	Severe corrosion attack seen with many black spots and black bumps, which were 1-2 mm above the surface of the coupon. These may be areas of localised corrosion.	The outermost corrosion product layer came off easily. The area under the bumps was smooth but there was a very adherent corrosion layer on the outer edges, which did not come off even with vigorous brushing.
Test 3b	Opaque dark yellow solution. Strain BH1 growth apparent. Reddish brown precipitates with large fibrous particles.	Corrosion product layer had fallen off. The sides showed a dark brown coloured corrosion layer.	The corrosion product layer was irregular.	The undersurface was smooth and appeared black with gritty shiny specks on it. The specks may be salt.

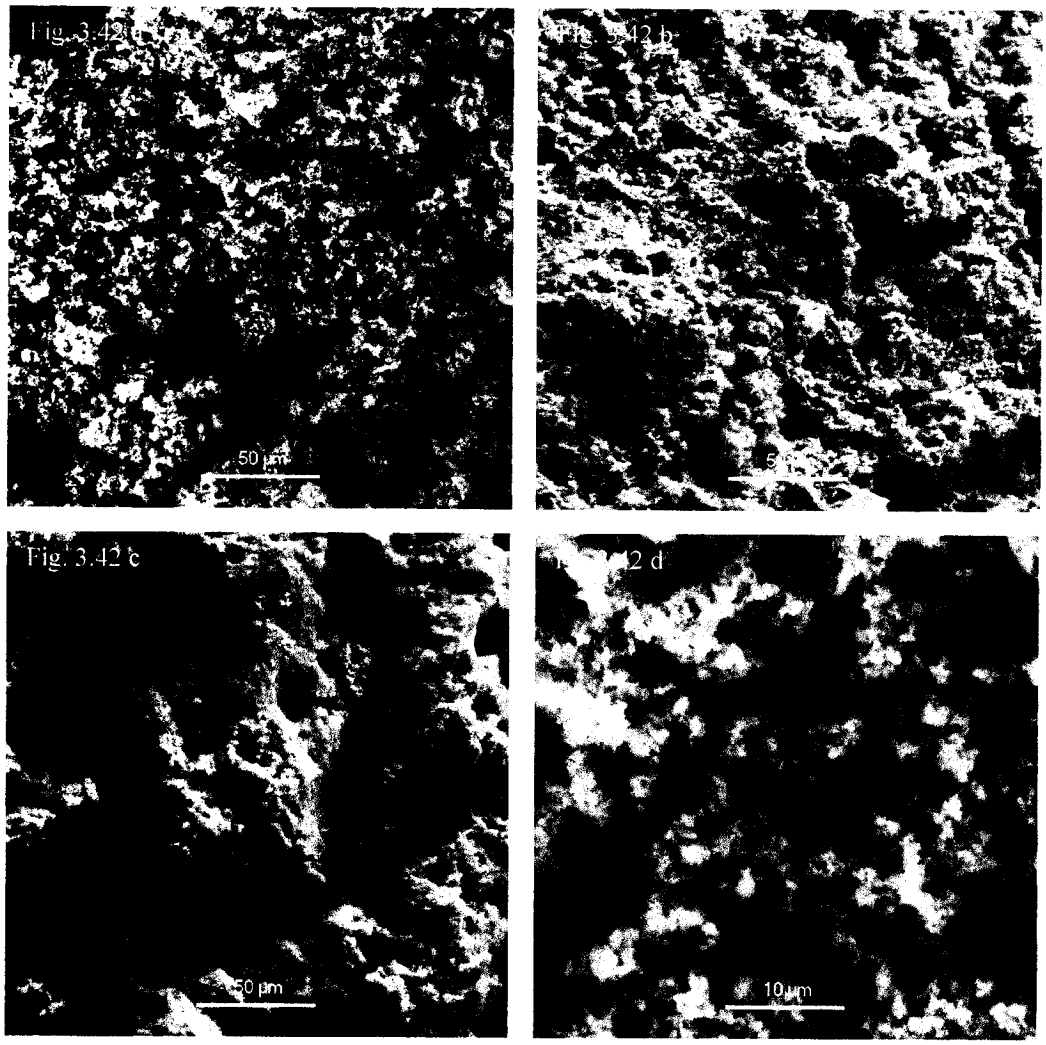

Figure 3.42 Low magnification micrographs showing the rough and irregular corrosion product layer on the metal coupon, in Test 1, on Day 22. The matrix seemed to have many holes. No clear crystal formations were visible.

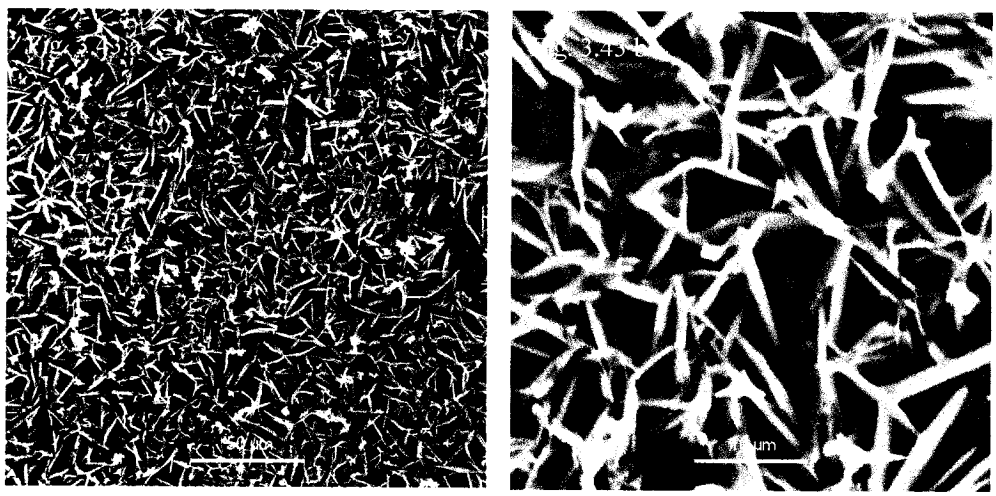

Figure 3.43 Flat needle like crystals were seen on the undersurface of the corrosion layer from metal coupon in Test 1, on Day 22.

Fig. 3.44 a

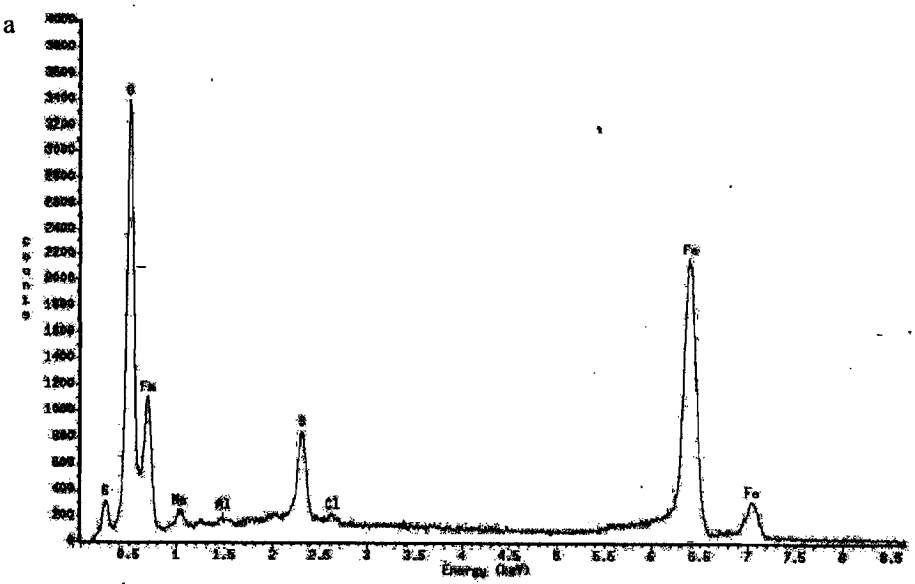

Fig. 3.44 b

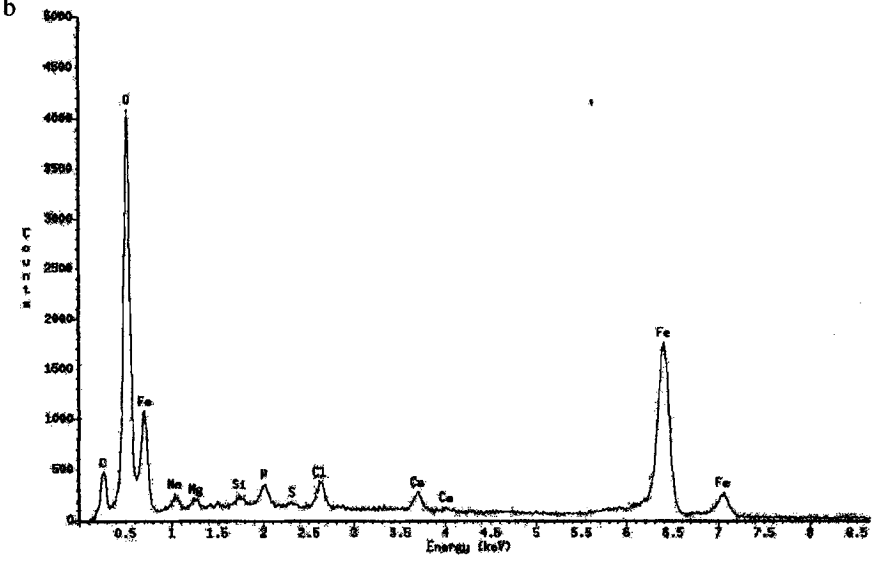

Figure 3.44 a) and b) EDX analysis of the corrosion product layer showed O and Fe peaks indicating the presence of iron oxides and hydroxides in the layer in Test 1 on Day 22 in two different samples.

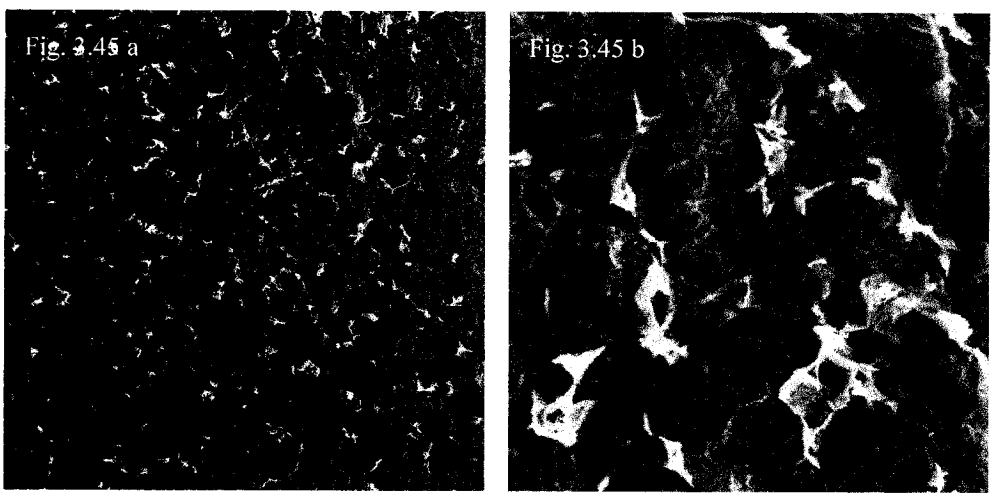

Figure 3.45 The bare metal surface from Test 1 on Day 22, after the corrosion product layer was washed off, appeared smooth, with some white flaky deposits.

Fig. 3.46 a

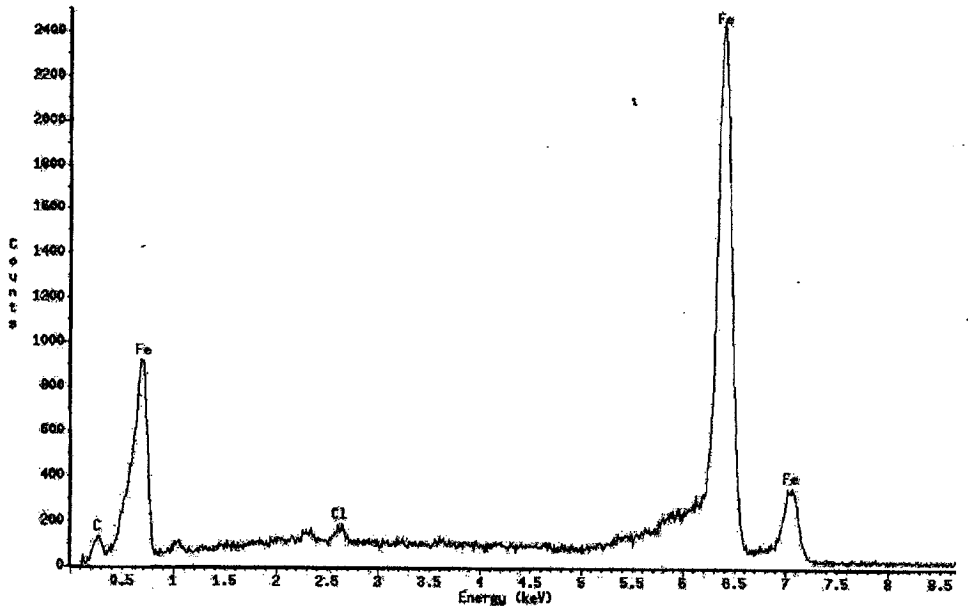

Fig. 3.46 b

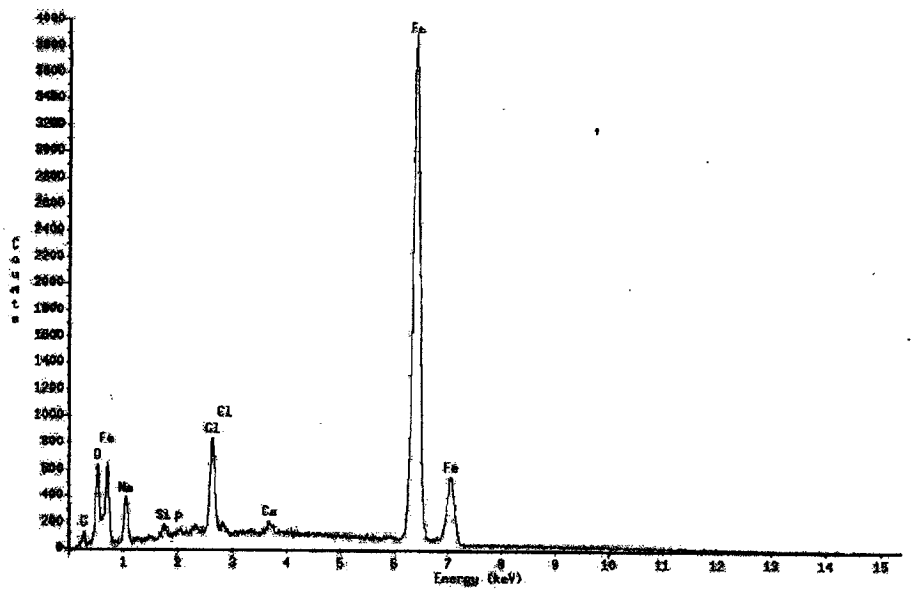

Figure 3.46 a) and b) EDX analysis of the bare metal surface revealed Fe as the main element in the uncorroded coupons in Test 1 on Day 1 in two different samples.

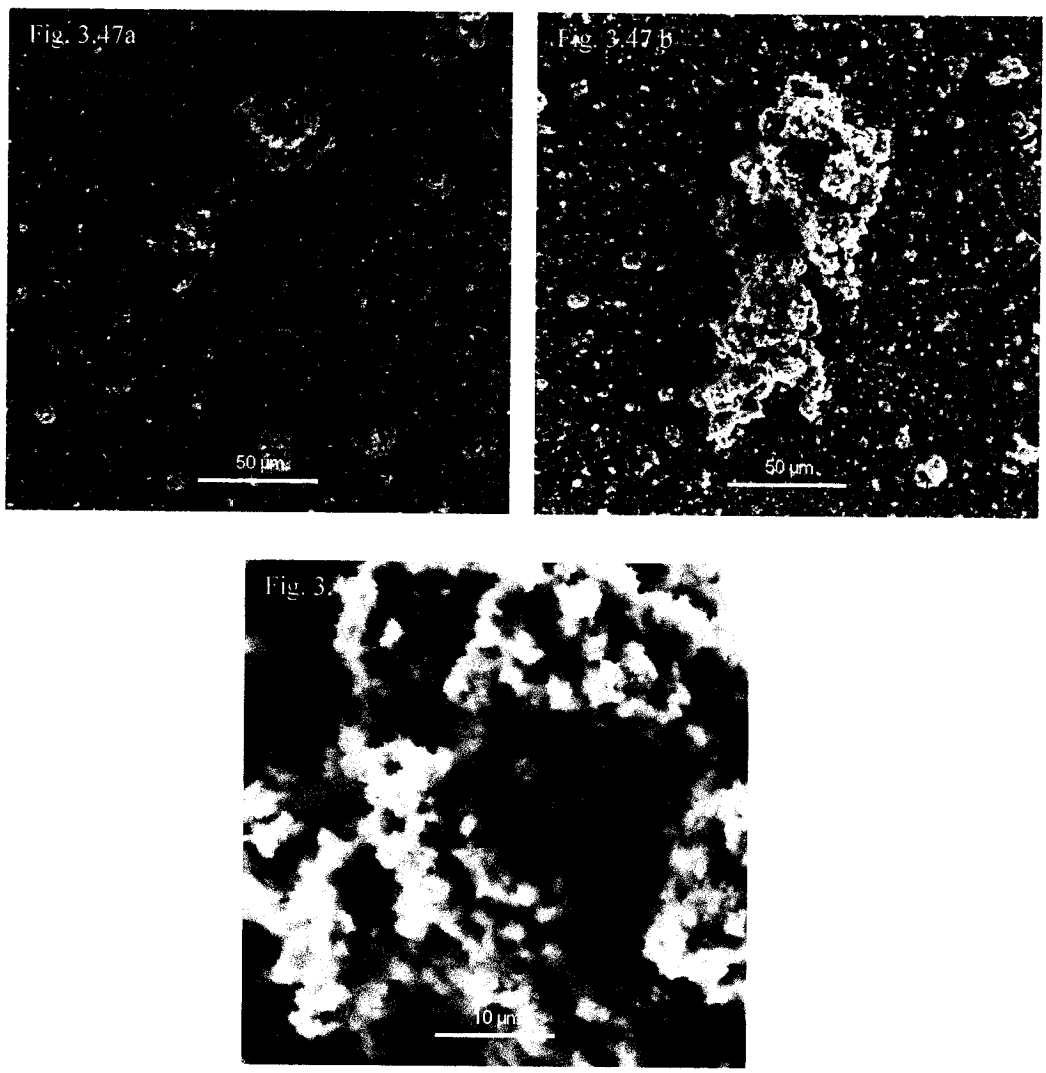

Figure 3.47 A thinner corrosion product layer was visible in some of the sterile samples (Test 4 on Day 22). It appeared relatively smooth with irregularly distributed bits of the rougher corrosion products.

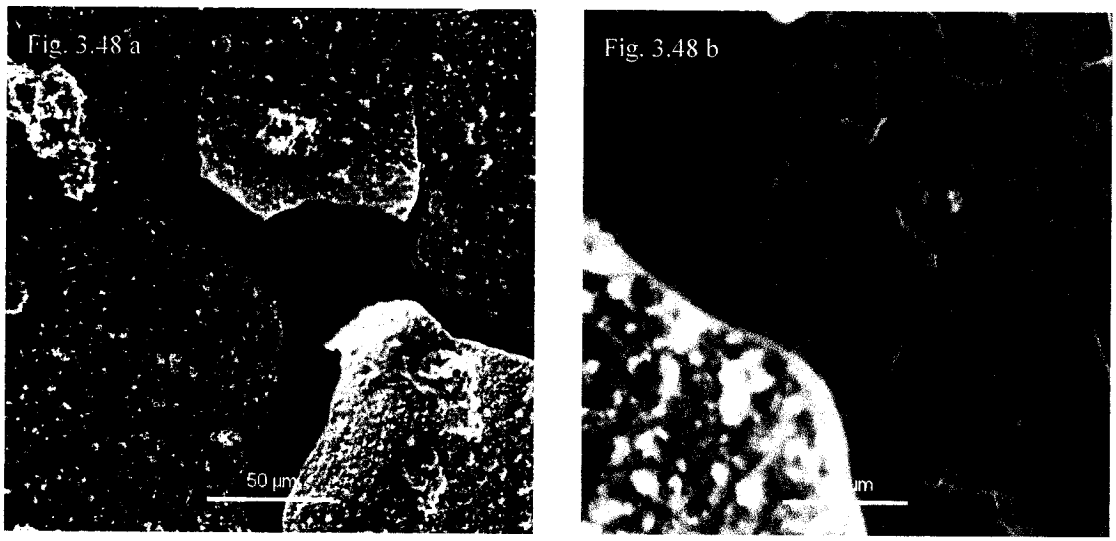

Figure 3.48 The smooth metal surface was visible in the areas where the corrosion product layer had cracked, in Test 4 on Day 22.

on the metal surface (Figure 3.49). The rougher corrosion products had higher O levels than Fe, and the Cl and Na peaks were smaller (Figure 3.50).

The surface of the coupons taken from Test 2 with strain BH1 showed a number of distinguishable formations. The general surface was very rough and irregular (Figure 3.51), showing high O and Fe peaks, demonstrating ferrous and ferric oxides (Figure 3.52). Rod shaped strain BH1 cells could be seen embedded within the corrosion products. They appeared as long transparent chains (Figure 3.53). The areas with the tubercles appeared like bumpy mountain ranges, which were very compact (Figure 3.54). There was a compact mass of corrosion products with small rounded particles embedded in the mass (Figure 3.55). These sites had small peaks of C, Cl, Ca and other elements in addition to Fe and O peaks. The smaller O peak (Figure 3.56), suggested that different corrosion products were being formed in these tubercles compared to the corrosion products in the sterile samples. In other areas, rosettes of discs covered by loose matrices (Figure 3.57), pointed disc-shaped crystal formations (Figure 3.58 a and b), and rounded ball-like formations were seen (Figure 3.58 c and d). All the structures had O and Fe peaks, but the Fe peak was more than twice that of the O peak (Figure 3.59). Based on their crystal structure and their elemental composition, the rosettes of discs in Figure 3.59, can be speculated to be goethite and, the smaller pointed disc-shaped formations in Figure 3.58 a and b, could be intermediate green rust crystals.

In coupons taken from samples (Test 4) that showed very little corrosion, the surface was smooth with cracks, and had irregularly distributed bits of rougher corrosion products (Figure 3.60), showing high Fe, Cl, O and Na peaks (Figure 3.61). At higher magnification, strain BH1 cells could be seen as transparent rods attached to the surface and the corrosion products (Figure 3.62).

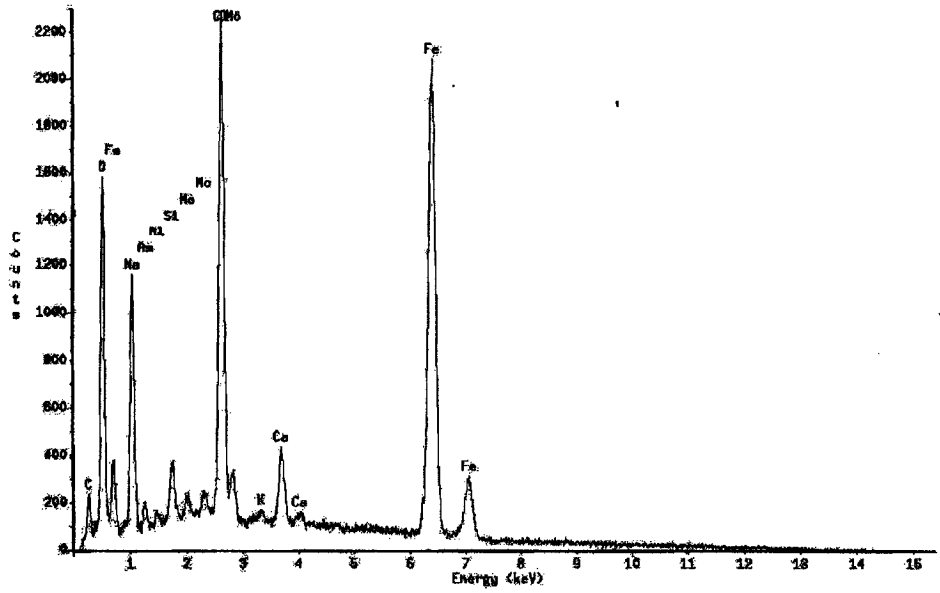

Figure 3.49 EDX analysis of the thinner corrosion layer showed not only high Fe and O peaks, but also high Cl and Na peaks indicating the presence of salt, probably precipitated from the media, in Test 3 on Day 22.

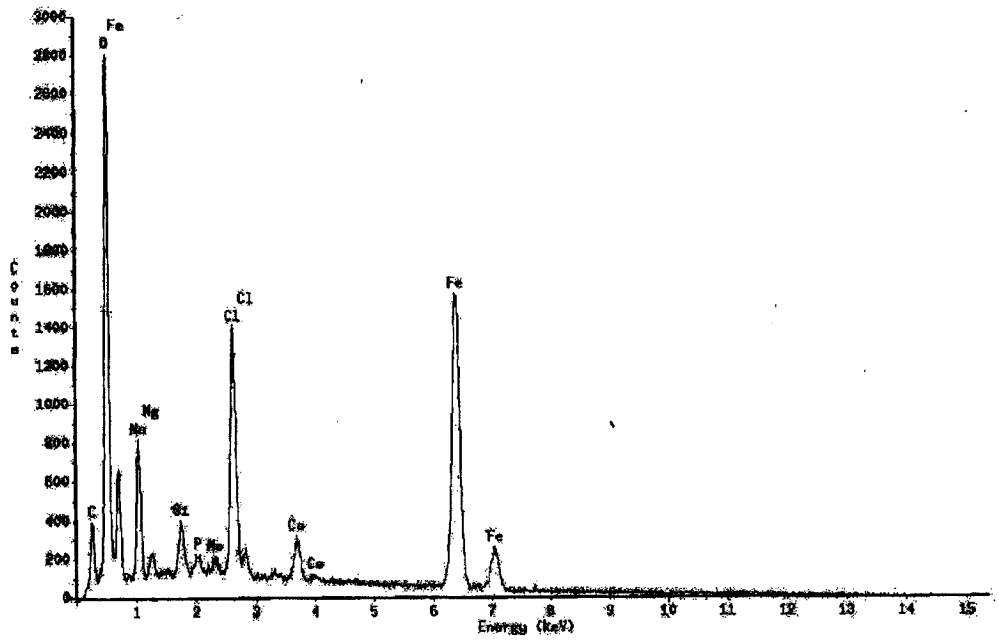

Figure 3.50 The irregularly distributed rougher corrosion products on the thinner corrosion layer showed high O peaks in Test 3 on Day 22, which was comparable to that of the corrosion product layer in the more corroded samples (Test 1). The Cl and Na peaks were higher than in those samples (Test 1).

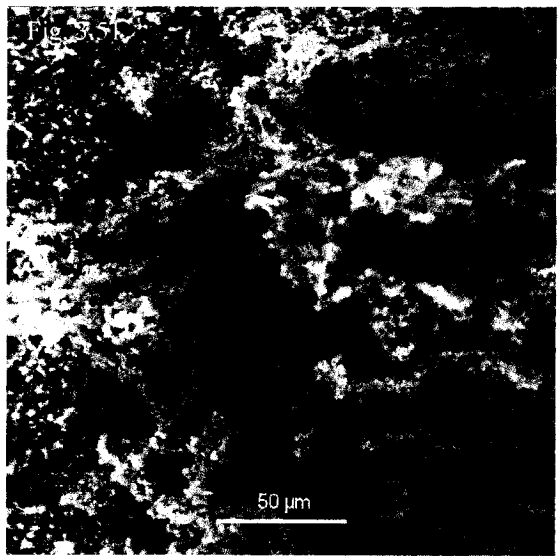

Figure 3.51 Low magnification micrograph showing the rough and irregular corrosion layer on the metal coupon placed in Test2 on Day 22.

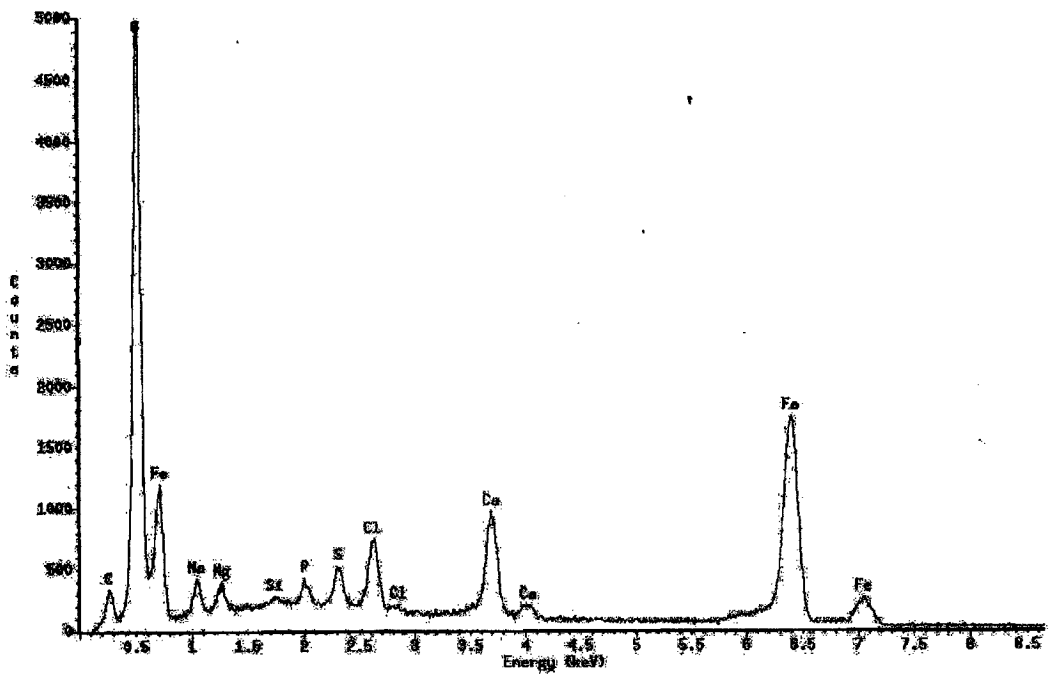

Figure 3.52 EDX analysis of the corrosion product layer, in Test 2 on Day 22, showed high O and Fe peaks, in addition to peaks in C, Ca and Cl.

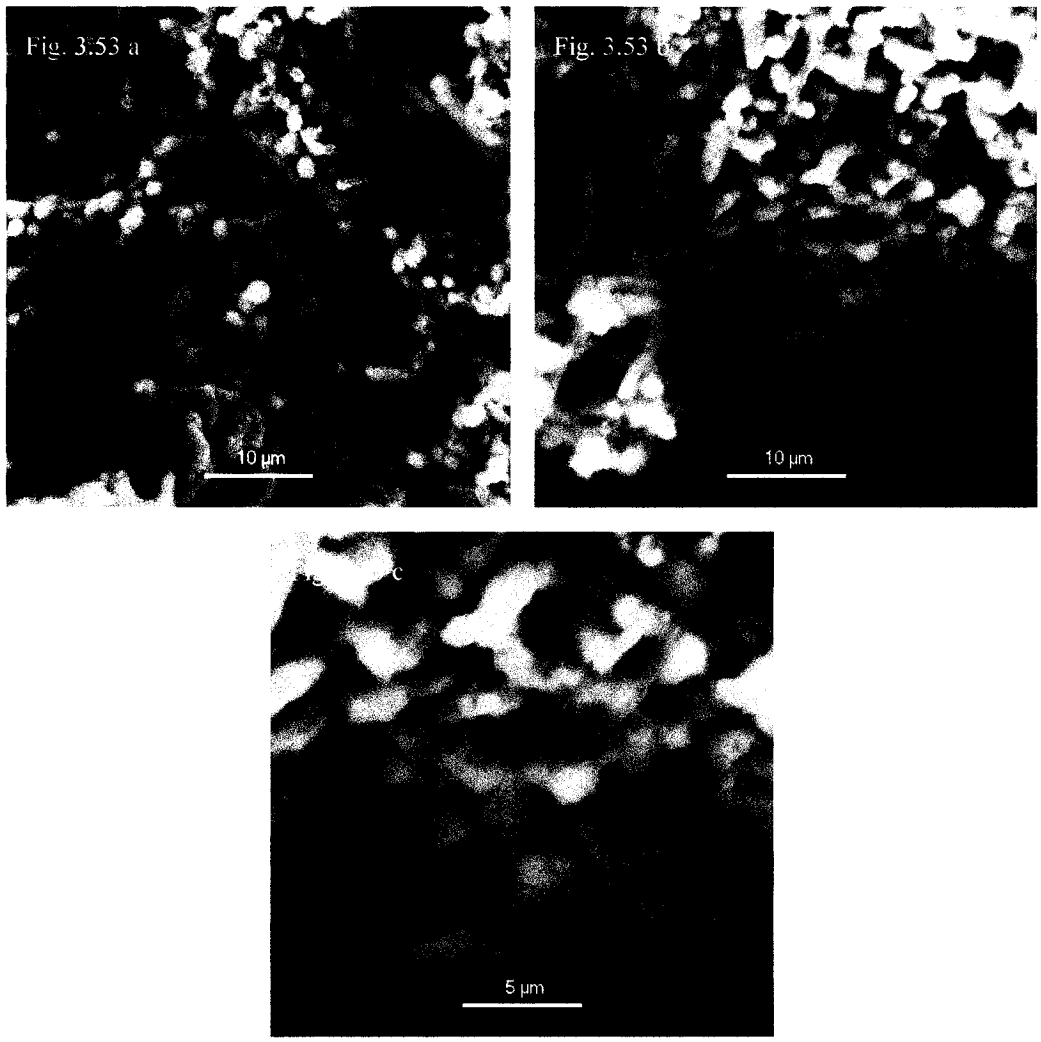

Figure 3.53 Transparent rod-shaped strain BH1 cells were seen embedded within the corrosion products on the metal coupons in Test 2 on Day 22.

.

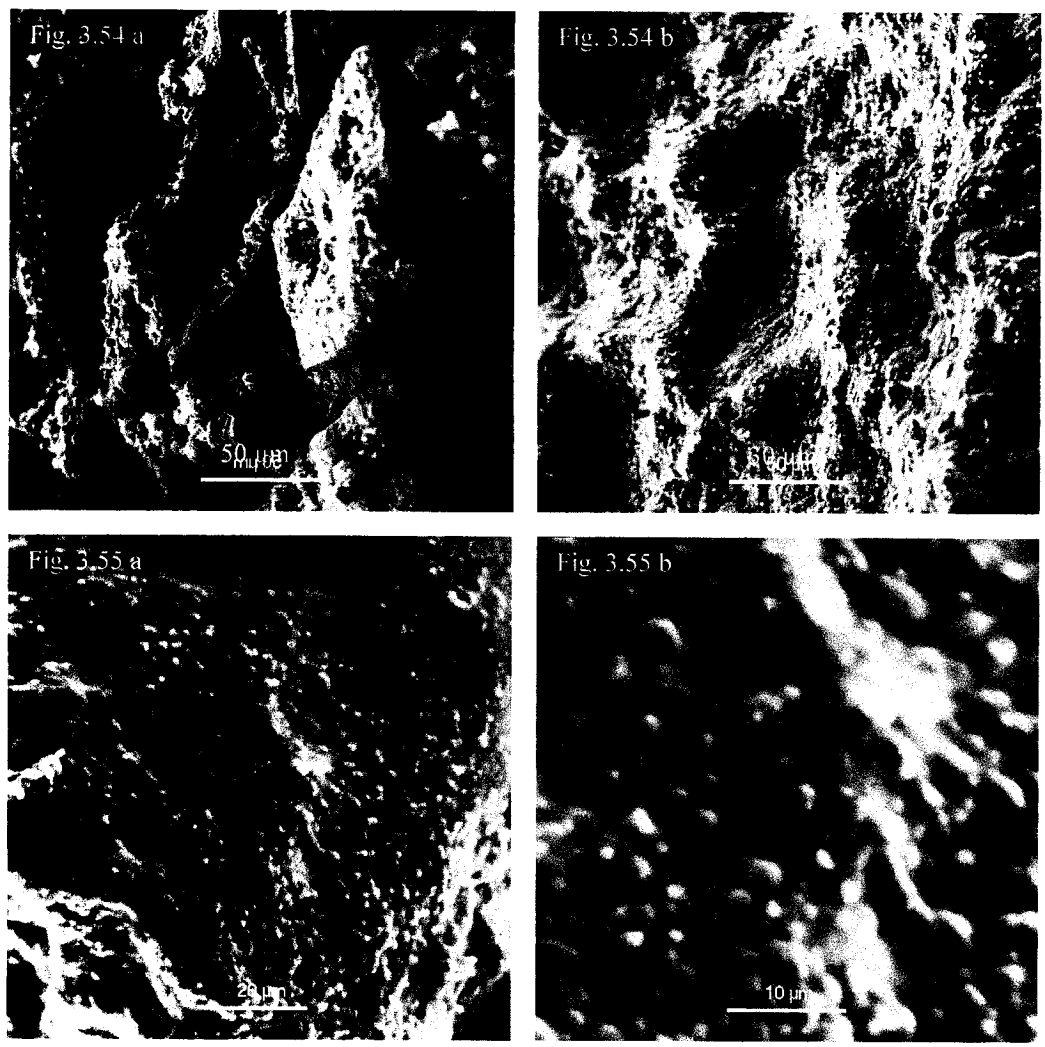

Figure 3.54 ESEM showing the corrosion layer on the metal coupon in Test 2 on Day 22, in the areas of the tubercles.

Figure 3.55 ESEM micrographs showing the compact mass of corrosion products in Test 2 on Day 22, in areas of the tubercles.

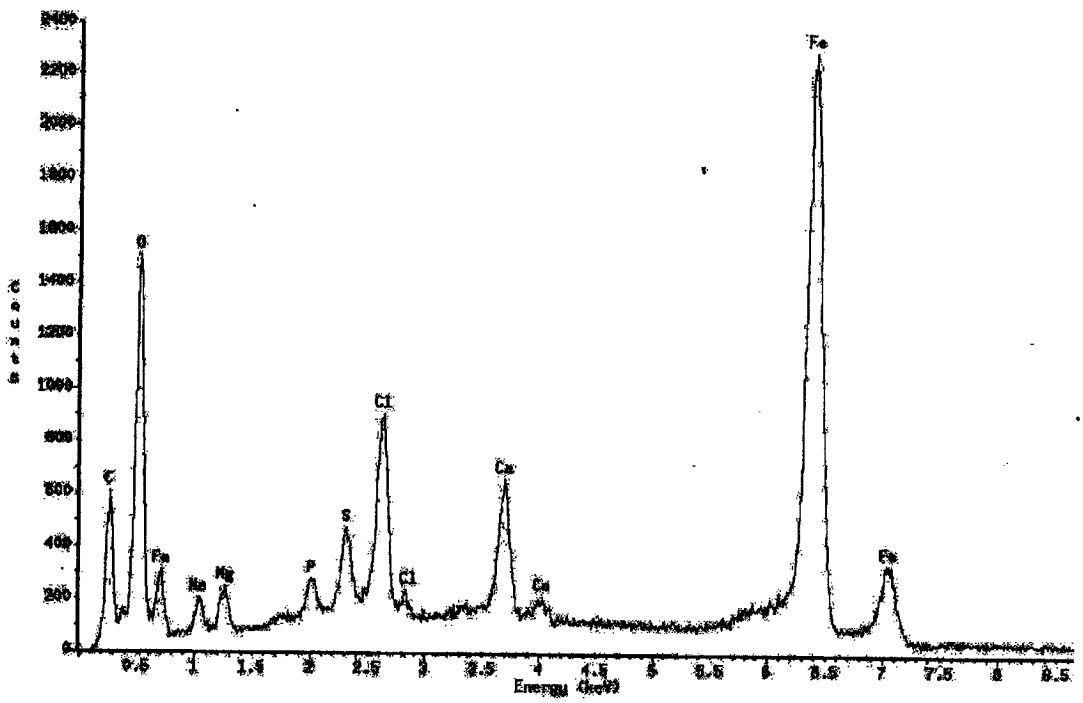

Figure 3.56 The lower O peak than the Fe peak in the bump areas of the corrosion layer, in Test 2 on Day 22, indicated that corrosion products different from those in the sterile samples (Test 1), were being formed. The C, Ca and Cl peaks were very prominent, pointing to a mixture of corrosion and microbiological products being formed.

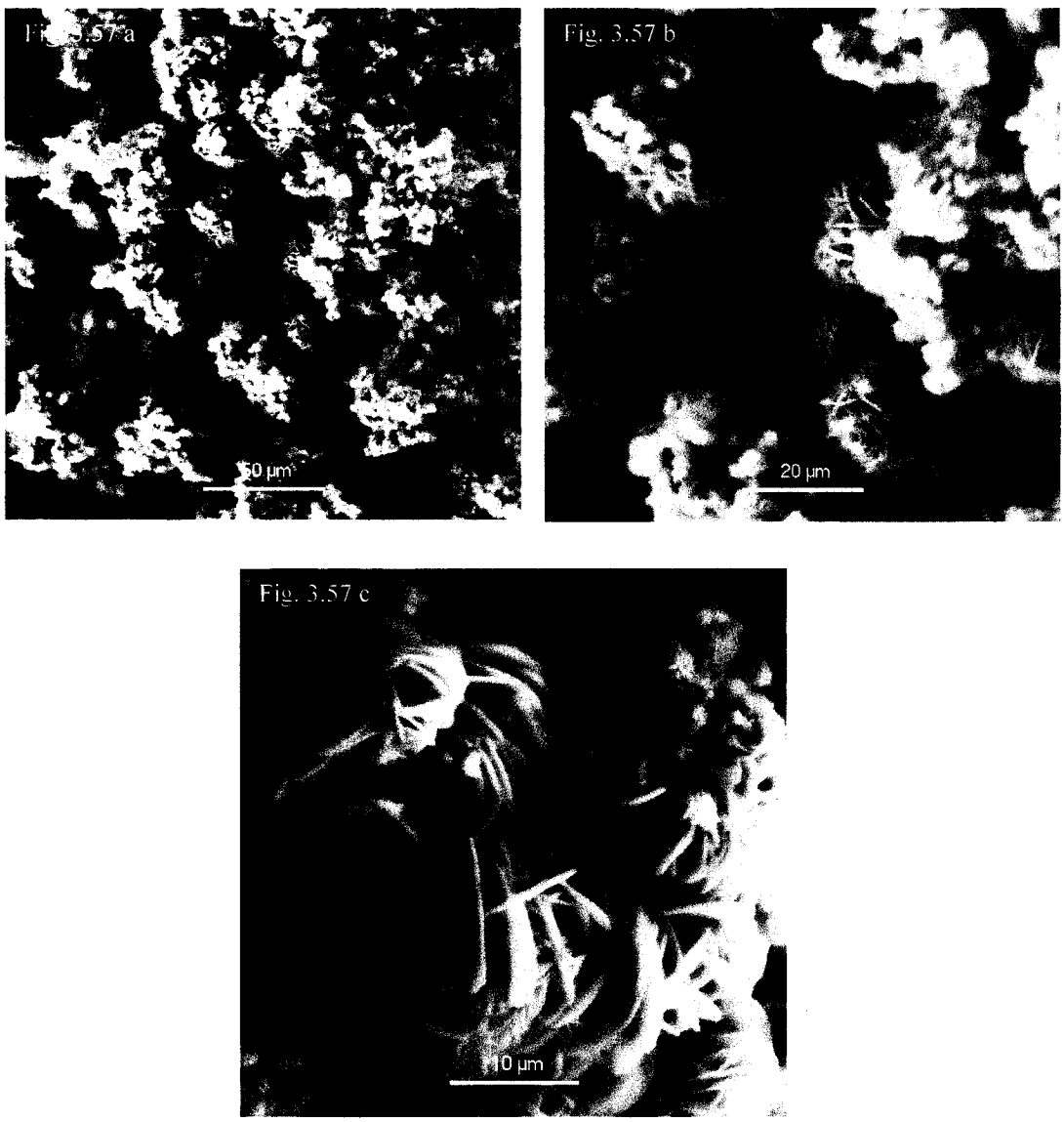

Figure 3.57 The corrosion layer had rosettes of disc-shaped crystals surrounded by a loose matrix, in Test 2 on Day 22 in areas close to the tubercles.

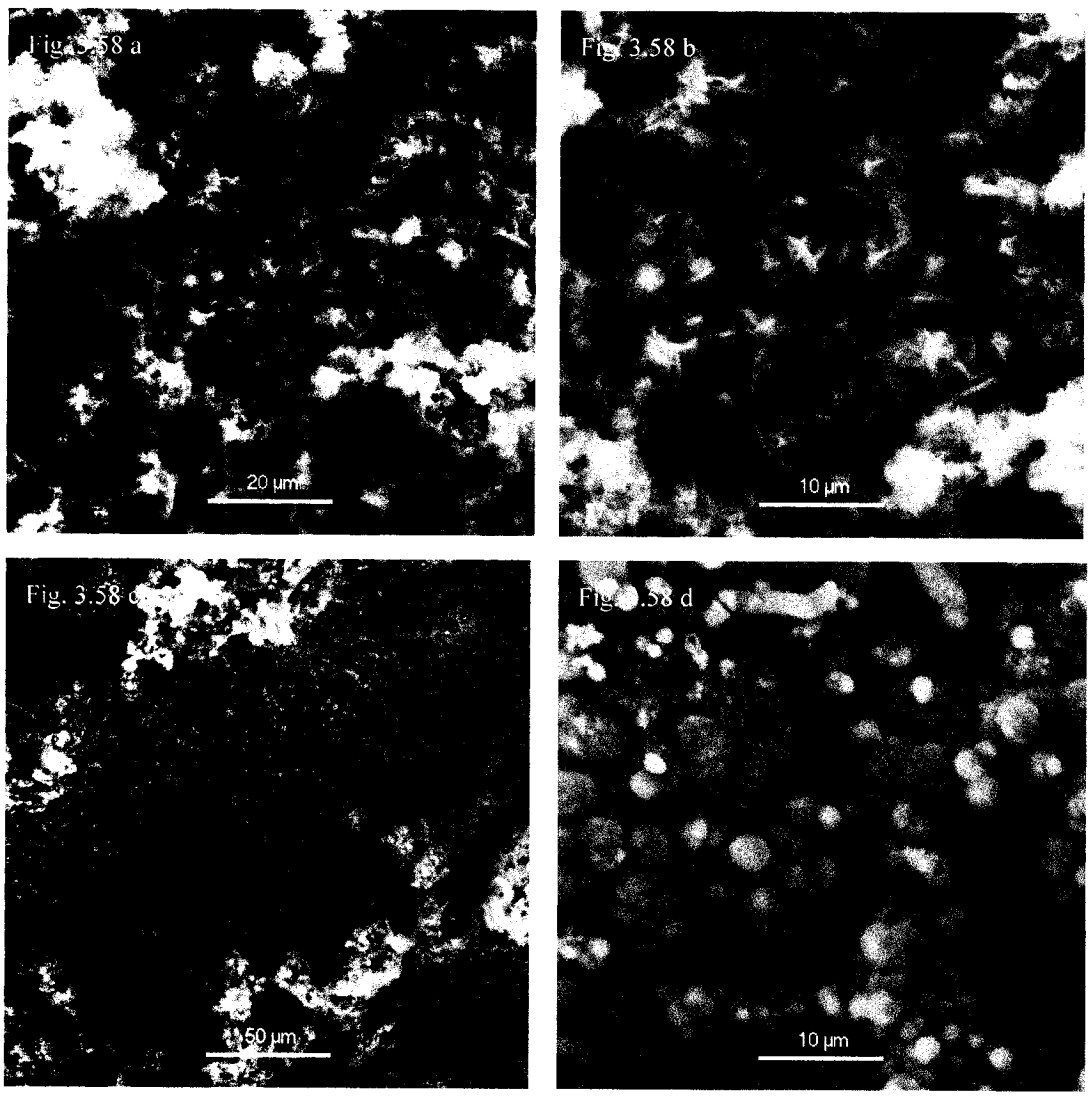

Figure 3.58 The corrosion layer also contained pointed disc-shaped crystal formations and, rounded ball-like formations in Test 2 on Day 22 in areas surrounding the tubercles.

Fig. 3.59 a

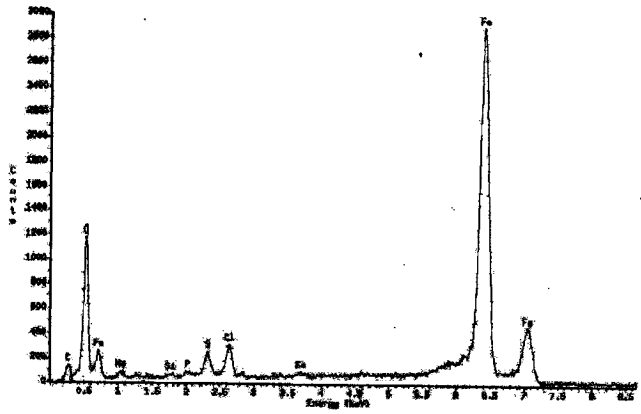

Fig. 3.59 b

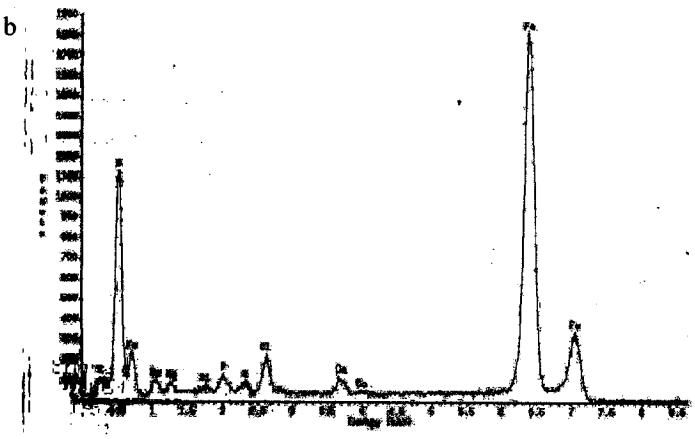

Fig. 3.59 c

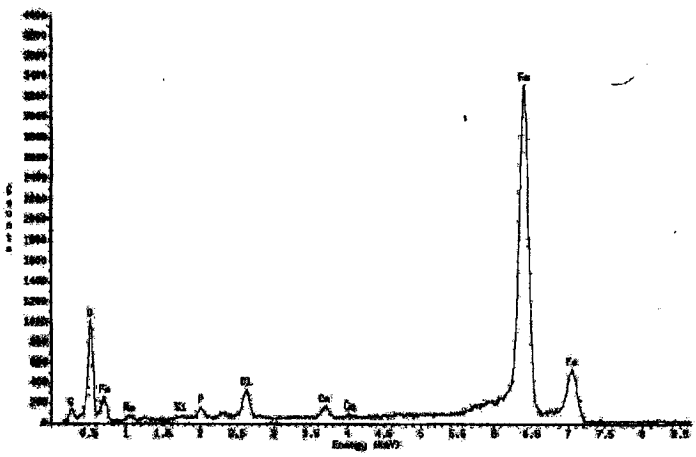

Figure 3.59 EDX analysis of the: a) rosettes of discs covered by loose matrices, b) pointed disc-shaped crystal formations, and c) rounded ball-like formations, showed O and Fe peaks, but the Fe peaks were more than twice those of the O peaks, in Test 2 on Day 22.

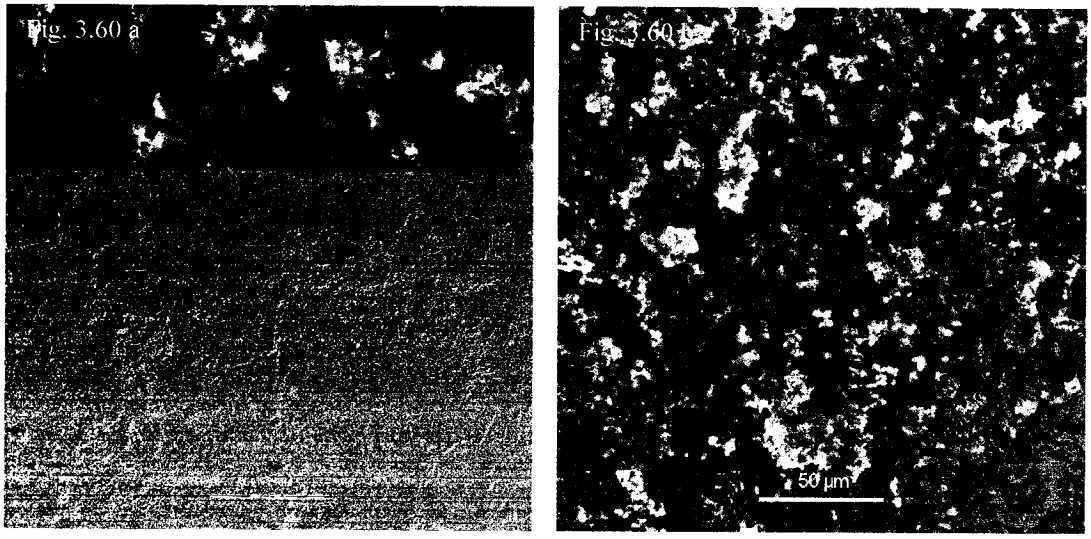

Figure 3.60 Low magnification micrographs of coupons taken from Test 4 on Day 22. The surface appeared smooth with: a) cracks, and b) irregularly distributed bits of rougher corrosion products.

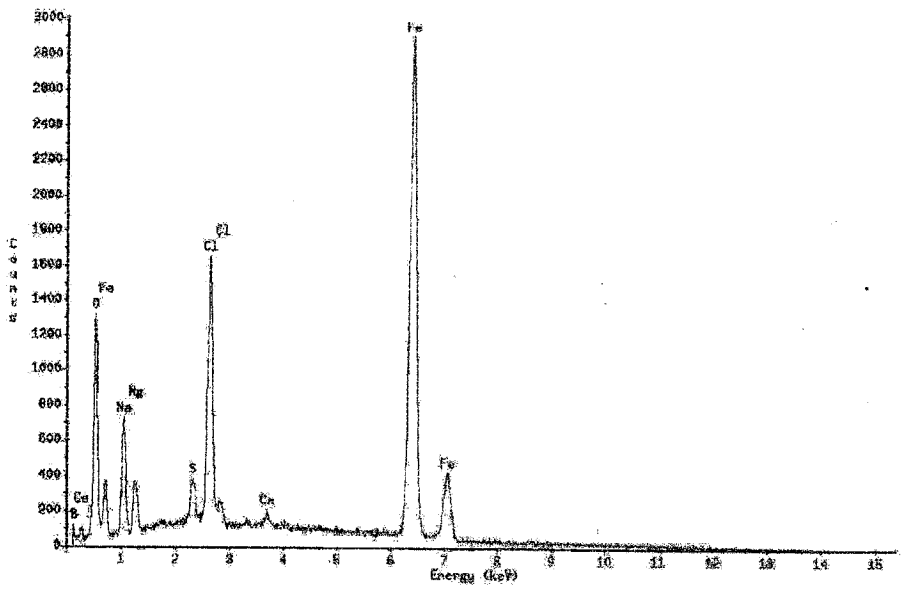

Figure 3.61 The very thin corrosion layer, in Test 4 on Day 22, showed high Fe, O, Cl and Na peaks.

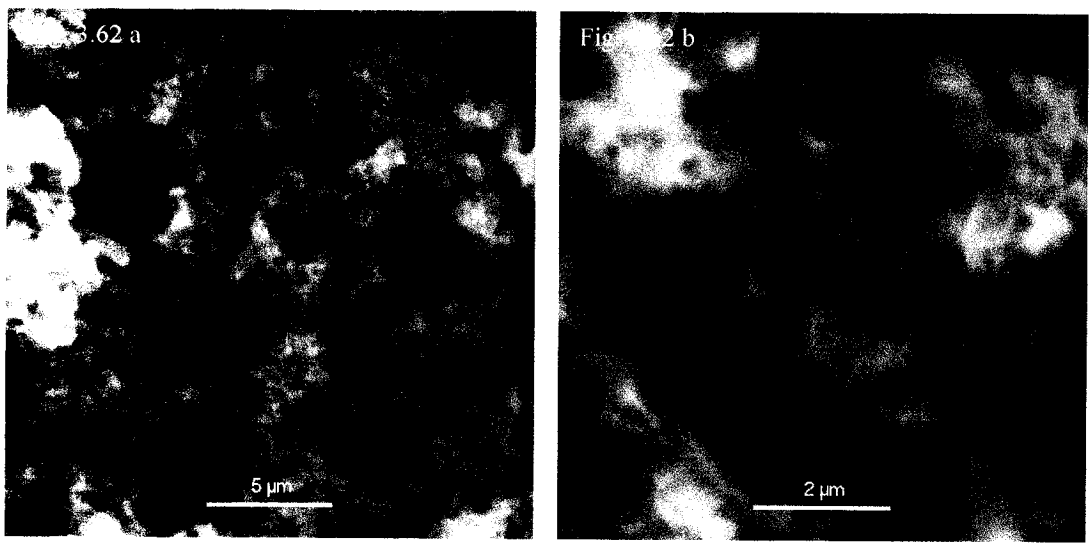

Figure 3.62 At higher magnification, strain BH1 cells were seen as transparent rods attached to the surface and the corrosion products, in Test 4 on Day 22.

Conclusion of corrosion results

1. Strain BH1 cells adhered to the coupon surfaces, thus behaving as barriers between the media and the coupon surface, and slowing down the corrosion process. Bumps of corrosion products, tubercles, were seen in these samples, and a type of pitting or localised corrosion was observed underneath the tubercles. In addition, the corrosion products formed in the samples with strain BH1 cells were different from the ones formed in sterile samples. This was illustrated by the continued adherence of the corrosion products to the coupon surface, in the bacterial samples, even after vigorous brushing. The distinct crystal formations visible through the ESEM, and the differences in the elemental composition of these formations from the ones found in sterile samples, again suggested, that strain BH1 plays a role in influencing the corrosion process.

2. Various physicochemical factors also affected the corrosion process. The agitation of the sample increased the rate of corrosion, perhaps due to the continued removal of the corrosion products from the surface, and the repeated exposure of the metal surface to the media or due to the increase in dissolved oxygen due to agitation. Decrease in temperature and oxygen in the sample tended to decrease the rate of corrosion. Under all the conditions tested, the rate of corrosion in the samples with strain BH1 was lower than the sterile samples.

3 The sequence of events taking place in the samples with strain BH1 can be hypothesized. The adherence of strain BH1 cells to the coupon surface leads to the formation of a barrier, which slows down the corrosion of the metal surface. However, in the agitated samples, the cells are intermittently sloughed off from the surface, in some areas. This causes the electrochemical corrosion reaction to proceed between the electrolyte and the metal surface, in those areas. Thus, an irregular buildup of corrosion products takes place over the surface. Over time, the build-up of strain BH1 cells and corrosion products, on the surface, leads to the formation of tubercles. Beneath these tubercles, a localized type of pitting corrosion is then initiated.

4. The roughness of the coupons increased the adherence of the corrosion products in the sterile samples. Under agitated conditions, the strain BH1 cells may have been able to adhere more strongly to the coupons with rougher surfaces. This, thus, slowed down the electrochemical corrosion reaction and also, prevented the formation of tubercles, in the rougher samples with strain BH1 cells. However, in the coupons with a smoother surface, the strain BH1 cells may not have been able to adhere as strongly and were easily sloughed off in some areas and, thus, the electrochemical corrosion reaction was able to proceed, causing an irregular build-up of corrosion products, on the surface. This, then, lead to the formation of tubercles in the smoother samples. Underneath these tubercles, the strain BH1 cells participated in the corrosion reaction in some way, leading to the formation of very adherent corrosion products.

4. DISCUSSION

"She is unsinkable". That is what they claimed, when the *Titanic* set off on her maiden and, last voyage. Now she rests 3.9 Km at the bottom of the ocean, a deep-sea grave for 1500 of those unlucky passengers who were on-board her, on that fateful night: 14th April, 1912. But this account is not of those passengers, but of other organisms that have since inhabited and claimed her as their home; the microorganisms that have changed her massive, solid frame into a fragile, rapidly disintegrating wreck.

Various studies (Stoffyn-Egli and Buckley, 1995; Wells and Mann, 1997; Cullimore *et al.*, 2002) have revealed the presence of sulphate-reducing bacteria, heterotrophic aerobic bacteria, slime-forming, microaerophilic iron-bacteria and other iron-oxidising bacteria, denitrifying bacteria, and a range of fungi, within the rusticles, that cover the ship's structures. One of these bacterial isolates, strain BH1 was the focus of the present study.

Identification of strain BH1

The 16S rRNA gene sequence comparison results revealed that strain BH1 belongs to genus *Halomonas* of family *Halomonadaceae*. It showed 98 % similarity with *H. variabilis* and, 96 % with *H. venusta*, *H. meridiana* and *H. aquamarina* (Table 19). The 16S rDNA phylogenetic consensus tree (Figure 4.1) determined by Arahal *et al.* (2002) showed that all these species were clustered in the same outgroup. The mean 16S rDNA sequence similarity for the outgroup was 97.4 % (Arahal *et al.*, 2002). Strain BH1 showed a mean 16S rDNA sequence similarity of 96.75 % with members of the outgroup suggesting that it may be a member of the outgroup.

Family *Halomonadaceae* belongs to the class gammaproteobacteria of the phylum *Proteobacteria* (Garrity and Holt, 2001). Members of the family *Halomonadaceae* are slight or moderate halophiles, found in intertidal zones, saline lakes and solar salt facilities. They are able to grow in NaCl concentrations varying from 0.1 - 32.5 %, but

Table 19: 16S rRNA gene sequence similarities between strain BH1 and other species of the family *Halomonadaceae.* Data taken from Arahal *et al.*, 2001, Arahal *et al.*, 2002, Berendes *et al.*, 1996, Bouchotrouch *et al.*, 2001, Dobson and Franzmann (unpublished, 1995), Dobson *et al.*, 1993, Duckworth *et al.*, 1996, Garriga *et al.*, 1998, Gauthier *et al.*, 1992, Mellado *et al.*, 1995, Miller *et al.*, 1994, Mormile *et al.*, 1999, Romano *et al.*, 1996, Thao *et al.*, 2000, Yoon *et al.*, 2001 and Yoon *et al.*, 2002.

Organism	**Strain**	**Percentage 16S rRNA gene sequence similarity**	**GenBank Accession number**
Halomonas alimentaria	YKJ-16	93%	AF211860
Halomonas aquamarina	DSM 30161	96%	AJ306888
Halomonas campisalis	ATCC 700597	93%	AF054286
Halomonas canadensis	DSM 6769	92%	AF211861
Halomonas cupida	ATCC 27124	91%	L42615
Halomonas desiderata	DSM 9502	94%	X92417
Halomonas elongata	ATCC 33173	92%	X67023
Halomonas eurihalina	ATCC 49336	92%	L42620
Halomonas halmophila	ATCC 19717	92%	AJ306889
Halomonas halodenitrificans	ATCC 13511	91%	L04942
Halomonas halodurans	ATCC 29686	93%	L42619
Halomonas halophila	DSM 4770	88%	M93353
Halomonas israelensis	DSM 6768	93%	AF211862
Halomonas magadiensis	NCIMB 13595	95%	X92150
Halomonas marina	ATCC 25374	92%	AJ306890
Halomonas marisflavae	KCCM 80003	91%	AF251143
Halomonas maura	DSM 13445	92%	AJ271864

Table 19: 16S rRNA gene sequence similarities between strain BH1 and other species of the family *Halomonadaceae*. Data taken from Arahal *et al.*, 2001, Arahal *et al.*, 2002, Berendes *et al.*, 1996, Bouchotrouch *et al.*, 2001, Dobson and Franzmann (unpublished, 1995), Dobson *et al.*, 1993, Duckworth *et al.*, 1996, Garriga *et al.*, 1998, Gauthier *et al.*, 1992, Mellado *et al.*, 1995, Miller *et al.*, 1994, Mormile *et al.*, 1999, Romano *et al.*, 1996, Thao *et al.*, 2000, Yoon *et al.*, 2001 and Yoon *et al.*, 2002 (continued).

Organism	Strain	Percentage 16S rRNA gene sequence similarity	GenBank Accession number
Halomonas meridiana	DSM 5425	96%	AJ306891
Halomonas pacifica	ATCC 27122	93%	L42616
Halomonas pantelleriensis	DSM 9661	94%	X93493
Halomonas salina	ATCC 49509	93%	AJ295145
Halomonas subglaciescola	DSM 4683	94%	AJ306892
Halomonas variabilis	DSM 3051	98%	AJ306893
Halomonas venusta	ATCC 27125	96%	AJ306894
Carnimonas nigrificans	CECT 4437	90%	Y13299
Chromohalobacter marismortui	ATCC 17056	93%	X87219
Chromohalobacter salexigens	ATCC 1705	92%	AJ295144
Zymobacter palmae	DSM 10491	90%	AF211871

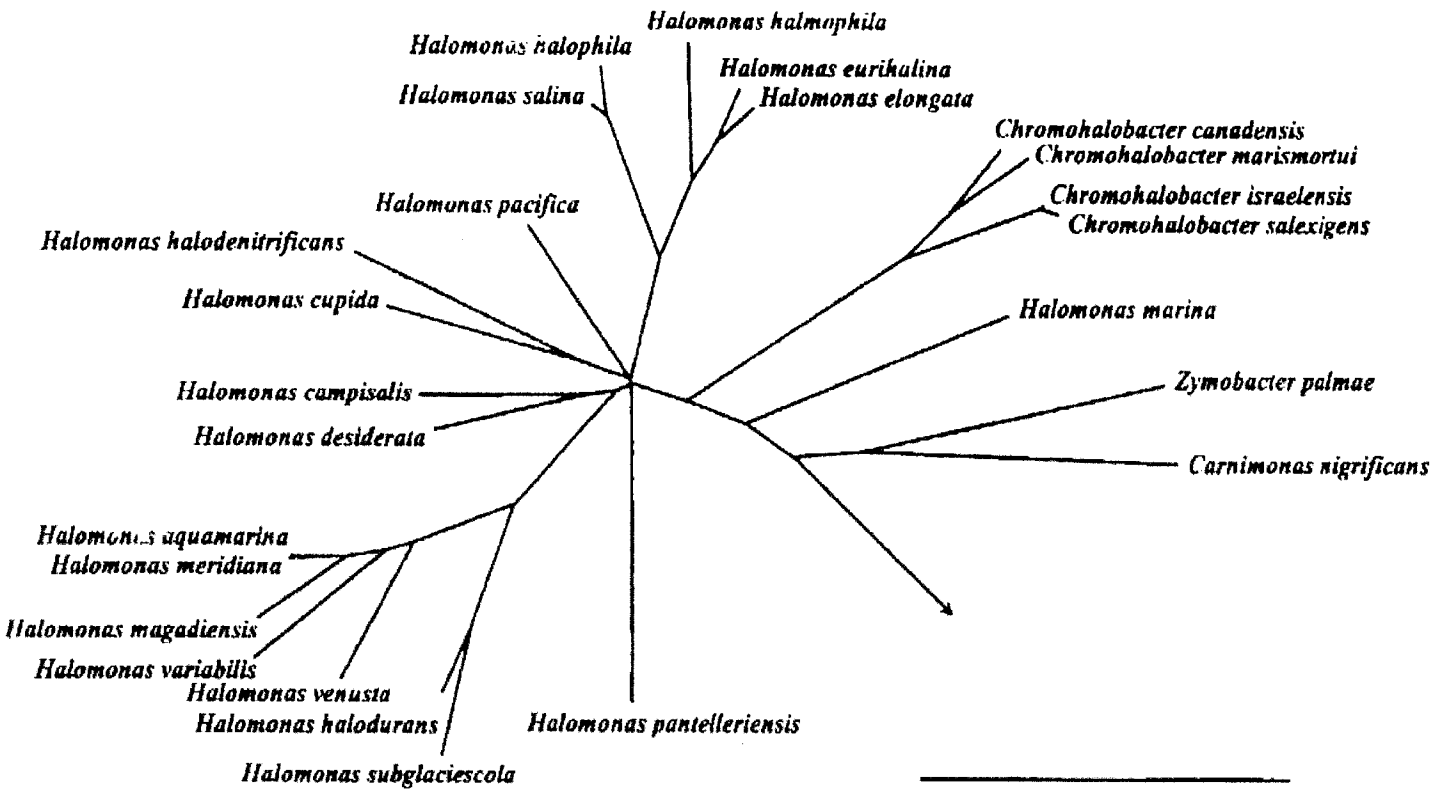

Figure 4.1 Phylogenetic consensus trees of members of the genera *Halomonas*, *Chromohalobacter*, *Zymobacter* and *Carimonas* constructed using 16S rDNA sequences. The arrow points to an outgroup, which has been removed to simplify the figure. Bar, 5% estimated sequence divergence. (Arahal *et al.*, 2002).

have an optimum of 8 % NaCl for growth. The type genus of this family, *Halomonas,* is rod shaped, Gram-negative, motile by 4 - 7 unsheathed lateral or polar flagella, halotolerant, forms white to yellow colonies and can survive in low dissolved oxygen (Vreeland *et al.,* 1980; Vreeland, 1984). The ultrastructure and light microscopy results illustrated all these characteristics in strain BH1.

The MIDI (fatty acid analysis) results identified strain BH1 as *Pseudomonas putida.* This disagreement in the identification, compared to the other test results, may be because the MIDI Microbial Identification System library used for the comparison of fatty acids did not include any members of family *Halomonadaceae.* That may also account for only 0.84 similarity index of strain BH1 with *P. putida.* Table 20 compares the fatty acids in strain BH1 with the fatty acids found in other species of *Halomonas* grown on similar media (TSA)- the fatty acid composition of bacterial cells varies with temperature, salinity and media composition (Monteoliva-Sanchez and Ramos-Cormenzana, 1986). It becomes apparent from the table that, the major fatty acids found in strain BH1 are similar to those found in other *Halomonas* species - $C_{16:0}$, $C_{18:1}$ ω7c, $C_{15:0}$ Iso 2OH and/or $C_{16:1}$ ω7c. Some of them have a high percentage of $C_{19:0}$ Cyclo ω8c, while strain BH1 does not. In other *Halomonas* species, grown on different media, also, the major fatty acids reported are $C_{18:1}$ ω7c, $C_{15:0}$ Iso 2OH and/or $C_{16:1}$ ω7c, $C_{16:0}$ and $C_{19:0}$ Cyclo 11-12 (Berendes *et al.,* 1996; Bouchotroch *et al.,* 2001; Franzmann and Tindall, 1990). This chemotaxonomic comparison further supports the inclusion of strain BH1 in genus *Halomonas.*

When the biochemical profile of strain BH1 was compared with the biochemical characteristics of other closely related species (Table 21 and 22), it was found that it showed the most similarities with *H. variabilis, H. desiderata* and *P. putida,*. However, *P. putida* is oval shaped, mono-flagellated and has only 87 % 16S rRNA gene sequence similarity, and *H. desiderata* is obligately alkaliphilic and has only 94% 16S rRNA gene sequence similarity.

Table 20: Cellular fatty acids profiles of strain BH1 and other *Halomonas* species grown on TSA. Values are percentages of total fatty acids. Data for *Halomonas pacifica, H. alimentaria, H. elongata, H. halodenitrificans,* and *H. cupida* taken from Yoon *et al.,* 2002 and data for *H. marisflavae* taken from Yoon *et al.,* 2001.

Fatty acid	Strain BH1	*H. pacifica*	*H. alimentaria*	*H. elongata*	*H. halodenitrificans*	*H. cupida*	*H. marisflavae*
10:0	-	2.4	1.9	2.7	-	2.8	1.1
10:0 3OH	2.84	0.3	0.2	0.9	-	0.2	-
12:0	1.64	1.6	-	3.6	0.6	3.9	2.2
12:0 2OH	5.13	0.1	0.1	0.1	-	0.2	1.9
12:0 3OH	3.78	5.9	5.2	7.5	6.9	7.1	9.1
12:1 3OH	0.17	-	-	-	-	-	-
14:0	0.28	0.2	1.2	0.1	0.4	0.2	0.9
15:0	0.22	0.2	0.6	0.1	0.1	0.1	-
16:0	27.65	26.0	27.0	24.8	24.7	23.4	28.0
16:0 3OH	-	-	-	0.2	-	-	-
17:0	0.28	0.4	0.2	0.3	0.2	0.6	-
17:0 Iso	0.13	0.3	-		-	0.1	-
17:0 cyclo	5.60	1.8	5.1	2.4	0.2	0.4	-
17:1 cyclo ω8c	0.2	-	-	-	-	0.2	-
18:0	0.51	0.4	0.2	0.3	0.2	0.6	1.1
18:1 ω7c	23.72	35.3	19.4	38.4	43.4	46.2	42.5
19:0 cyclo ω8c	0.35	14.3	12.9	12.7	0.8	1.3	0.8
^Summed feature 3	27.50	9.6	24.2	4.9	22.6	12.1	12.4
*** Other fatty acids**	-	1.2	1.8	0.6	-	0.5	-

^Summed feature 3 represents 16:1 ω7c and/or Iso 15:0 2OH

***Other fatty acids represent 18:1 cyclo ω9c and/or 11 methyl 18:1 ω7c and/or 19:0 and/or 20:2 cyclo ω6.9c and/or unknown fatty acids**

Table 21: Differential features among strain BH1 and other member of the family *Halomonadaceae.* Data was taken from Fendrich, 1988, Akagawa and Yamasato, 1989, James *et al.,* 1990, Arahal *et al.,* 2002.

Characteristic	Strain BH1	*Halomonas variabilis*	*Halomonas aquamarina*	*Halomonas meridiana*	*Halomonas venusta*
Rod - shaped	+	curved rods	+	+	+
Size of cells : length (µm)	2.0 - 6.0	1.0 - 3.0	4.0 - 6.0	1.9 - 4.5	
width (µm)	0.5 – 0.8	0.5 - 0.8	0.4 - 0.8	0.6 - 1.0	
Flagella present:	+	+	+	+	+
How many	2 - 6	1			
Kind	Pe	P	Pe	L	Pe
Colony characteristics	circular, off-white, raised	light brown, raised round			
NaCl tolerance range	0 - 20%	1.5 - 5.0%	0 - 20%	1 - 20%	
Optima	2.2 - 8%	2%			
Temperature (°C) range	4 - 37	15 - 37	5 - 40	0 - 55	4 – 40
Optima	27	31 - 34			
pH range	6.0 - 9.0	6.5 - 8.4	5.0 - 9.0	5.0 - 9.0	
Optima	7.0 - 8.0	7.5			
% 16S rRNA gene similarity	100%	98%	96%	96%	96%
Nitrate reduced to nitrite	-	-	-	-	+
Catalase	+	+			
Oxidase	+				
Glucose utilized	+	-	+	+	+
Glycerol	+	+	+	+	+
Sucrose	-	-	+	+	+
Mannose	+	-	+	+	-
Cellobiose	borderline	-			
Ornithine	-	-			
Lysine	-	-			
Gluconate	-				

Table 21: Differential features among strain BH1 and other member of the family *Halomonadaceae.* Data was taken from Fendrich, 1988, Akagawa and Yamasato, 1989, James *et al.,* 1990, Arahal *et al.,* 2002 (continued).

Characteristic	Strain BH1	*Halomonas variabilis*	*Halomonas aquamarina*	*Halomonas meridiana*	*Halomonas venusta*
Lactose	-	-			
Urease	-	+	-	+	+
Esculin	-	+	-	-	-
β-Galactosidase (ONPG)	-	-			
Indole	-	-			
Methyl red	-	-			
Voges-Proskauer	-	-			
Starch	-	-			

Table 22: Differential features among strain BH1 and other member of the family *Halomonadaceae* and *Pseudomonadaceae*. Data was taken from Arahal *et al.*, 2002, Berendes *et al.*, 1996, Vreeland *et al.*, 1980, Palleroni, 1984.

Characteristic	Strain BH1	*Halomonas magadiensis*	*Halomonas desiderata*	*Halomonas elongata*	*Pseudomonas putida*
Rod - shaped	+	.+	+	+	oval
Size of cells : length (µm)	2.0 - 6.0	4.0 - 6.0	1.0 - 2.6		2.0 - 4.0
width (µm)	0.5 – 0.8	0.6 - 0.8	0.4 - 0.6		0.7 - 1.1
Flagella present:	+	+	+	+	+
How many	2 - 6			4 - 7	1
Kind	Pe		Pe	P/L	P
Colony characteristics	circular, off-white, raised	round, cream coloured, raised		white raised round	
NaCl tolerance range	0 - 20%	0 - 20%	0 - 18%	0.1 - 32.5%	
Optima	2.2 - 8%	0 - 7%		3 - 8%	
Temperature (°C) range	4 - 37	20 - 50	10 - 45	15 - 45	
Optima	27	37	37 - 42		25 - 30
pH range	6.0 - 9.0	7.0 - 11.0	7.0 - 11.0	5.0 - 9.0	
Optima	7.0 - 8.0	9.0 - 10.0	9.0 - 10.0		
% 16S rRNA gene similarity	100%	95%	94%	92%	87%
Nitrate reduced to nitrite	-	+	+	+	
Catalase	+	+	+	+	+
Oxidase	+		+	+	+
Glucose utilized	+	+	+	+	+
Glycerol	+	+	+	+	+
Sucrose	-	+	+	+	-
Mannose	+	+	+	+	+
Cellobiose	borderline	+		+	-
Ornithine	-	+		+	+
Lysine	-	+		+	

Table 22: Differential features among strain BH1 and other member of the family *Halomonadaceae* and *Pseudomonadaceae.* Data was taken from Arahal *et al.,* 2002, Berendes *et al.,* 1996, Vreeland *et al.,* 1980, Palleroni, 1984 (continued).

Characteristic	Strain BH1	*Halomonas magadiensis*	*Halomonas desiderata*	*Halomonas elongata*	*Pseudomonas putida*
Gluconate	-	+	+	+	+
Lactose	-	+		+	-
Urease	-		-	+	
Esculin	-	+		+	
β-Galactosidase (ONPG)	-				
Indole	-	-	-		
Methyl red	-				
Voges-Proskauer	-		-		
Starch	-	-	-	-	-

Amann *et al.* (1992) showed that at high 16S rRNA gene homology values, DNA-DNA reassociation had a higher species resolving power than sequence analysis. Stackebrandt and Goebel (1994) showed that eventhough the correlation between 16S rRNA gene homology and DNA-DNA reassociation values was non-linear, yet, at sequence homologies below 97.5 %, it was unlikely that two organisms would have more than 60 to 70 % DNA similarity. Thus it seems unlikely that strain BH1 may be a strain of *P. putida* (87 %) or *H. desiderata* (94 %). The high (98 %) 16S rRNA gene sequence homology with *H. variabilis* advocates the need for DNA-DNA hybridization to be performed between *H. variabilis* and strain BH1. The significant differences in morphology- *H. variabilis* being obligately aerobic, vibrio-shaped and monoflagellated (Fendrich, 1988) - nevertheless, allude to strain BH1 being a new species of genus *Halomonas*.

Crude oil degradation

Petroleum and petroleum products, as pollutants, occupy an intermediary position between naturally degradable products and extremely recalcitrant man-made organics (Atlas and Bartha, 1972). The degradation and dispersion of crude oil by marine bacteria has been the subject of extensive research (Atlas and Bartha, 1972; Jobson *et al.*, 1972; Horowitz *et al.*, 1975; Cerniglia and Heitcamp, 1989; Leahy and Colwell, 1990; Delille and Siron, 1993, Siron *et al.*, 1995; Hedlund and Staley, 2001). A large number of species belonging to a wide range of genera exhibit the ability to breakdown and utilize the different components of crude oil (Floodgate, 1984).

Bouchotroch *et al.* (2000), Béjar *et al.* (1998) and Quesada *et al.* (1993) have studied this ability in two different species of *Halomonas*. Exopolysaccharides produced by *H. eurihalina* and *H. maura*, a newly identified species, showed great potential in emulsifying various hydrocarbons, some even better than control surfactants. *Halomonas salina*, another member of this family, has shown potential to degrade petroleum hydrocarbons (Bruheim and Eimhjellen, 1998).

In this study strain BH1 was tested for its ability to utilize Santa Barbara crude oil, by monitoring the increase in biomass as a function of time. No such increase was recorded even after 12 days of incubation at 27 °C - the temperature for maximum growth of the strain BH1. Even supplementing the artificial seawater medium with different concentrations of nitrogen and phosphorus – exogenous sources of which are known to enhance emulsification of oil (Reisfeld *et al.*, 1972; Bridle and Bos, 1971) – did not show any change in oil dispersion. Strain BH1 cells were found to be viable in Marine broth when removed from the test solution, indicating that they were not able to utilise the carbon in the crude oil.

Another way to perhaps test strain BH1 could be to extract its EPS and test them for degradation or dispersion of individual hydrocarbons. Also, supplementing BHS medium with a carbon source like glucose may allow the growth of strain BH1 cells, which may then be able to produce metabolites that are able to emulsify the hydrocarbons in crude oil.

Corrosion

Corrosion is a phenomenon that can have many adverse technical, economic and even social consequences, as it can lead to the deterioration in the properties of a metal (NACE, 1982; During, 1997). As corrosion is the result of a chemical or electrochemical interaction of a metal with its environment (NACE, 1982), it can be influenced by many factors: temperature, pH, dissolved oxygen, surface area, agitation, concentration of various electrolytes, stress, surface roughness, metal composition, polarization effect and even microorganisms (Wulpi, 1966; NACE, 1984; Fontana, 1986; ASM Metals Handbook, 1987; Borenstein, 1994; Sawant and Venugopal, 1996; During 1997; Medilanski *et al.*, 2002).

In an aqueous environment, it is the electrochemical corrosion reaction that takes place between the metal and the electrolyte, resulting in a flow of current between the different

portions of the metal that act as cathode and anode (Borenstein, 1994). This corrosion reaction can be affected by polarization, i.e. the accumulation of reaction products at one of the electrodes, which can then result in a halting of the corrosion process (During, 1997).

In the tests conducted on mild steel coupons, it was observed that the rate of corrosion was higher in the agitated samples compared to the static samples. Various authors (Ostroff, 1979; Borenstein, 1994; During, 1997) have reported that increased velocity of a system prevents the build up corrosion products at the electrodes, by constantly stripping them off and, thus, decreases the rate of polarization at the electrodes. This, in turn, exposes the bare metal surface and results in a higher rate of corrosion. The increased rate of corrosion in the agitated samples thus indicated that concentration polarization was taking place in the static samples.

In addition, the tests showed that there was a decrease in the rate of corrosion with a decrease in temperature and, dissolved oxygen in the sample. The decrease in corrosion due to decrease in temperature could be due to various factors: decrease in the rate of the electrochemical reactions (NACE, 1984), decrease in the current (Borenstein, 1994), and, decrease in the rate of diffusion of oxygen to the metal surface (ASM Metals Handbook, 1987).

Dissolved oxygen plays a primary role in the corrosion of steels (ASM Metals Handbook, 1987). In an aerated system, it continually depolarises the cathode by utilizing the protons that are being generated at the cathode (NACE, 1984). Whereas, in the deaerated system, a protective Fe_3O_4 layer is formed over the metal surface, that reduces or stops the corrosion (Borenstein, 1994). The reduction in corrosion, in the test samples, due to lower dissolved oxygen suggests that primarily an oxygen corrosion process was taking place in the samples.

Microorganisms, are also known, to affect corrosion. They are capable of forming biofilms by adhering to metal surfaces in aqueous environments (Fleming and Geesey, 1991; Verran and Hissett, 1997; White *et al.*, 1997). When mild steel coupons were placed in media containing strain BH1 cells, it was observed that strain BH1 cells were able to adhere to the surface. Most bacterial cells are recognised to have a net negative charge on their surface. In Gram-negative bacteria, acidic lipopolysaccharides and proteins in the outer cell membrane, are all sources of negative charge (Wicken, 1985). Strain BH1 cells probably interacted with the metal because they were negatively charged and therefore, electrostatically attracted to the positively charged iron surface, adhering to the surface using polymers (Cullimore, 1993). In addition, even if the net charge on both the metal surface and the bacterial cell was similar, the high ionic strength of the medium (Marine broth), would eliminate the electrostatic repulsion barrier, allowing adhesion to take place (Fletcher, 1996).

Also, in the present study, it was inferred that strain BH1 cells were more strongly adherent to rougher surfaces. This is in agreement with different researchers who have reported that higher surface roughness increases the extent of bacterial accumulation (Vanhaecke *et al.*, 1990; Verran *et al.*, 1991; Verran *et al.*, 1994; Barnes *et al.*, 1999), and adhesion takes place preferentially at surface irregularities (Geesey *et al.*, 1996).

Under all the physicochemical conditions tested, the results of the samples with strain BH1 were similar to the sterile controls, in that there was a decrease in the rate of corrosion with decrease in temperature and oxygen, and an increase with increase in agitation. But the rate of corrosion, in all the samples with strain BH1 cells, was lower compared to the sterile samples. This indicated that the adherent strain BH1 cells acted as a barrier, preventing the metal surface from coming in contact with the medium, thus slowing down corrosion. Gaylarde and Videla (1987) have emphasised the role of microbial adherence in the induction of passivity, in the process of microbially-induced corrosion.

However, the corrosion process was not entirely halted, but changed. The surface of the metal coupon was covered with tubercles (scattered knob-like mounds of corrosion and microbial products) and underneath these, localised corrosion or pitting was observed. This was, in contrast to, the uniform corrosion seen in the sterile samples. Various case histories, reported in the Corrosion Atlas (During, 1997), showing similar type of corrosion build-up, have been classified under oxygen corrosion and microbially induced corrosion. These phenomenon, which leads to localised or pitting corrosion are initiated by the formation of oxygen-concentration cells (Figure 4.2) over the metal surface (Videla, 2001).

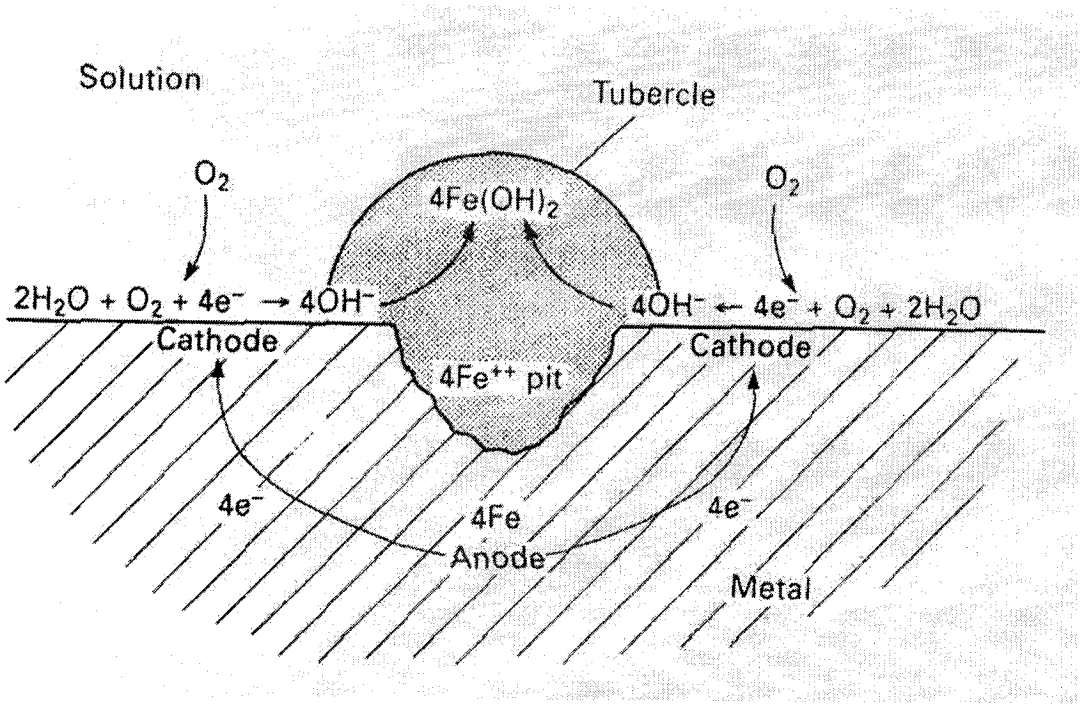

Figure 4.2 Oxygen concentration under tubercle (Tiller, 1986)

The initial oxidation and reduction reactions in an aerated system are:

M (Metal) $\longrightarrow$ $M^+ + e^-$ (oxidation reaction)

$O_2 + 2H_2O + 4e^- \longrightarrow 4\ OH^-$ (reduction reaction)

The microbial biofilms and the corrosion products together form knob-like mounds, tubercles, over the surface of the metal and create oxygen concentration cells (Tiller, 1986; Fleming and Geesey, 1991; Borenstein, 1994). Underneath the tubercles, the oxygen concentration is lowered because of low diffusion rate. But the oxidation reaction continues and a pit is initiated. So, to support the oxidation reaction underneath the tubercles, the rate of oxygen reduction, on the surface not covered by tubercles, increases. This leads to an excess of M^+ ions within the pit. To balance these, chloride ions from the electrolyte are attracted to the pit, leading to a lowering of pH, which can further accelerate the corrosion rate within the pit (Borenstein, 1994).

This type of microbially influenced corrosion has been reported in iron oxidising bacteria like *Gallionella*, *Sphaerotilus*, *Leptothrix*, etc., (Tatnall, 1981; Fleming and Geesey, 1991; During, 1997). Iron oxidising bacteria are chemolithotrophs that utilize the energy generated by the oxidation of Fe^{3+} to Fe^{2+} to produce ATP (Moat and Foster, 1988; Fleming and Geesey, 1991). They can also grow as heterotrophs (Moat and Foster, 1988). Low, cone-shaped, red-brown mounds, made up of deposits of metal oxide, are typically observed on top of the pits that are formed due to the oxygen concentration cells, which are initiated by the attachment of the iron-oxidising bacteria to the metal surface (Kobrin, 1976; Borenstein, 1994). The localised corrosion seen underneath the tubercles, in the present study, supports the theory that a similar kind of mechanism may be taking place when strain BH1 cells adhere to the metal surface.

The ESEM micrographs and the EDX analysis illustrated the formation of goethite (Roh *et al.*, 2000) and green rust crystals (Gu *et al.*, 1999) in the samples with strain BH1. Cells of strain BH1 were seen embedded within these corrosion products. Various authors (Edyvean, 1984; Myneni *et al.*, 1997; Gu *et al.*, 1999; Watson *et al.*, 1999; Phillips *et al.*, 2000; Roh *et al.*, 2000) have characterised the formation of corrosion products like goethite, lepidocrocite, magnetite, green rust, etc, under oxidising conditions, in the presence of microorganisms. Videla (2001) also reported the formation

of goethite and hematite as corrosion products, on carbon steels, when exposed to a mixed culture of SRB (sulphate-reducing bacteria) and *Vibrio*. The formation of similar corrosion products as found in other documented cases of microbially influenced corrosion, adds weight to the conclusion that strain BH1 is involved in microbially influenced corrosion of mild steel coupons.

Different members of the class gammaproteobacteria, e.g. *Pseudomonas*, *Vibrio*, *Escherichia*, etc, have been implicated in microbially induced corrosion (Tatnall, 1981; Gaylarde and Videla, 1987; Dowling *et al.* 1988; Videla, 2001). However, this is the first report of any member of family *Halomonadaceae*, belonging to genus *Halomonas*, being involved in microbially influenced corrosion.

Titanic and the rusticles

The complex structures of the rusticles, found on the *Titanic*, with their goethite-dominated mesh-like matrix, iron-plate like structures, porous spongelike regions, water channels, ducts and thread-like spans, provide various sites with a range of physicochemical conditions suitable for the growth of diverse and site-focused microbes (Stoffyn-Egli and Buckley, 1995; Mann, 1997; Pellegrino and Cullimore, 1997; Wells and Mann, 1997; Cullimore and Johnston, 2000). Stoffyn-Egli and Buckley (1995) identified a wide array of mineral precipitates, within the rusticles, that were stable at very different oxidation-reduction potentials and pH conditions (6.0 - 8.2). In addition, Brown (1997) reported that the restricted flow of water within some of the structures creates higher salt concentrations than the surrounding seawater. Since strain BH1 has a wide pH (6.0 – 9.0) and salt tolerance range (0.26 to 20 % NaCl), it would be able to survive in a number of different formations within the rusticles. The rod-shaped formations covered by lepidocrocite that were found on the outer surface of the iron-oxyhydroxide shell of the rusticles, as reported by Stoffyn-Egli and Buckley (1995), and Wells and Mann (1997) are very similar in size and shape to strain BH1 cells.

The crystal structures and formations seen in the dark knob-like mounds (tubercles) formed on the surface of metal coupons with strain BH1, resemble the goethite and green rust matrices found in rusticles (Stoffyn-Egli and Buckley, 1995; Cullimore and Johnston, 2000; Cullimore *et al.,* 2002). Since strain BH1 was originally isolated from rusticles, these results implicate their role in the formation of these rusticles. However, they, almost certainly, must have been interacting and forming consortial associations with other bacterial, fungal and microbial communities, found within the rusticles. Many corrosion scientists have documented that corrosion processes are enhanced, when a wide variety of microorganisms are present in a biofilm (Tatnall, 1981; Gaylarde and Johnston, 1982; Dowling *et al.,* 1990; Jain, 1995) formed over the metal surface.

Cullimore *et al.* (2002) suggest that consortia may be vital or transient, depending upon whether the strains involved in their formation can function independently, when removed from the consortium. Since strain BH1 was successfully cultured in the laboratory, it lends support to the understanding that the rusticles are made of transient consortia, containing species that may have arrived from the water column (Takami *et al.,* 1997; Simon *et al.,* 2002) as macroaggregates and attached to the *Titanic* or the rusticles and helped in their growth.

The rusticles, in addition to being habitats for various species of microorganisms, can have other impacts. The ability of the tubercles and rusticles to extract iron from steel structures can have various implications for the ship industry, pipelines, oil rigs, water wells and other steel-fabricated structures, by affecting the integrity of these structures. In addition, the iron that is released from rusticles, as "red dust" and "yellow colloids", into the ocean, may have a health impact, as it may be able to enter the food chain (Cullimore *et al.,* 2002). Nevertheless, this may also be a way in which the iron from these structures is returned back into the natural biogeochemical cycles. The structures of the tubercles and rusticles also provide various sites with a potential for bioaccumulation of other hazardous chemicals within their matrices (Alford, 1999; Cullimore *et al.,* 2002).

Thus, there is a continuing need to study and understand the microbially influenced processes taking place in the rusticles.

Future research

DNA-DNA hybridization studies with other species of the genus *Halomonas,* which have closely related 16S rRNA gene sequences, will help to determine the species identity of strain BH1. If the DNA homology values are low, then it would indicate that strain BH1 is a new species of genus *Halomonas*, which can then be named and classified.

Strain BH1 could be tested for the production of exopolysaccharides. These could be extracted and evaluated for their potential industrial applications: food, pharmaceutical and petroleum industries. Perhaps the EPS polymers may be better capable of emulsifying and viscosifying the hydrocarbons found in petroleum and petroleum products.

The exact mechanism of microbially influenced corrosion (MIC) of strain BH1 can be determined by carrying out electrochemical tests like, corrosion potential measurements (Hadley, 1943; Wanklin and Spruit, 1952), redox potential measurements (Starkey and Wight, 1945), potentiodynamic-sweep techniques (Salvarezza *et al.,* 1979), split-cell measurements (Little *et al.,* 1986), etc (Videla, 2001). The role of other species of genus *Halomonas* in MIC can be investigated.

Deep oceanic degradation of steel structures can be understood by studying the *RMS Titanic*. Cullimore and Johnston (2000) have initiated in situ studies of the corrosion rates and rusticle formation processes, by placing platforms with different types of steel at the site of the wreck. The observation and results of that study will help in gaining a better understanding of the consortial nature of microbes, perhaps even to identify the pioneer species and to understand the various stages of rusticle development. Other

members of the consortia could be identified and characterised. Fluorescently-labelled DNA probes, consisting of single-stranded oligonucleotide sequences, designed from the conserved regions of the 16S rRNA gene of strain BH1, can be used to visualise the presence of the strain in the rusticles by *in situ* hybridisation (Amann and Schleifer, 2001). This can assist in identifying the niche of strain BH1 within the rusticles. Probes could also be designed to see if other members of family *Halomonadaceae* were also part of the rusticular consortium.

The results of this study can be related to the rusticle-like structures that cause plugging of water wells and may even help in designing strategies for their control.

5. CONCLUSION

Strain BH1, recovered from the rusticles of the *Titanic*, was found to be Gram negative, rod-shaped, and peritrichously flagellated. Its 16S rRNA gene sequence showed that it belonged to genus *Halomonas* of family *Halomonadaceae*. The pH, temperature and salt tolerance ranges were 6.0 to 9.0, 4 °C to 37 °C and 0.26 to 20.0 % NaCl, respectively. It was found to be catalase and oxidase positive; methyl red and urease negative. It was unable to grow on starch, sucrose, mannitol, inositol, sorbitol, rhamnose, amygdalin, arabinose, erythritol, adonitol, B-methyl-xyloside, dulcitol, a-methyl-D-mannoside, a-methyl-D-glucoside, esculin, salicin, lactose, maltose, trehalose, inulin, glycogen, and 2-keto-gluconate. It was able to utilize glucose, arginine, citrate, melibiose, ribose, L-arabinose, D-xylose, galactose, D-fructose, D-mannose, and D-fucose. The major fatty acids found in strain BH1: $C_{16:0}$, $C_{18:1}\omega7c$ and $C_{15:0}$ Iso 2OH and/or $C_{16:1}$ $\omega7c$, were similar to those found in other species of *Halomonas*. Strain BH1 showed 98 % 16S rRNA gene sequence similarity with *Halomonas variabilis*. At this high level of gene sequence similarity, DNA-DNA hybridisation is required to confirm whether it is a strain of *H. variabilis* or a novel species.

Strain BH1 was unable to utilise the hydrocarbons present in Santa Barbara crude oil, for growth.

Strain BH1 was able to cause microbially influenced corrosion, by adhering to the surface of mild steel coupons, and causing the development of oxygen concentration cells. The sequence of events taking place between the metal and strain BH1 cells can be hypothesized. Strain BH1 cells adherent to the coupon surface, act as a barrier between the metal surface and the electrolytes in the medium, slowing down the corrosion. However, in the agitated samples, the cells are intermittently sloughed off from the surface, in some areas. This causes the electrochemical corrosion reaction to proceed in those areas. Thus, an irregular buildup of corrosion products takes place over the surface. Over time, the build-up of strain BH1 cells and corrosion products, on the surface, leads

to the formation of tubercles. Beneath these tubercles, oxygen concentration cells are created, which cause localized corrosion or pitting.

The rate of corrosion was influenced by physicochemical factors like temperature, dissolved oxygen, and agitation. A decrease in temperature and dissolved oxygen resulted in a decrease in the rate of corrosion. Similarly, agitation had a direct influence on the rate of corrosion. Compared to sterile samples, the corrosion products were more adherent in the samples with strain BH1, indicating that different corrosion products were being formed in each. ESEM demonstrated various structural formations: rosettes of discs covered by loose matrices, pointed disc-shaped crystal formations, and rounded ball-like formations, in the samples with strain BH1. Rod-shaped strain BH1 cells were seen embedded within the corrosion products. EDX analysis implied that the ferrous and ferric, hydroxide and oxyhydroxide crystals seen may be goethite and green rust.

Rusticles with their complex structural formations, composed, predominantly, of goethite, lepidocrocite and green rust, provide various sites for the existence of strain BH1. In addition, its capability of causing microbially influenced corrosion suggests that it might play a role in the formation of these rusticles, or might, be a species just occupying a niche within the rusticles. However, the rusticles are not single-species structures, but a result of the cooperative action of a multiplicity of microbial and higher forms. Thus, strain BH1 is, probably, a member of a transient consortium of species that have colonized the rusticles.

Most of the previous studies on rusticular microorganisms have only identified the categories/groups of microorganisms found in conjuction with the rusticles. Strain BH1 is the first isolate from the rusticles, whose exact genus identification has been determined. This is also the first report of any member of genus *Halomonas*, found at that those depths. The unique habitat from which it was isolated, and its ability to influence corrosion, substantiates the novelty of the strain.

6. REFERENCES

AGHTM Biofilm European Working Group 1997 Standard method to evaluate aquatic biofilms. In: *Biofilms in the aquatic environment*, C.W. Keevil, A. Godfree, D. Holt and C. Dow (eds), The Royal Society of Chemistry, Cambridge. pp. 210 - 219.

Akagawa, M. and Yamasato, K. 1989 Synonymy of *Alcaligenes aquamarina*, *Alcaligenes faecalis* subsp. *homari*, and *Deleya aesta*: *Deleya aquamarina* comb. nov. as the type species of the genus *Deleya*. *International Journal of Systematic Bacteriology* **39**: 462 – 466.

Albaiges, J. 1989 Marine pollution: an introduction. In: *Marine pollution*, J. Albaiges (ed.), Hemisphere Publishing Corp., New York. pp. 1 - 10.

Alford, G. 1999 Discussion: Final Comment. In: *The Application of Heat and Chemicals in the Control of Biofouling Events in Wells*, G. Alford and D.R. Cullimore (eds.), Lewis Publishers, Boca Raton, FL. pp. 157 – 162.

Allison, D.G. and Sutherland, I.W. 1987 The role of exopolysaccharides in adhesion of freshwater bacteria. *Journal of General Microbiology* **133**: 1319 - 1327.

Amann, R. and Schleifer, K-H, 2001 Nucleic acid probes and their application in environmental microbiology. In: Bergey's Manual of Systematic Bacteriology, D.R. Boone and R.W. Castenholz (eds.), 2nd Edition, Springer, New York. pp. 67 – 99.

Amann, R.I., Lin, C., Key, R., Montgomery, L. and Stahl, D.A. 1992 Diversity among *Fibrobacter* strains: towards a phylogenetic classification. *Systematic and Applied Microbiology* **15**: 23 - 31.

Arahal, D.R., Garcia, M.T., Ludwig, W., Schleifer, K.H. and Ventosa, A. 2001 Transfer of *Halomonas canadensis* and *Halomonas israelensis* to the genus *Chromohalobacter* as *Chromohalobacter canadensis* comb. nov. and *Chromohalobacter israelensis* comb. nov. *International Journal of Systematic and Evolutionary Microbiology* **51**(4): 1443 – 1448.

Arahal, D.R., Wolfgang, L., Schleifer, K.H. and Ventosa, A. 2002 Phylogeny of the family *Halomonadaceae* based on 23S and 16S rDNA sequence analyses. *International Journal of Systematic and Evolutionary Microbiology* **52**: 241 – 249.

ASM Metals Handbook 1987 *Corrosion*. Vol 13. ASM International, Metals Park, OH.

Atlas, R.M. 1984 *Petroleum Microbiology*. Macmillan Press, New York. 692 pp.

Atlas, R.M. and Bartha, R. 1972 Degradation and mineralization of petroleum by two bacteria isolated from coastal waters. *Biotechnology and Bioengineering* **14**: 297 – 308.

Austin, B. 1988 Microbiology of the deep sea. In: *Marine Microbiology*, B. Austin (ed) Cambridge University Press, Cambridge. pp. 133 - 176.

Ballard, R.D. 1989 *The Discovery of the Titanic.* Penguin/Madison Press Books, Ontario, 238 pp.

Barnes, L-M., Lo, M. F., Adams, M.R. and Chamberlain, A.H.L. 1999 Effect of milk proteins on adhesion of bacteria to stainless steel surfaces. *Applied and Environmental Microbiology* **65:** 4543 - 4548.

Béjar, V., Llamas, I., Calvo, C. and Quesada, E. 1998 Characterisation of exopolysaccharides produced by 19 halophilic strains of the species *Halomonas eurihalina. Journal of Biotechnology* **61**: 135 - 141.

Benson, H.J. 1998 *Microbiological applications: Laboratory Manual of General Microbiology.* 7th ed. The McGraw-Hill Companies Inc., Dubuque, Iowa. 468 pp.

Berendes, F., Gottschalk, G., Heine-Dobbernack, E., Moore, E.R.B. and Tindall, B.J. 1996 *Halomonas desiderata* sp. nov., a new alkaliphilic, halotolerant and denitrifying bacterium isolated from a municipal sewage works. *Systematic and Applied Microbiology* **19**: 158 - 167.

Beveridge, T.J., Popkin, T.J. and Cole, R.M. 1994 Electron Microscopy. In: *Methods for General and Molecular Bacteriology,* P. Gerhardt, R.G.E. Murray, W.A. Wood, N.R. Krieg (eds.), American Society for Microbiology, Washington, DC.

Blasco, S. Bedford Institute of Oceanography, Dartmouth, NS, Canada. Personal communication.

Bockris, J.O.M. and Reddy, A.K.N. 1970 *Modern Electrochemistry.* Vol. 2. MacDonald & Co., London. pp. 1267 - 1350.

Booth, G.H. 1971 *Microbial corrosion.* Monograph CE/1. Mills & Boon.

Borenstein, S.W. 1994 Microbiologically influenced corrosion handbook, Industrial Press Inc., New York.

Bouchotrouch, S., Quesada, E., Izquierdo, I., Rodriguez, M. and Béjar, V. 2000 Bacterial exopolysaccharides produced by newly discovered bacteria belonging to the genus *Halomonas*, isolated from hypersaline habitats in Morocco. *Journal of Industrial Microbiology and Biotechnology* **24**: 374 – 378.

Bouchotrouch, S., Quesada, E., del Moral, A., Llamas, I. and Béjar, V. 2001 *Halomonas maura* sp. nov., a novel moderately halophilic, exopolysaccharide-producing bacterium. *International Journal of Systematic and Evolutionary Microbiology* **51**: 1625 - 1632.

Brenner, D.J., McWhorter, A.C., Leete Knutson, J.K. and Steigerwalt, A.G. 1982 *Escherichia vulneris*, a new species of *Enterobacteriaceae* associated with human wounds. *Journal of Clinical Microbiology* **15**: 1133 – 1140.

Brenner, D.J., Staley, J.T. and Krieg, N.R. 2001 Classification of prokaryotic organisms and the concept of bacterial speciation. In: *Bergey's Manual of Systematic Bacteriology*, D.R. Boone and R.W. Castenholz (eds.), 2nd Edition, Vol 1, Springer-Verlag, New York. pp. 27 – 31.

Bridle, A.L. and Bos, J. 1971 Biological degradation of mineral oil in sea water. *Journal of Inst. Petroleum* **57**: 270 – 277.

Brown, M. 1997 The identification of a bacteria pure cultured from and analysis of the elemental and structural composition of a rusticle taken from the *R.M.S. Titanic*. B.Sc. (Honours) thesis, Dalhousie University.

Bruheim, P. and Eimhjellen, K. 1998 Chemically emulsified crude oil as substrate for bacterial oxidation: differences in species response. *Canadian Journal of Microbiology* **44**: 195 - 199.

Cerniglia, C.E. and Heitcamp, M.A. 1989 Microbial degradation of polycyclic aromatic hydrocarbons in the aquatic environment. In: *Metabolism of polycyclic aromatic hydrocarbons in the aquatic environment*, U. Varanasi (ed), CRC Press, Boca Raton, FL. pp 41 – 68.

Christensen, B.E. 1989. The role of extracellular polysaccharide biofilms. *Journal of Biotechnology* **10**: 181 - 202.

Christensen, B.E. and Characklis, W.G. 1990 Physical and chemical properties of biofilms. In: *Biofilms*, W.G. Characklis and K.C. Marshall (eds.), John Wiley, New York. pp. 93 - 130.

Cooksey, K.E. 1992 Extracellular polymers in biofilms. In: *Biofilms: Science and Technology*, L.F. Melo, M.M. Fletcher and T.R. Bott (eds.), Kluwer Academic Publishers, Dordrecht. pp. 137 - 147.

Costerton, J.W., Cheng, K.-J., Geesey, G.G., Ladd, T.I., Nickel, J.C., Dasgupta, M. and Marrie, T.J. 1987 Bacterial biofilms in nature and disease. *Annual Review of Microbiology* **41**: 435 - 464.

Costerton, J.W., Lewandowski, Z., Caldwell, D.E., Korber, D.R. and LappinScott, H.M. 1995 Microbial biofilms. *Annual Reviews of Microbiology* **49**: 711 - 745.

Costerton, J.W., Marrie, T.J. and Cheng, K.J. 1985 Phenomena of bacterial adhesion. In *Bacterial Adhesion*, D.C. Savage and M. Fletcher (eds.), Plenum Press, New York. pp. 3 - 43.

Crosa, J., Brenner, D.J. and Falkow, S. 1973 Use of a single-strand specific nuclease for the analysis of bacterial and plasmid DNA homo- and heteroduplexes. *Journal of Bacteriology* **115**: 904 – 911.

Cullimore, D.R. 1993. *Practical Manual of Ground Water Microbiology*. CRC Press, Boca Raton, FL.

Cullimore, D.R. 1999 IV Titanic: the connection between rusticles and clogging. In: *The Application of Heat and Chemicals in the Control of Biofouling Events in Wells,* Alford, G.A. and Cullimore, D.R. (eds.), Lewis Publishers, Boca Raton, FL.

Cullimore, D.R. and Johnston, L. 2000 Biodeterioration of the RMS *Titanic*. *Canadian Chemical News* Nov/Dec: 14 – 15.

Cullimore, D.R., Pellegrino, C. and Johnston, L. 2002 *RMS Titanic* and the emergence of new concepts on consortial nature of microbial events. *Reviews of Environmental Contamination and Toxicology* **173**: 117 - 141.

Delille, D. and Siron, R. 1993 Effect of dispersed oil on heterotrophic bacterial communities in cold marine waters. *Microbial Ecology* **25**: 263 – 273.

Dexter, S.C. 1976 Influence of substrate wettability on the formation of bacterial slime films on solid surfaces immersed in natural seawater. In *Proceedings of the 4th International Congress on Marine Corrosion and Fouling*, Juan Les Pins, Antibes, France. pp. 137 - 144.

Difco 1984 *DIFCO MANUAL Dehydrated Culture Media and reagents for Microbiology*. 10th ed. Difco Laboratories, Michigan, 1155 pp.

Dobson , S. J., McMeekin, T. A. and Franzmann, P. D. 1993 Phylogenetic relationships between some members of the genera *Deleya*, *Halomonas* and *Halovibrio*. *International Journal of Systematic Bacteriology* **43**: 665 - 673.

Dowling, N.J.E., Guezennec, J., Lamoine, M.L., Tunlid, A. and White, D.C. 1988 Analysis of carbon steels affected by bacteria using electrochemical impedance and direct counting techniques. *Corrosion* **44**: 869 – 874.

Dowling, N.J.E., White, D.C., Buchanan, R.A., Danko, J.C., Vass, A. and Brooks, S. 1990 Microbiologically influenced corrosion of 6 % molybdenum stainless steels and AISI 316: comparison with ferric chloride testing. In: *The Conference Proceedings of the National Association of Corrosion Engineers*, Corrosion/90, Paper no. 532, Las Vegas.

Duckworth, A.W., Grant, W.D., Jones, B.E. and Van Steenbergen, R.P. 1996 Phylogenetic diversity of soda lake alkaliphiles. *FEMS Microbiology Ecology* **19**: 181 - 191.

During, E.D.D. 1997 *Corrosion Atlas. A collection of illustrated case histories.* Elsevier Science Publishers B.V., Netherlands. 689 pp.

Edwards, U., Rogall, T., Blöcker, H., Emde, M. and Böttger, E.C. 1989 Isolation and direct complete nucleotide determination of entire genes. Characterization of coding for 16S ribosomal RNA. *Nucleic Acid Research* **17**(19): 7843 - 7853.

Edyvean, R.G.J. 1984 Interactions between microfouling and the calcareous deposit formed on cathodically protected steel in seawater. In: *Proceedings of the 6th International Congress on Marine Corrosion and Fouling. Marine Biology.* Athens, Greece. pp. 469 – 483.

Fendrich, C. 1988 *Halovibrio variabilis* gen. nov. sp. nov., *Pseudomonas halophila* sp. nov. and a new halophilic aerobic coccoid eubacterium from great salt lake, Utah, USA *Systematic and Applied Microbiology* **11**: 36 – 43.

Fleming, H.C. and Geesey, G.G. 1991 *Biofouling and Biocorrosion in Industrial Water Systems.* Springer-Verlag, New York.

Flemming, H.C., Wingender, J., Moritz, R., Borchard, W. and Mayer, C. 1997 Physico-chemical properties of biofilms – a short review. In: *Biofilms in the aquatic environment*, C.W. Keevil, A. Godfree, D. Holt and C. Dow (eds.), The Royal Society of Chemistry, Cambridge. pp. 1 - 12.

Fletcher, M. 1996 Bacterial attachment in aquatic environments: a diversity of surfaces and adhesion strategies. In: *Bacterial adhesion, Molecular and Ecological diversity*, M. Fletcher (ed), Wiley-Liss, Inc., New York. pp. 1 - 24.

Flint, S.H., Brooks, J.D. and Bremer, P.J. 2000 Properties of the stainless steel substrate, influencing the adhesion of thermo-resistant streptococci. *Journal of Food Engineering* **43**: 235 - 242.

Floodgate, G.D. 1984 The fate of petroleum in the marine ecosystems. In: *Petroleum Microbiology,* R.M. Atlas (ed), Macmillan Publishing Co., New York. pp 355 - 397.

Fontana, M. 1986 *Corrosion Engineering.* McGraw-Hill, New York.

Franzmann, P.D. and Tindall, B.J. 1990 A chemotaxonomic study of members of the family *Halomonadaceae. Systematic and Applied Microbiology* **13**: 142 – 147.

Garriga, M., Ehrmann, M.A., Arnau, J., Hugas, M. and Vogel, R.F. 1998 *Carnimonas nigrificans* gen. nov., sp. nov., a bacterial causative agent for black spot formation on cured meat products. *International Journal of Systematic Bacteriology* **48**(3): 677 – 686.

Garrity, G.M. and Holt, J.G. 2001 The Road Map to the Manual. In: *Bergey's Manual of Systematic Bacteriology*, D.R. Boone and R.W. Castenholz (eds.), 2nd Edition, Vol 1, Springer-Verlag, New York. pp. 119 – 166.

Gauthier, M.J., Lafay, B., Christen, R., Fernandez, L., Acquaviva, M., Bonin, P. and Bertrand, J.C. 1992 *Marinobacter hydrocarbonoclasticus* gen. nov., sp. nov., a new, extremely halotolerant, hydrocarbon-degrading marine bacterium. *International Journal of Systematic Bacteriology.* **42**: 568 - 576.

Gaylarde, C.C. and Johnston, J..M. 1982 The effect of *Vibrio anguillarum* on the anaerobic corrosion of mild steel by *Desulfovibrio vulgaris. International Biodeterioration Bulletin* **18**: 111 – 116.

Gaylarde, C.C. and Videla, H.A. 1987 Localised corrosion induced by a marine *Vibrio. International Biodeterioration* **23**: 91 – 104.

Geesey, G.G., Gillis, R.J., Avci, R., Daly, D., Hamilton, M., Shope, P. and Harkin, G. 1996 The influence of surface features on bacterial colonization and subsequent substratum chemical changes of 316L stainless steel. *Corrosion Science* **38**: 73 - 95.

Gerhardt, P., Murray, R.G.E., Wood, W.A. and Krieg, N.R. 1994 *Methods for General and Molecular Bacteriology.* American Society for Microbiology, Washington, D.C. 791 pp.

Gibson, W.L. and Brown, L.R. 1975 The metabolism of parathion by *Pseudomonas aeruginosa. Developments in Industrial Microbiology* **16**: 77 - 87.

Gillis, M., Vandamme, P., de Vos, P., Swings, J. and Kersters, K. 2001 Polyphasic Taxonomy. In: *Bergey's Manual of Systematic Bacteriology*, D.R. Boone and R.W. Castenholz (eds.), 2nd Edition, Vol 1, Springer-Verlag, New York. pp. 43 – 48.

Giovannoni, S. and Rappé, M. 2000 Evolution, diversity, molecular ecology of marine prokaryotes. In *Microbial Ecology of the Oceans*, D.L. Kirchman (ed), Wiley-Liss, Inc., New York. pp. 47 - 84.

Gu, B., Phelps, T.J., Liang, L., Dickey, M. J., Roh, Y., Kinsall, B.L., Palumbo, A.V. and Jacobs, G.K. 1999 Biogeochemical dynamics in zero-valent iron columns: Implications for permeable reactive barriers. *Environmental Science and Technology* **33**: 2170 - 2177.

Hadley, R.F. 1943 The influence of *Sporovibrio desulfuricans* on the current and potential behaviour of corroding iron. National Bureau of Standards Corrosion Conference.

Hamilton, W.A. 1985 Sulphate-reducing bacteria and anaerobic corrosion. *Annual Review of Microbiology* **39**: 195 - 217.

Hedlund, B.P. and Staley, J.T. 2001 *Vibrio cyclotrophicus* sp. nov., a polycyclic aromatic hydrocarbon (PAH)-degrading marine bacterium. *International Journal of Systematic and Evolutionary Microbiology* **51**: 61 – 66.

Horowitz, A., Gutnick, D. and Rosenberg, E. 1975 Sequential growth of bacteria on crude oil. *Applied Microbiology* **30**(1): 10 - 19.

Jahn, A. and Nielsen, P.H. 1996 Extraction of extracellular polymeric substances from biofilms using a cation exchange resin. *Water Science.and Technology* **32**: 125 - 132.

Jain, D.K. 1995 Microbial colonization of the surface of stainless steel coupons in a deionized water system. *Water Research* **29**(8): 1869 - 1876.

James, S.R., Dobson, S.J., Franzmann, P.D. and McMeekin, T.A. 1990 *Halomonas meridiana*, a new species of extremely halotolerant bacteria isolated from Antarctic saline lakes. *Systematic and Applied Bacteriology* **13**: 270 – 277.

Jobson, A., Cook, F.D. and Westlake, D.W.S. 1972 Microbial utilization of crude oil. *Applied Microbiology* **23**(6): 1082 - 1089

Johnston, C.S. 1980 Sources of hydrocarbons in the marine environments. In: *Oily Water Discharges*, C.S. Johnston and R.J. Morris (eds.), Applied Science, London. pp. 41 - 62.

Kiorboe, T. 2001 Formation and fate of marine snow: small-scale processes with large-scale implications. *Scientia Marina* **65**: 57 - 71.

Kirchman, D.L. and Williams, P.J. le B. 2000 Introduction. In: *Microbial Ecology of the Oceans*, D.L. Kirchman (ed), Wiley-Liss, Inc., New York. pp. 1 - 11.

Kobrin, G. 1976 Corrosion by microbiological organisms in natural waters. *Materials Performance* **15**(17): 38.

Lazarova, V. and Manem, J. 1995 Biofilm characterization and activity analysis in water and wastewater treatment. *Water Research* **29**: 2227 - 2245.

Leahy, J.G. and Colwell, R.R. 1990 Microbial degradation of hydrocarbons in the environment. *Microbiological Reviews* **54**: 305 – 315.

Little, B.J., Wagner, P., Gerchakov, S.M., Walch, M. and Mitchell, R. 1986 The involvement of a thermophilic bacterium in corrosion processes. *Corrosion* **42**: 533 - 536.

Low, S. 1991 Titanica. IMAX Film, Imax Corporation/TMP (1991) I Limited Partnership.

Ludwig, W. and Klenk, H-P 2001 Overview: A phylogenetic backbone and taxonomic framework for prokaryotic systematics. In: *Bergey's Manual of Systematic Bacteriology*, D.R. Boone and R.W. Castenholz (eds.), 2nd Edition, Vol 1, Springer-Verlag, New York. pp. 49 – 65.

Ludwig, W. and Schleifer, K.H. 1994 Bacterial phylogeny based on 16S and 23S rRNA sequence analysis. *FEMS Microbiological Reviews* **15**: 155 – 173.

Ludwig, W., Strunk, O., Klugbauer, S., Klugbauer, N., Weiznegger, M., Neumaier, J., Bachleitner, M. and Schleifer, K.H. 1998 Bacterial phylogeny based on comparative sequence analysis. *Electrophoresis* **19**: 554 – 568.

MacInnis, J.B. 1992 Unlocking the secrets. In: *Titanic In a New Light,* S. Shulman (ed), Thomasson-Grant, Inc., Charlottesville. pp. 89 - 94.

Mann, H. Dalhousie University, Halifax, NS, Canada. Personal communication.

Mann, H. 1997 A close-up look at *Titanic's* rusticles. *Voyage* **25**: 47 - 48.

Marshall, K.C. 1985 Mechanisms of bacterial adhesion at solid-water interfaces. In: *Bacterial Adhesion*, D.C. Savage and M. Fletcher (eds.), Plenum Press, New York. pp. 133 - 161.

Medilanski, E., Kaufmann, K., Wick, L.Y., Wanner, O. and Harms, H. 2002 Influence of the surface topography of stainless steel on bacterial adhesion. *Biofouling* **18**: 193 - 203.

Mellado, E., Moore, E.R., Nieto, J.J. and Ventosa, A. 1995 Phylogenetic inferences and taxonomic consequences of 16S ribosomal DNA sequence comparison of *Chromohalobacter marismortui*, *Volcaniella eurihalina* and *Deleya salina* and reclassification of *V. eurihalina* as *Halomonas eurihalina* comb. nov. *International Journal of Systematic Bacteriology* **45**(4): 712 - 716.

Miller, J.M., Dobson, S.J., Franzmann, P.D. and McMeekin, T.A. 1994 Reevaluating the classification of *Paracoccus halodenitrificans* with sequence comparisons of 16S ribosomal DNA. *International Journal of Systematic Bacteriology* **44** (2): 360 - 361.

Minas, W. and Gunkel, W. 1995 Oil pollution in the North Sea - a microbiological point of view. *Helgoländer Meeresunters* **49**: 143 - 158.

Moat, A.G. and Foster, J.W. 1988 *Microbial Physiology*: Carbohydrate metabolism and energy production, 2nd edition, John Wiley & Sons, Inc., New York. pp. 118 – 220.

Monteoliva-Sanchez, M. and Ramos-Cormenzana, A. 1986 Effect of growth temperature and salt concentration on the fatty acid composition of *Flavobacterium halmephilum* CCM2831. *FEMS Microbiology Letters* **33**: 51 – 54.

Mormile, M.R., Romine, M.F., Garcia, M.T., Ventosa, A., Bailey, T.J. and Peyton, B.M. 1999 *Halomonas campisalis* sp. nov., a denitrifying, moderately haloalkaliphilic bacterium. *Systematic and Applied Microbiology* **22** (4) 551 - 558.

Myneni, S.C.B., Tokunaga, T.K. and Brown, G.E. 1997 Abiotic selenium redox transformation in the presence of Fe (II, III) oxides. *Science* **278**: 1106 – 1109.

NACE 1982 *Forms of Corrosion Recognition and Prevention, Handbook 1*. Houston, TX.

NACE 1984 *Corrosion Basics, An Introduction*. Houston, TX.

NCBI National Centre of Biotechnology (1988) [online]
Available:
www.ncbi.nlm.nih.gov/
Accessed on September 2003

Neu, T.R. 1991 Polysaccharide in Biofilmen. *Jahrbuch f. Biotechnol.*, **4**. Ausg., Carl Hanser Verlag, München

Neu, T.R. and Marshall, K.C. 1990 Bacterial polymers: physicochemical aspects of their interactions with interfaces. *Journal of Biomaterial Applications* **5**: 107 - 133.

Olsen, G.J. and Woese, C.R. 1993 Ribosomal RNA: a key to phylogeny. *FASEB Journal* **7**: 113 – 123.

Olsen, G.J., Woese, C.R. and Overbeek, R. 1994 The winds of (evolutionary) change: breathing a new life into microbiology. *Journal of Bacteriology* **176**: 1 – 6.

Ostroff, A.G. 1979 *Introduction to Oilfield Water Technology*. National Association of Corrosion Engineers, Houston, TX.

Palleroni, N.J. 1984 Gram Negative Aerobic Rods and Cocci: Family Pseudomonadaceae, Genus *Pseudomonas*, *Pseudomonas putida*. In: *Bergey's Manual of Systematic Bacteriology*, N. R. Kreig and J. G. Holt (eds.), vol 1., Williams and Wilkins, Baltimore. pp. 140 – 169.

Patel, R.N. and Hou, C.T. 1983 Enzymatic transformation of hydrocarbons by methonotrophic organisms. *Developments in Industrial Microbiology* **23**: 187 - 205.

Pellegrino, C. 2000 *Ghosts of the Titanic*. Harper Morrow, New York.

Pellegrino, C. and Cullimore, D.R. 1997 A study of the bioarcheology of a physically disrupted sunken vessel. *Voyage* **25**: 39 – 46.

Phaff, H.J. 1986 Ecology of yeasts with actual and potential value in biotechnology. *Microbial Ecology* **12**: 31 - 42.

Phillips, D.H., Gu, B., Watson, D.B., Roh, Y., Liang, L. and Lee, S.Y. 2000 Performance evaluation of a zerovalent iron reactive barrier: Mineralogical characteristics. *Environmental Science and Technology* **34**: 4169 – 4176.

Postgate, J.R. 1994 *The outer reaches of life*. Cambridge University Press, Cambridge.

Quesada, E., Béjar, V. and Calvo, C. 1993 Exopolysaccharide production by *Volcaniella eurihalina. Experientia* **49**: 1037 – 1041.

Ravin, A.W. 1963 Experimental approaches to the study of bacterial phylogeny. *Amateur Naturalist* **97**: 307 – 325.

Raymond, D. 1974 Metabolism of methylnaphthalenes and other related aromatic hydrocarbons by marine bacteria. Ph.D. Dissertation, Rutgers University.

Reisfeld, A., Rosenberg, E. and Gutnick, D. 1972 Microbial degradation of crude oil: Factors affecting the dispersion in sea water by mixed and pure cultures. *Applied Microbiology* **24**(3): 363 – 368.

Rice, T. 2000 *Deep Ocean,* J. Morris (ed), The Natural History Museum, London.

Robinow, C.F. 1960 Morphology of bacterial spores, their development and germination. In: *The bacteria*, I.C. Gunsalus and R.Y. Stanier (eds.), Vol.1, Academic Press Inc., New York. pp. 207 – 248.

Rodriguez-Valera, F. 1992 Biotechnological potential of halobacteria. In*: The Archaebacteria: Biochemistry and Biotechnology,* M.J. Danson, D. W. Hough and G.G. Lunt (eds.*),* Portland Press, London and Chapel Hill. pp 135 - 148.

Roh, Y., Lee, S. Y. and Elless, M. P. 2000 Characterization of corrosion products in the permeable reactive barriers. *Environmental Geology* **40**(1-2): 184 – 194.

Romano, I., Nicolaus, B., Lama, L., Manca, M.C. and Gambacorta, A. 1996 Characterization of haloalkaliphilic strictly aerobic bacterium, isolated from Pantelleria island. *Systematic and Applied Microbiology* **19**: 326 - 333.

Salvarezza, R.C., Mele, M.F.L. de and Videla, H.A. 1979 The use of pitting potential to study the microbial corrosion of 2024 aluminium alloy. *International Biodeterioration Bulletin* **15**: 125 – 132.

Sanders, P. 1997 Problems caused by biofilms in the oil industry. In: *Biofilms in the aquatic environment*, C.W. Keevil, A. Godfree, D. Holt and C. Dow (eds.), The Royal Society of Chemistry, Cambridge. pp. 109 - 119.

Sawant, S.S. and Venugopal, C. 1996 Effect of exposure angle on the marine atmospheric corrosion of mild steel. *Corrosion Prevention and Control* **43**(1): 35 - 38.

Scheuerman, T.R., Camper, A.K. and Hamilton, M.A.1998 Effects of substratum topography on bacterial adhesion. *Journal of Colloid Interface Science* **208:** 23 - 33.
Silver, M.W., Shanks, A.L. and Trent, J.D. 1978 Marine snow: microplankton habitat and source of small-scale patchiness in pelagic populations. *Science* **201**: 371 - 373.

Simon, M., Grossart, H.P., Schweitzer, B. and Ploug, H. 2002 Microbial ecology of organic aggregates in aquatic ecosystems. *Aquatic Microbial Ecology* **28**(2): 175 - 211.

Siron, R., Pelletier, É. and Brochu, C. 1995 Environmental factors influencing the biodegradation of petroleum hydrocarbons in cold seawater. *Archives of Environmental Contamination and Toxicology* **28**: 406 – 416.

Stackebrandt, E. and Goebel, B.M. 1994 Taxonomic note: a place for DNA-DNA reassociation and 16S rRNA sequence analysis in the present species definition in bacteriology. *International Journal of Systematic Bacteriology* **44**(4): 846 - 849.

Starkey, R.L. and Wight, K.M. 1945 *Anaerobic Corrosion of Iron in Soil*. American Gas Association, New York.

Stoffyn, P. and Buckley, D.E. 1992 The Titanic 80 years later: Initial observations on the microstructure and biogeochemistry of corrosion products. In: *Proceedings of the 50th Annual Meeting of the Electron Microscopy Society of America*, G.W. Bailey, J. Bentley and J.A. Small (eds.), EMSA, San Francisco Press, Inc., San Francisco. pp. 1330 - 1331.

Stoffyn-Egli, P. and Buckley, D.E. 1993 The *Titanic*: From metals to minerals. *Canadian Chemical News* **45**(9): 26 - 28.

Stoffyn-Egli, P. and Buckley, D.E. 1995 The micro-world of the *Titanic*. *Chemistry in Britain* **31**: 551 - 553.

Stratagene: Tools and Technologies for Life Sciences n.d. [online]
Available:
http://www.stratagene.com/vectors/maps/pdf/pBluescript%20II%20SK%2B_%20webpg.pdf
Accessed on January 2002

Sutherland, I.W. 1990 *Biotechnology of Microbial Exopolysaccharides,* J. Baddiley, N.H. Higgins and W.G. Potter (eds.), Cambridge University Press, Cambridge.

Sutherland, I.W. 1998 Novel and established applications of microbial polysaccharides. *Trends in Biotechnology* **16**: 41 – 46.

Takami, H., Inoue, A., Fuji, F. and Horikoshi, K. 1997 Microbial flora in the deepest sea mud of the Mariana Trench. *FEMS Microbiology Letters* **152**(2): 279 - 285.

Tatnall, R.E. 1981 Fundamentals of bacteria induced corrosion. *Materials Performance* **19**(9): 32.

Taylor, R.L., Verran, J., Lees, G.C. and Ward, A.J.P. 1998 The influence of substratum topography on bacterial adhesion to polymethyl methacrylate. *Journal of Materials Science. Materials in Medicine* **9**: 17 - 22.

Thao, M.L., Moran, N.A., Abbot, P., Brennan, E.B., Burckhardt, D.H. and Baumann, P. 2000 Cospeciation of psyllids and their primary prokaryotic endosymbionts. *Applied and Environmental Microbiology* **66**(7): 2898 – 2905.

Tiller, A.K. 1982 Aspects of Microbial Corrosion. In: *Corrosion Process*, R.N. Parkins (ed), Applied Science. pp. 115-160.

Tiller, A.K. 1986 A review of the European research effort on microbial corrosion between 1950 and 1984. In: *Biologically Induced Corrosion*, S.C. Dexter (ed), NACE Reference Book No. 8, National Association of Corrosion Engineers, Houston, TX.

Tombs, M. and Harding, S.E. 1998 *An Introduction to Polysaccharide Biotechnology.* Taylor and Francis, London.

Turner, J.T. 2002 Zooplankton fecal pellets, marine snow and sinking phytoplankton blooms. *Aquatic Microbial Ecology* **27**(1): 57 - 102

Uhlinger, D.J. and White, D.C. 1983 Relationship between physiological status and formation of extracellular polysaccharide glycocalyx in *P. atlantica. Applied and. Environmental. Microbiology* **45**: 64 - 70.

Vance, I., Stanley, S.O. and Brown, C.M. 1979 A microscopical investigation of bacterial degradation of wood pulp in simulated marine environment. *Journal of General Microbiology* **114**: 69 - 74.

Vandamme, P., Pot, B., Gillis, M., de Vos, P., Kersters, K. and Swings, J. 1996 Polyphasic Taxonomy, a consensus approach to bacterial systematics. *Microbiological Reviews* **60**: 407 – 438.

Vanhaecke, E., Remon, J-P., Moors, M., Raes, F., de Rudder, D. and van Peteghem, A. 1990 Kinetics of *Pseudomonas aeruginosa* adhesion to 304 and 316 L stainless steel: role of cell surface hydrophobicity. *Applied and Environmental Microbiology* **56**: 788 - 795.

van Loosdrecth, M.C.M., Lyklema, J., Norde, W. and Zehnder, A.J.B. 1989 Bacterial adhesion - a physiochemical approach. *Microbial Ecology* **17**: 1 - 15.

van Loosdrecth, M.C.M., Lyklema, J., Norde, W. and Zehnder, A.J.B. 1990 Influence of interfaces on microbial activity. *Microbiological Reviews* **54**: 75 - 87.

Verran, J. and Hisett, T. 1997 The effect of substratum surface defects upon retention of, and biofilm formation by, microorganisms from potable water. In: *Biofilms in the aquatic environment*, C.W. Keevil, A. Godfree, D. Holt and C. Dow (eds.), The Royal Society of Chemistry, Cambridge. pp. 25-33.

Verran, J. et al., 1991 The effect of surface roughness on adhesion of *Candida albicans* to acrylic. *Biofouling* **3**: 183.

Verran, J. Taylor, R.L. and Lees, G.C. 1994 The use of image analysis to quantify microorganisms adherent on surfaces. *Binary-Computing in Microbiology* **6**: 55.

Videla, H.A. 1986 Mechanisms of MIC. In: *Proceedings of Argentine-USA Workshop on Biodeterioration* (CONICET-NSF), H.A. Videla (ed), Aquatec Química S.A., Sao Paulo, Brazil. pp. 43 - 63.

Videla, H.A. 2001 Microbially induced corrosion: an updated overview. *International Biodeterioration and Biodegradation* **48**: 176 – 201.

Videla, H.A., Mele, M.F.L. de and Brankevich, G. 1987 Microfouling of several metal surfaces in polluted seawater and its relation with corrosion. Paper no. 365, *CORROSION* 87. National Association of Corrosion Engineers, Houston, TX.

Voronin, A.M., Kochetkov, V.V., Starovoytov, I.I. and Skryabin, G.K.1977 pBS2 and pBS3 plasmids controlling oxidation of naphthalene in bacteria of the genus *Pseudomonas*. *Moscow Doklady Akademii Nauk* **237**: 1250 - 1208.

Vreeland, R.H. 1984 Genus *Halomonas*, Other Genera, Section 4. In: *Bergey's Manual of Systematic Bacteriology,* N.R. Krieg and J.G. Holt (eds.). 1st ed. Vol 1, Williams and Wilkins, Baltimore.

Vreeland, R.H., Litchfield, C.D., Martin, E.L. and Elliot, E. 1980 *Halomonas elongata*, a new genus and species of extremely salt-tolerant bacteria. *International Journal of Systematic Bacteriology* **30**(2): 485 - 495.

Vreeland, R.H. and Martin, E.L. 1980 Growth characteristics, effects of temperature, and ion specificity of the halotolerant bacterium *Halomonas elongata. Canadian Journal of Microbiology* **26**: 746 – 752.

Wanklin, J.N. and Spruit, C.I.P. 1952 Influence of sulphate-reducing bacteria on the corrosion potential of iron. *Nature* **169**: 928 – 929.

Watson, D., Gu, B., Phillips, D. H. and Lee, S. Y. 1999 *Evaluation of permeable reactive barriers for removal of uranium and other inorganics at the Department of Energy Y-12 Plant, S-3 disposal ponds.* ORNL/TM-1999-143, Oak Ridge National Laboratory, Oak Ridge, TN.

Wayne, LG., Breener, D.J., Colwell, R.R., Grimont, P.A.D., Kandler, O., Krichevsky, M.I., Moore, L.H., Moore, W.E.C., Murray, R.G.E., Stackebrandt, E., Starr, M.P. and Truper, H.G. 1987 Report of the ad hoc committee on reconciliation of approaches to bacterial systematics. *International Journal of Systematic Bacteriology* **37**: 463 – 464.

Wells, W. and Mann, H. 1997 Microbiology and formation of rusticles from the *R.M.S. Titanic. Resource and Environmental Biotechnology* **1**: 271 - 281.

White, D.C., Kirkegaard, R.D., Palmer, R.J. Jr., Flemming, C.A., Chen, G., Leung, K.T., Phiefer, C.B. and Arrage, A.A. 1997 The biofilm ecology of microbial biofouling, biocide resistance and corrosion. In: *Biofilms in the aquatic environment*, C.W. Keevil, A. Godfree, D. Holt and C. Dow (eds.), The Royal Society of Chemistry, Cambridge. pp. 120 - 130.

Wicken, A.J. 1985 Bacterial cell walls and surfaces. In: *Bacterial adhesion, Mechanism and Physiological significance*, D.C. Savage and M. Fletcher (eds.), Plenum press, New York. pp. 45 - 70.

Woese, C.R.1987 Bacterial evolution. *Microbiological Reviews* **51**: 221 – 271.

Woese, C.R., Maniloff, J., and Zablen, L.B. 1980 Phylogenetic analysis of the mycoplasmas. *Proceedings of the Natural Academy of Sciences* (Washington) **77**: 494 - 498.

Woese, C.R., Weisburg, W.G., Hahn, C.M., Paster, B.J., Zablen, L.B., Lewis, B.J., Macke, T.J., Ludwig, W. and Stackebrandt, E. 1985 The phylogeny of purple bacteria: The gamma subdivision. *Systematic and Applied Microbiology* **6**: 25 – 33.

Wulpi, D.J. 1966 *How Components Fail.* ASM International, Metals Park, OH.

Yamikov, M.M., Golyshin, P.N., Lang, S., Moore, E.R.B., Abraham, W-R., Lünsdorf, H. and Timmis, K.N. 1998 *Alcanivorax borkumensis* gen. nov., sp. nov., a new, hydrocarbon-degrading and surfactant-producing marine bacterium. *International Journal of Systematic Bacteriology.* **48**: 339 - 348.

Yoon, J-H, Choi, S.H., Lee, K-C, Kho, Y.H., Kang, K.H. and Park, Y-H. 2001 *Halomonas marisflavae* sp. nov., a halophilic bacterium isolated from the Yellow Sea in Korea. *International Journal of Systematic and Evolutionary Microbiology* **51**: 1171 – 1177.

Yoon, J-H, Lee, K-C, Kho, Y.H., Kang, K.H., Kim, C-J and Park, Y-H. 2002 *Halomonas alimentaria* sp. nov., isolated from jeotgal, a traditional Korean fermented seafood. *International Journal of Systematic and Evolutionary Microbiology* **52**: 123 – 130.

7. APPENDIX A

Bacto Marine Agar 2216 (dehydrated)

Ingredients per liter

Bacto Peptone	5 g	Potassium Bromide	0.08 g
Bacto Yeast Extract	1 g	Strontium Chloride	0.034 g
Ferric Citrate	0.1 g	Boric Acid	0.022 g
Sodium Chloride	19.45 g	Sodium Silicate	0.004 g
Magnesium Chloride	8.8 g	Sodium Fluoride	0.0024 g
Sodium Sulfate	3.24 g	Ammonium Nitrate	0.0016 g
Calcium Chloride	1.8 g	Disodium Phosphate	0.008 g
Potassium Chloride	0.55 g	Bacto Agar	15 g
Sodium Bicarbonate	0.16 g		

Final pH 7.6 ± 0.2 at 25 °C.

Use 55.1 g per liter.

Bacto Marine Broth 2216 (dehydrated)

Ingredients per liter

Bacto Peptone	5 g	Potassium Bromide	0.08 g
Bacto Yeast Extract	1 g	Strontium Chloride	0.034 g
Ferric Citrate	0.1 g	Boric Acid	0.022 g
Sodium Chloride	19.45 g	Sodium Silicate	0.004 g
Magnesium Chloride	8.8 g	Sodium Fluoride	0.0024 g
Sodium Sulfate	3.24 g	Ammonium Nitrate	0.0016 g
Calcium Chloride	1.8 g	Disodium Phosphate	0.008 g
Potassium Chloride	0.55 g		
Sodium Bicarbonate	0.16 g		

Final pH 7.6 ± 0.2 at 25 °C.

Use 37.4 g per liter.

Bacto Triple Sugar Iron Agar (dehydrated)

Ingredients per liter

Bacto Beef Extract	3 g	Bacto Sucrose	10 g
Bacto Yeast Extract	3 g	Ferrous Sulfate	0.2 g
Bacto Peptone	15 g	Sodium Chloride	5 g
Proteose Peptone, Difco	5 g	Sodium Thiosulfate	0.3 g
Bacto Dextrose	1 g	Bacto Agar	12 g
Bacto Lactose	10 g	Bacto Phenol Red	0.024 g

Final pH 7.4 ± 0.2 at 25 °C.

Prepare as specified by manufacturer.

Bushnell Hass Broth (dehydrated)

Ingredients per litre

Magnesium Sulfate	0.2 g
Calcium Chloride	0.02 g
Monopotassium Phosphate	1 g
Dipotassium Phosphate	1 g
Ammonium Nitrate	1 g
Ferric Chloride	0.05 g

Final pH 7.0 ± 0.2 at 25 °C.

Dissolve 3.25 g per litre of distilled water.

Epon Araldite resin composition

Araldite	4.6 g
TAAB 812	6.1 g
DDSA	11.9 g
DMP30	0.5 g

Add all the components to a plastic beaker. Mix them well by placing on a vortexer for 5 - 10 min.

Reagents for genetic analysis experiments

1 Kb ladder

TE	150 µl
6X dye	40 µl
1Kb DNA ladder	10 µl

1 M HCl

dH_2O	90.38 ml
10.4 M HCl	9.62 ml

First add dH_2O to the beaker and then slowly add HCl.

10 M NaOH

Dissolve 40 g NaOH in 70 ml of dH_2O.
Adjust volume to 100 with dH_2O.

20 % SDS

Dissolve 4 g of SDS in 20 ml of dH_2O.

Agarose gel

Agarose	0.7 g
1% TAE	100 ml

Add 0.7 g of agarose in 100 ml of 1 % TAE. Boil and then allow it to cool before pouring it into a casting tray.

Ampicillin stock (50 mg/ ml)

Amp powder	0.5 g
ddH_2O	10 ml

Filter sterilize with a 0.2 µm membrane and store at 4 °C.

Coomassie blue

Isopropanol	125 ml
Acetic acid	50 ml
Coomassie blue	0.2 g
dH_2O	325 ml

Filter sterilize with 0.2 μm membrane.

Glycerol 50 % (w/v)

Weigh out 50 g of glycerol in 100 ml beaker. Add 30 ml dH_2O. Stir to mix. Then add dH_2O to make volume 100 ml. Autoclave for 30 min.

GTE

50 mM Glucose
25 mM Tris
10 mM EDTA

Filter sterilize through a 0.2 μm membrane and store at 4 °C.

High salt solution

1.0 mM NaCl
20 mM Tris
1.0 mM EDTA

Adjust final pH to 7.5.

IPTG (200 mg/ml)

IPTG	0.2 g
H_2O	1 ml

Filter sterilize with 0.2 μm membrane.

KAc solution

5 M KAc	60 ml
Glacial acetic acid	11.5 ml
dH_2O	28.5 ml

L B Broth

Tryptone	10 g
Yeast extract	5 g
NaCl	10 g
dH_2O	1 L

Adjust final pH 7.5 at 25 °C. Add 1.5 % agarose (15 g/l) to make plates.

Low salt solution

20 mM NaCl
20 mM Tris
1.0 mM EDTA

Adjust final pH to 7.5.

RNase (10mg/ml)

10 mM Tris-HCl (pH 7.5)
15 mM NaCl
RNase powder

Add 0.1 g RNase powder to 5 ml of dH_2O and stir. Then add 200 µl of 0.5 M Tris-HCl and 75 µl of 2 M NaCl. Make the volume 10 ml by adding dH_2O. Heat the solution to 100 °C for 15 min. Slowly cool to room temperature. Store at -20 °C.

TAE buffer

Tris base	121 g
0.5 M EDTA (pH 8.0)	50 ml
Glacial acetic acid	28.55 ml

Mix 121 g of Tris-base with 50 ml of 0.5 M EDTA and stir. Then add 28.55 ml glacial acetic acid and add dH_2O to make volume 500ml.

TE buffer

10 mM Tris-HCl (pH 8.0)
1 mM EDTA

Tetracycline stock (10mg/ml)

Tetracycline powder	0.1 g
95% ethanol	10 ml

Tfm buffer 1

10 mM Tris
150 mM NaCl

Dissolve 1.21 g Tris and 8.76 g NaCl in 800 ml of dH_2O.
Adjust pH to 7.5 with 1 M HCl.
Add dH_2O to make volume 1 L and autoclave.

Tfm buffer 2

50 mM $CaCl_2$

Dissolve 7.35 g $CaCl_2.2H_2O$ in 1 L of dH_2O and autoclave.

Tfm buffer 3

10 mM Tris
50 mM $CaCl_2.2H_2O$
10 mM $MgSO_4$

Dissolve 0.12 g Tris, 0.735 g $CaCl_2.2H_2O$ and 0.25 g $MgSO_4.7H_2O$ in 70 ml dH_2O.
Adjust pH to 7.5 with 1 M HCl.
Add dH_2O to make volume 100 ml

Filter sterilize with 0.2 μm membrane

X-gal (10 mg/ml)

X-gal	0.05 g
Dimethylformamide	5 ml

Preparation of competent *E. coli* cells

Inoculate 50 ml of LB broth, containing 75 µl of tetracycline (10mg/ml), with 0.5 ml of an overnight culture of *E. coli* cells. Incubate at 37 °C with vigorous shaking until OD at 600 nm = 0.35 (3 h).
Harvest the cells at 10,000 g. Then wash them with 50 ml cold Tfm 1 and leave at 4 °C for 30 min. Centrifuge the cells for 15 min.
Resuspend the pellet in 50 ml cold Tfm 2. Vortex to mix the cells with the buffer. Leave the cells on ice for 45 min. Centrifuge and gently wash the cells in 3 ml of Tfm 2.
Add 2 ml glycerol. Dispend 0.22 ml/ tube and freeze at – 70 °C, immediately.
The cells should remain competent for at least 1 month under these conditions.

Restriction enzymes

All the enzymes were purchased from Invitrogen (Burlington)

*Bam*H1	10 U/µl
*Cla*I	10 U/µl
*Hin*cII	10 U/µl
*Hin*dIII	10 U/µl
*Kpn*I	10 U/µl
*Not*I	15 U/µl
*Pst*I	10 U/µl
*Sma*I	10 U/µl
*Xba*I	10 U/µl

8. APPENDIX B

Nelson lab report

FINAL REPORT

ORGANISM IDENTIFICATION

PROCEDURE NO. SOP/MBG/006I.1, SOP/MBG/038G.1, SOP/MBG/027I.1

LABORATORY NO. 221560

PREPARED FOR:

BHAVLEEN KAUR
DALHOUSIE UNIVERSITY
DEPT. OF BIOLOGICAL ENGINEERING
"N" BLDG., SEXTON CAMPUS, PO BOX 1000
HALIFAX, NOVA SCOTIA
CANADA B3J 1Z1

SUBMITTED BY:

NELSON LABORATORIES, INC.
6280 SOUTH REDWOOD ROAD
SALT LAKE CITY, UT 84123-6600
UNITED STATES OF AMERICA
801-963-2600

NELSON
LABORATORIES

ORGANISM IDENTIFICATION

LABORATORY NUMBER:	221560
PROCEDURE NUMBER:	SOP/MBG/006I.1, SOP/MBG/038G.1, SOP/MBG/027I.1
SAMPLE SOURCE:	Dalhousie University
SAMPLE IDENTIFICATION:	Halomonas Biochemical analysis P.O. #P9011244
DEVIATIONS:	None
DATA ARCHIVE LOCATION:	Sequentially by lab number
SAMPLE RECEIVED DATE:	29 Oct 2002
LAB PHASE START DATE:	30 Oct 2002
LAB PHASE COMPLETION DATE:	27 Nov 2002
REPORT ISSUE DATE:	02 Dec 2002
TOTAL NUMBER OF PAGES:	12

INTRODUCTION:

The organism submitted was identified by colony morphology, Gram stain reaction, cell morphology, biochemical testing, and MIDI (fatty acid analysis).

ACCEPTANCE CRITERIA:

A Gram stain is considered acceptable if the positive and negative control organisms have acceptable Gram stains.

The MIDI results are considered acceptable if the calibration data is acceptable, if the positive control organisms have a similarity index value of 0.600 or higher (for the yeast control the similarity index should be 0.500 or higher), if the negative control (or blank) has no named peaks, and if the library search report is interpreted according to the guidelines explained in this report.

Biochemical test results are considered valid if the positive and negative (if applicable) controls are acceptable.

PROCEDURE:

Gram Stain:

The test organism was plated on soybean casein digest agar and incubated at 30-35°C until growth was observed. Colonies present after incubation were isolated and examined for colony morphology, Gram stain reaction, and cell morphology.

NELSON
LABORATORIES

MIDI:

The MIDI Microbial Identification System (MIS) was used to identify the organism. The test organism was plated on trypticase soy broth agar and incubated at 27-29°C until growth was observed. The fatty acids were extracted from the test organisms and analyzed by gas chromatography. The results were then compared against the MIS Library. The MIS Library Search Report lists the most likely matches to the unknown composition, and provides a similarity index for each match. If the search results in more than one possible match, the suggested identities are listed in the descending probability. When applicable, subspecies level identifications are printed.

The MIS Similarity Index is a numerical value which expresses how closely the fatty acid composition of an unknown compares with the mean fatty acid composition of the strains used to create the library entry listed as its match. This value is a software generated calculation of the distance, in multi-dimensional space between the profile of the unknown and the mean profile of the closest library entry. It is an expression of the relative distance from the population mean. An exact match of the fatty acid makeup of the unknown and the mean of the library entry would result in a similarity index of 1.000. As each fatty acid varies from the mean percentage, the similarity index will decrease in proportion to the cumulative variance between the composition of the unknown and the library entry.

The MIS Similarity Index assumes that species of microorganisms have normal Gaussian distribution (the classic "bell shaped curve") and that the mean of the population in any series of traits (e.g., fatty acid percentages) characterizes the group. Most of the population falls somewhere near the mean, but individuals will differ in composition and thus may show considerable variance from the mean.

The following guidelines are used when interpreting the MIS Similarity Index. Strains with a similarity index of 0.500 or higher with a separation of 0.100 between the first and second choice are considered good library comparisons. If the similarity index is between 0.300 and 0.500 and well separated from the second choice (0.100 separation), it may be a good match but an atypical strain (it would fall very low on a normal distribution curve). A value lower than 0.300 suggests that the organism is not in the database, but indicates the most closely related species.

Biochemical Tests:

The organism was then tested using appropriate biochemical tests and test kits as documented in standard microbiology literature.

NELSON
LABORATORIES

Dalhousie University
Lab Number 221560

Organism Identification
Page 5

TABLE 1. Morphology Results

ISOLATE NUMBER	COLONY MORPHOLOGY	MICROSCOPIC MORPHOLOGY
1	Tan, Raised, Round	Negative rods

NELSON
LABORATORIES

Dalhousie University
Lab Number 221560

Organism Identification
Page 6

TABLE 2. MIDI Similarity Index Table

ISOLATE NUMBER	ORGANISM	SIMILARITY INDEX
1	*Pseudomonas putida* biotype A	0.841

NELSON
LABORATORIES

Dalhousie University
Lab Number 221560

Organism Identification
Page 7

TABLE 3. Api 20E results

TEST	24 hr RESULT[a]	48 hr RESULT[b]
ONPG	Negative	Negative
Arginine	Positive	Positive
Lysine	Negative	Negative
Ornithine	Negative	Negative
Citrate	Positive	Positive
Urease	Negative	Negative
TDA	Negative	Negative
Indole	Negative	Negative
VP	Negative	Negative
Gelatinase	Negative	Negative
Glucose	Negative	Positive
Mannitol	Negative	Negative
Inositol	Negative	Negative
Sorbitol	Negative	Negative
Rhamnose	Negative	Negative
Sucrose	Negative	Negative
Melibiose	Negative	Positive
Amygdalin	Negative	Negative
Arabinose	Negative	Negative
Oxidase	Positive	Positive

[a] The 24 hr profile is a "Good ID to genus" for *Pseudomonas fluorescens/putida*.

[b] The 48 hr profile is an "Excellent ID" for *Pseudomonas fluorescens/putida* or *Pseudomonas aeruginosa*

NELSON LABORATORIES

Dalhousie University
Lab Number 221560

Organism Identification
Page 8

TABLE 4. Api 50CH results

TEST	RESULT
Glycerol	Positive
Erythritol	Negative
D-Arabinose	Borderline
L-Arabinose	Positive
Ribose	Positive
D-Xylose	Positive
L-Xylose	Borderline
Adonitol	Negative
B-Methyl-xyloside	Negative
Galactose	Positive
Glucose	Positive
D-Fructose	Positive
D-Mannose	Positive
L-Sorbose	Negative
Rhamnose	Borderline
Dulcitol	Negative
Inositol	Negative
Mannitol	Negative
Sorbitol	Negative
a-Methyl-D-mannoside	Negative
a-Methyl-D-glucoside	Negative
N-Acetyl-glucosamine	Negative
Amygdalin	Negative
Arbutine	Negative
Esculin	Negative

NELSON
LABORATORIES

Dalhousie University
Lab Number 221560

Organism Identificatior
Page 9:

TABLE 4. Api 50CH results (cont.)

TEST	RESULT
Salicin	Negative
Cellobiose	Borderline
Maltose	Negative
Lactose	Negative
Melibiose	Positive
Sucrose	Negative
Trehalose	Negative
Inulin	Negative
Melezitose	Negative
D-Raffinose	Negative
Starch	Negative
Glycogen	Negative
Xylitol	Negative
B-Genitiobiose	Borderline
D-Turanose	Negative
D-Lyxose	Borderline
D-Tagatose	Negative
D-Fucose	Positive
L-Fucose	Negative
D-Arabitol	Negative
L-Arabitol	Negative
Gluconate	Negative
2-Keto-Gluconate	Negative
5-Keto-Gluconate	Negative

NELSON
LABORATORIES

Dalhousie University
Lab Number 221560

Organism Identification
Page 10

TABLE 5. Biochemical test results

TEST	RESULT
Oxidase	Positive
Catalase	Positive
Starch	Negative
Methyl Red	Negative
Nitrate	Negative
Urease	Positive

NELSON
LABORATORIES

REFERENCES:

Balows, A. et al. (ed.), 1992. The Prokaryotes, Second Edition. Springer-Verlag, New York.

Dwokin, M. et al, (ed.). 1998. The Prokaryotes, Third Edition. New York: Springer-Verlag. <http://link.springer-ny.com:6335/contents/index.html>

Holt, J.G. et al. (ed.), 1994. Bergey's Manual of Determinative Bacteriology, Ninth Edition. Williams & Wilkins. Baltimore, MD

Holt, J.G. et al. (ed.), Bergey's Manual of Systematic Bacteriology, Volume 1: 1984; Volume 2: 1986; Volume 3: 1989; Volume 4: 1989. Williams & Wilkins. Baltimore, MD

Murray, R.P., et al. (ed.), 1999. Manual of Clinical Microbiology, Seventh Edition. American Society for Microbiology, Washington, D.C.

Joklik, Wolfgang K., et al. (ed.) 1995. Zinsser Microbiology, 20th. McGraw Hill, Monterey, CA

AEROSPRAY Microbiology Gram Slide Stainer/Cytocentrifuge service manual. 1997. Wescor, Inc.

AEROSPRAY Microbiology Gram Slide Stainer/Cytocentrifuge user manual. 1997 Wescor, Inc.

Sherlock Operating Manual. Version 3.0. September 1999. MIDI, Inc. Newark, DE.

MIDI Training Manuals. 1996, 1998. MIDI, Inc. Newark, DE.

Barnett, J.A., R.W. Payne, and D. Yarrow. 1990. The Yeasts: Characterization and Identification. Second edition. Cambridge University Press, Cambridge, England.

Larone, Davise H. 1995. Medically Important Fungi: A Guide to Identification, Third Edition. American Society for Microbiology, Washington, D.C.

Gilman, J.C. 1957. A Manual of Soil Fungi, Second Edition. The Iowa State University Press. Ames, IA.

MacFaddin, J.F., 2000. Biochemical Tests for Identification of Medical Bacteria, Third Edition. Lippincott William & Wilkins, Philadelphia, PA

NELSON
LABORATORIES

E02B037.87A [146] 221560-1

Volume: DATA1 File: E02B037.87A Seq Counter: 36 ID Number: 146
Type: Stat Bottle: 74 Method: TSBA40
Created: 11/4/02 9:51:41 AM
Sample ID: 221560-1

RT	Response	Ar/Ht	RFact	ECL	Peak Name	Percent	Comment1	Comment2
1.726	3.386E+8	0.026	----	7.015	SOLVENT PEAK	----	< min rt	
2.278	336	0.024	----	8.142		----	< min rt	
3.180	342	0.027	----	9.984		----		
3.503	580	0.028	----	10.472		----		
4.243	13903	0.030	1.073	11.425	10:0 3OH	2.84	ECL deviates 0.003	
4.761	8199	0.031	1.048	12.000	12:0	1.64	ECL deviates 0.000	Reference -0.006
5.151	199	0.027	----	12.345		----		
6.133	26722	0.036	1.007	13.178	12:0 2OH	5.13	ECL deviates 0.001	
6.285	864	0.034	1.004	13.290	12:1 3OH	0.17	ECL deviates 0.002	
6.511	19852	0.037	0.999	13.456	12:0 3OH	3.78	ECL deviates 0.002	
6.992	493	0.035	----	13.812		----		
7.246	1511	0.036	0.985	13.999	14:0	0.28	ECL deviates -0.001	Reference -0.004
8.780	1182	0.037	0.965	15.001	15:0	0.22	ECL deviates 0.001	Reference -0.001
9.236	481	0.038	----	15.275		----		
10.140	151415	0.049	0.953	15.819	Sum In Feature 3	27.50	ECL deviates -0.003	16:1 w7c/15 iso 2OH
10.443	152585	0.043	0.951	16.001	16:0	27.65	ECL deviates 0.001	Reference 0.000
11.535	747	0.040	0.944	16.631	17:0 ISO	0.13	ECL deviates 0.001	Reference 0.000
11.815	1090	0.047	0.943	16.792	17:1 w8c	0.20	ECL deviates 0.000	
11.981	31233	0.045	0.942	16.888	17:0 CYCLO	5.60	ECL deviates 0.000	Reference -0.001
12.172	1551	0.047	0.941	16.999	17:0	0.28	ECL deviates -0.001	Reference -0.003
13.633	133261	0.050	0.934	17.825	18:1 w7c	23.72	ECL deviates 0.002	
13.940	2849	0.045	0.933	17.999	18:0	0.51	ECL deviates -0.001	Reference -0.003
14.721	666	0.042	----	18.443		----		
15.530	1994	0.046	0.927	18.903	19:0 CYCLO w8c	0.35	ECL deviates 0.001	Reference -0.002
----	151415	----	----	----	Summed Feature 3	27.50	16:1 w7c/15 iso 2OH	15:0 ISO 2OH/16:1w7c

ECL Deviation: 0.002
Reference ECL Shift: 0.003
Number Reference Peaks: 9
Total Response: 551718
Total Named: 548957
Percent Named: 99.50%
Total Amount: 524851

Matches:

Library	Sim Index	Entry Name
TSBA40 4.10	0.841	Pseudomonas-putida-biotype A*
	0.475	Pseudomonas-savastanoi pv. oleae
	0.459	Pseudomonas-syringae-syringae

Data File C:\SHERLOCK\RAW\E02B03.787\A00146A3.D Sample Name: 146
Sherlock Id: 221560-1

Injection Date : 11/4/02 9:55:52 AM
Sample Name : 146 Vial : 74
Acq. Operator : WARCHER1657 Inj : 1
Inj Volume : 2 µl
Method : C:\HPCHEM\1\METHODS\$MIDI$2.M
Last changed : 11/4/02 9:51:42 AM by WARCHER1657
MIDI Aerobe method saved on ChemStation Version 4.02
Switched to new integration algorighm 11-Nov-98

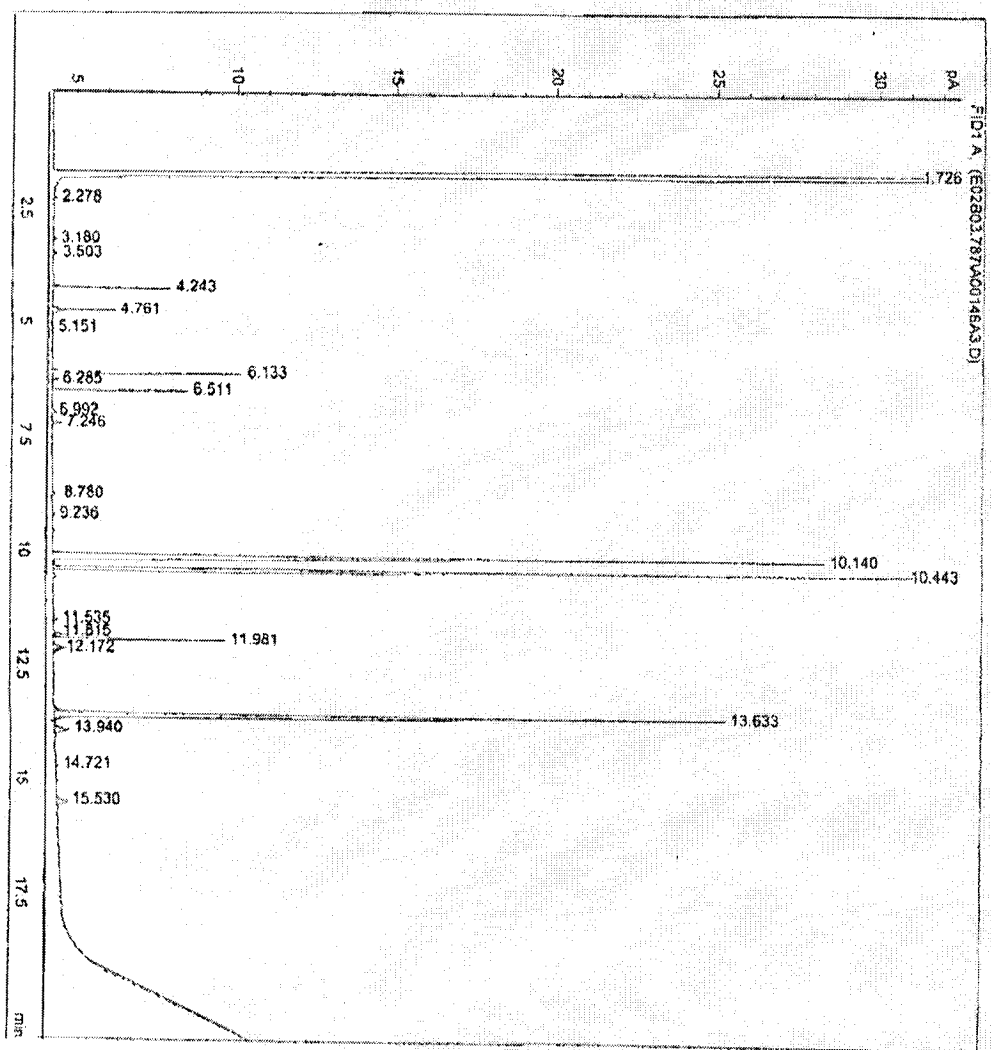

*** End of Report ***

9. APPENDIX C

Figure 9.1 Illustration of the multiple cloning sites in the plasmid pBluescript SK + (Stratagene: Tools and Technologies for Life Sciences, n.d.).

f1 (+) origin 138–444
β-galactosidase α-fragment 463–816
multiple cloning site 653–760
***lac* promoter 817–938**
pUC origin 1158–1825
ampicillin resistance (*bla*) ORF 1976–2833

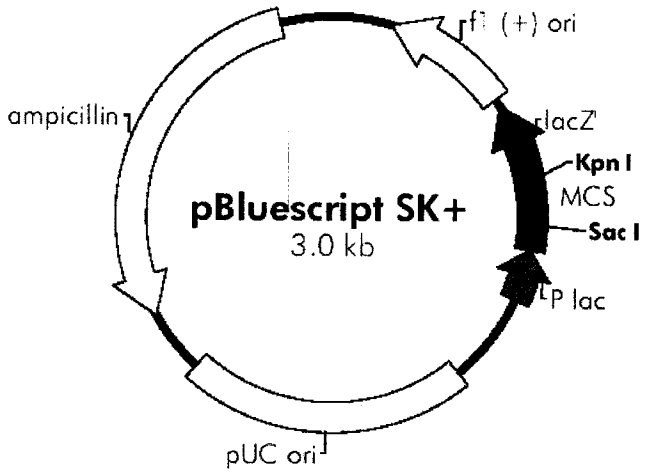

pBluescript SK (+/–) Multiple Cloning Site Region (sequence shown 601–826)